COMMUNICATIONS QUARTERLY

THE JOURNAL OF COMMUNICATIONS TECHNOLOGY

Fall 1998

$9.95

- Build a 160-Meter Class-E PA with Low-Cost Power Switching MOSFETs
- Radiation Characteristics of TABA HF Camp/Mobile Antenna through Experimentation and Modeling
- Unusual Low-Frequency Signal Propagation at Sunrise—Ap Index Reaches 101!
- Simple Scalar Measurements Yield Complex Impedance Measurements
- A Brief Guide to Surface-Mount Technology
- Quarterly Computing Reviews *Toroid Pro* and *Ironcore Novice* Programs
- Junk Science Meets the Skeptic

U.S. $9.95

83>

0 73361 64880 8

M2 BUILDS THE BEST ROTATOR SYSTEM!
THE 0R2800DC HERE'S WHY:

HOUSING DIMENSIONS

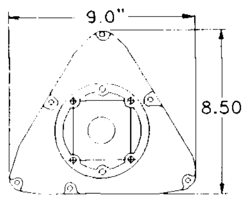

BOTTOM VIEW

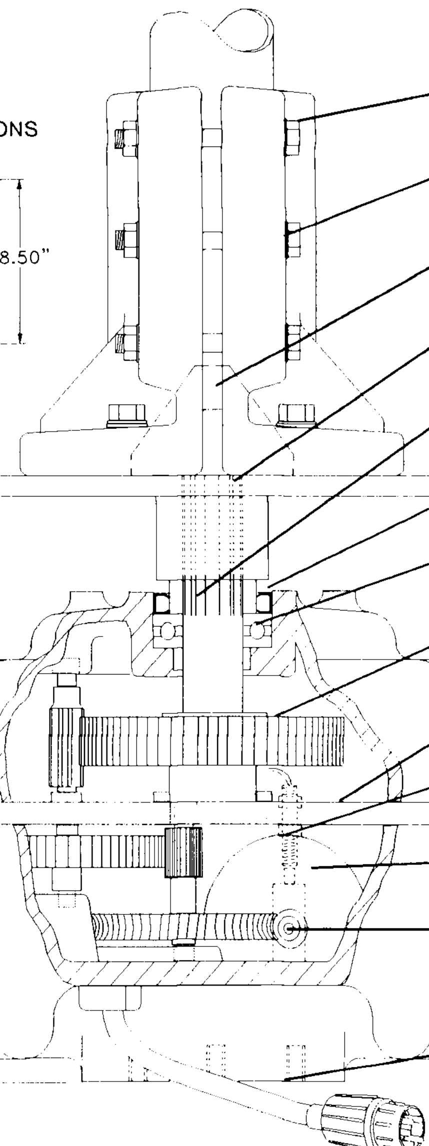

- Ductile iron, massive, toothed mast clamps
- *Grade 5, 3/8-24 steel hardware*
- Self-centering mast guide
- Drive plate accepts masts up to 3-1/8"O.D.
- **NEW! 6-SPLINED OUTPUT SHAFT AND HUB**
- Water seal to keep moisture out.
- 2000 lb thrust bearing for low friction
- Massive hardened steel main gear
- Prop-pitch style torque plate
- Magnetically actuated pulse counting switch for accurate heading display and target accuracy
- **NEW! DC motor - higher starting torque**
- Precision wormdrive - cannot be reversed by mast torque; NO BRAKE RQD.
- Standard Ham M etc. 3" x 3" bolt pattern +2 xtra holes,- fits inside towers like Rohn 25 & up, Triex LM-354 & up U.S.Towers TX438 & up.

OR-2800P SPECIFICATIONS

Wind Area Capacity	35 sq.ft.
Starting Torque	3500 in. lbs.
Rotating Torque	2800 in. lbs.
Braking Torque	17000 in. lbs.
Vertical Load Capacity	1800 lbs.
Height of just the positioner	9.75"
Total height to top of clamps	15.75"
Mast Size (O.D.)	1.75-3"
Rotation Speeds / 360°	70 TO 110 sec.
Rotation Range	0-360° ±14°
Readout resolution	0.1°
Travel Accuracy	± .5°
Input Voltage	110 / 220 VAC
Motor voltage	28-42 VAC
Cable req. - min.	3-#18, 2-#22
Weight (rotator unit)	42 lbs.
Shipping Weight	53 lbs.UPS

CONTROL UNITS
RC2800P Programmable Control Unit WITH WITH DIGITAL READOUT also for prop pitches.

RC2800PRK DUAL for AZ-AZ or AZ-EL control of OR2800, MT3000A, and NEW MT1000
All control units feature RS232 port for computer control. Manual operation standard plus 10 programmable presets plus and 1 flexible preset, Programmable Speed and Ramped start and stop, 0.5° target accuracy. (Works with many logging programs plus Nova and Skymoon for satellite and moon tracking). No other hardware required.

7560 N. Del Mar Ave, Fresno, CA 93711 (209) 432-8873 FAX: 432-3059
Em: m2sales@aol.com or www.m2inc.com

COMMUNICATIONS QUARTERLY

THE JOURNAL OF COMMUNICATIONS TECHNOLOGY

CONTENTS

Volume 8, Number 4 Fall 1998

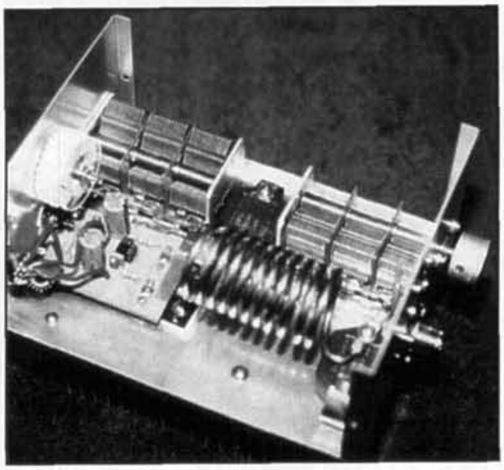

page 9

page 47

On the Cover: Jack Belrose, VE2CV, poses beside the van used in the Amateur Radio Station 40th anniversary demonstration at the Communications Research Centre Open House in Shirleys Bay, Nepan, Ontario, Canada. Photo by Janice Lang. Courtesy of the Communications Research Centre.

EDITORIAL

Securing the ham home for winter

I returned home from running errands one morning in October to find the OM digging holes for antenna radials across our dirt driveway. An old splitting maul was playing the part of trench digger and Rick, K1BQT, was wishing he had some sort of power tool to do the job. "Got to get these trenches deep enough so the snowblower won't rip 'em up this winter. The radials we ran into the woods can just lay on the ground, but these have got to be buried! I wonder if one of those power edgers I saw at the Black & Decker Outlet would work? I need to get this done before the ground freezes."

All over the snow belt, the annual fall preparations for securing ham homes for winter are well underway. In between weekend visits to the local fall hamfests, wires must be launched into the trees, antennas must be secured or taken down, and any outdoor ham work one doesn't want to deal with when the icy gales are blowing must be attended to. Our home is no exception.

Squeezing into small places and playing on the roof

In early September, one of the jobs that fell to Rick was to install a 2-meter radio in the car my son and I share. This was truly a labor of love as the car is a GEO Metro, which requires the smallest possible rig and sculpting of the center console to make it fit besides. But no one should be out on our slippery winter New Hampshire roads without a way to communicate in case of emergency, so Rick spent a weekend squashed in the front seat of our car.

The end of September found us mucking about on the roof, laying down a new covering of roofing asphalt, as the roofing contractor we'd called never bothered to show. Not only will our efforts ensure that we remain dry this winter when the ice dams build up on the eaves, but they will enable us to climb up and de-ice, raise and lower, and repair antennas without fear of falling through an old leaky roof. Of course, until the stuff dries, there's little chance of falling—right now it's easier to get stuck than fall. Fortunately, Rick took down all the experimental antennas he thought might not make it through the winter before we climbed the roof with our goo and brushes!

Cleaning up the yard

In preparation for the winter snow and ice, Rick has also put new wire on all the wire antennas and checked all the ropes in the trees around our yard, making sure to replace any worn lines. Next, he picked up all the aluminum from the yard and stowed it carefully in the crawl space beneath the house. (This was no mean feat, as it meant taking apart several unused antenna designs and gathering up many stray elements strewn about during various experiments. I helped by denuding the yard of black electrician's tape and tie-wrap ends!) Then, we fixed and labeled all the feedline disconnects coming into the house to prevent later crawls through the snow piled against the house.

Putting up that last antenna before the snow flies

This past weekend saw our resident antenna guru out in the yard with a bow and arrow, attempting to put up a 160-meter inverted L to go with those radials I mentioned. These efforts usually go fairly smoothly, but Murphy was busy this day. The antenna is not yet in the trees, but good weather is predicted for the upcoming weekend, offering the opportunity for a second attempt.

And, just this morning, Rick was thinking about those radials again. "I wonder," he mused, "if I should take a little time this evening and run up to the Black & Decker Outlet and buy one of those nifty little edgers?" I suspect he probably will as, like a squirrel collecting nuts, he is determined to be ready when those first snowflakes fly. As, I suspect, are all hams who live in these northern climes!

Terry Littlefield, KA1STC
Editor

P.S. Rick did, indeed, buy his edger last night. A test by the light of the floods on the house indicated it was great idea. However, work has halted for the time being, as the skies are poring rain today with more of the same predicted for the weekend...

A publication of
CQ Communications, Inc.
25 Newbridge Road
Hicksville, NY 11801-USA

Editorial Offices: P.O. Box 465, Barrington, NH 03825. Telephone/FAX: (603) 664-2515. **Business Offices:** 25 Newbridge Road, Hicksville, NY 11801. Telephone: (516) 681-2922. FAX: (516) 681-2926.

Communications Quarterly is published four times a year (quarterly) by *CQ Communications, Inc. Communications Quarterly* is the philosophical successor of *Ham Radio Magazine* founded by T.H. "Skip" Tenney, Jr., W1NLB and James R. Fisk, W1HR. Subscription prices (all in U.S. Dollars): Domestic—one year $33.00; two years $62.00. Canada/Mexico—one year $39.00; two years $74.00. Foreign Air Post—one year $46.00; two years $88.00.

Periodical postage paid at Hicksville, NY and additional mailing offices.

Postmaster: Please send change of address to Communications Quarterly, CQ Communications, Inc., 25 Newbridge Road, Hicksville, NY 11801. ISSN 1053-9344.

Printed in U.S.A.

The book you've been waiting for...

CQ Amateur Radio Equipment Buyer's GUIDE

This information-packed book is your most reliable, unbiased source for detailed information on practically every piece of Amateur Radio equipment and every accessory item currently offered for sale in the United States. From the biggest HF transceiver to Ham computer software, it's in the CQ Amateur Radio Equipment Buyer's Guide, complete with specs and prices. There are over 2100 product listings (3100 including transceiver accessories!).

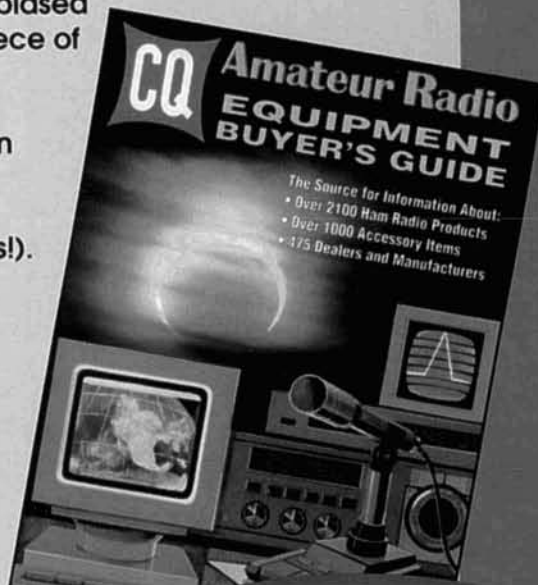

Product listings cover: HF Transceivers, VHF/UHF Multi-Mode Transceivers, VHF/UHF Base/Mobile Transceivers, Handheld Transceivers, Receivers and Scanners, HF Linear Amplifiers, VHF/UHF Power Amplifiers, Transceiver Accessories, Repeaters, Packet and RTTY Equipment, Amateur Television, HF Antennas, VHF/UHF Antennas, Accessories for Antennas, Antenna Rotators, Towers and Masts, Antenna Tuners, Measurement and Test Equipment, Ham Software, Training Tapes, Publications, and Miscellaneous Accessories. Thousands of products are described; many are illustrated.

Only $15.95
Plus $4.00 Shipping & Handling

The CQ Amateur Radio Equipment Buyer's Guide also includes the most comprehensive directory anywhere of Ham product manufacturers and dealers n the USA, complete with phone numbers, FAX numbers, Web sites, and e-mail addresses. Dealer and Manufacturer listings include major products manufactured or sold, and service and repair policies, where applicable, with 475 dealers and manufacturers listed. These listings alone are worth their weight in gold.

The CQ Amateur Radio Equipment Buyer's Guide is jam-packed with solid information and great reading. In addition to being an incredible source of insight into the current state of Ham Radio technology, it will continue to be a reliable Ham equipment reference source for many years to come.

For Fastest Service call 1-800-853-9797 or FAX 516-681-2926

CQ Communications, Inc., 25 Newbridge Road, Hicksville, NY 11801

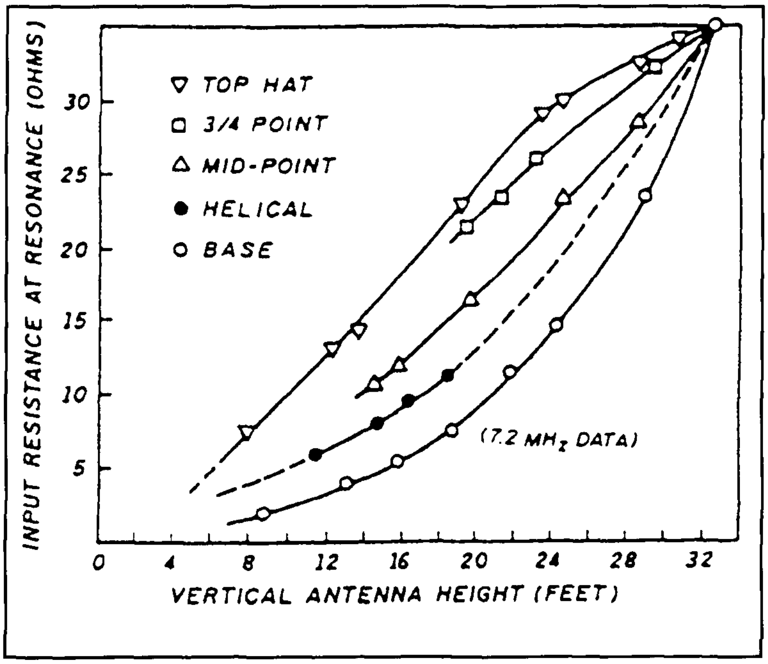

Figure 1. Measured values from Jerry Sevick, W2FMI's antennas erected over a nearly lossless ground system for several representative types from his 1973 article, "Short Radial Systems for Short Verticals," in *QST*. Used with permission of the author.

A word about short verticals

Dear Editor:

Several years ago I wrote three successive articles in the old *Ham Radio* magazine. They were about antennas, dealing exclusively with the design of short verticals ("Marconi" antennas; current-fed at the base, and all shorter than a quarter-wave). The most important (and fascinating to me) is the large diversity in their radiation resistances from type to type and, hence, their feedpoint impedances. An admonishment, however, is necessary here: One "sees" the radiation resistance at the antenna input *only* when ground and other circuit resistances characteristically approach "zero." Loss of energy from other sources, like horizontally polarized radiation from a set of "raised radials," also will appear as a resistance *measured at the antenna input terminals*. They all will appear to be *in series* with the radiation resistance.

Those, in turn, define the gamut of matching circuits and their values. The subject of the aforementioned articles, and this letter, is to demonstrate, by measurement and calculation, the range of impedances (really resistances, because all were adjusted for resonance).

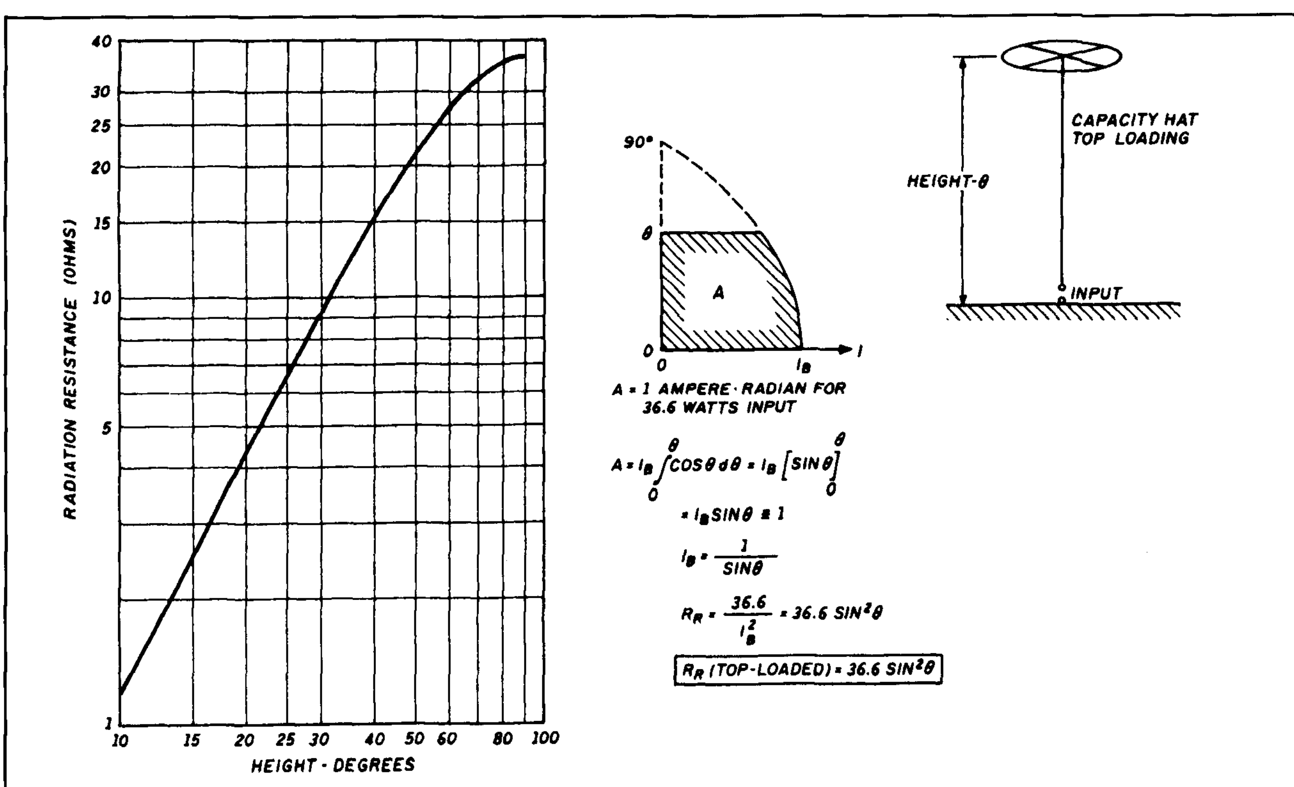

Figure 2. The curve and its derivation for the top-loaded Marconi vertical. The curve is computed from the expression in the rectangular box.

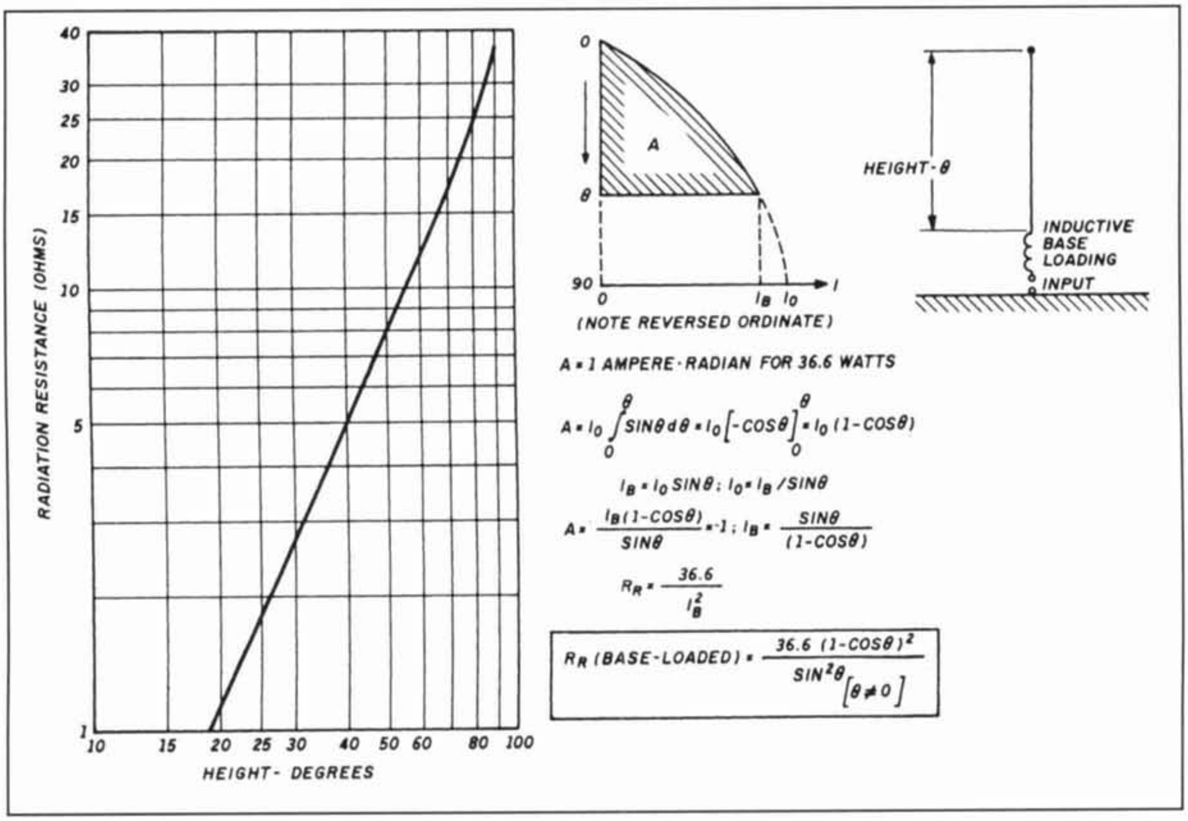

Figure 3. The curve and its derivation for the base-loaded Marconi vertical.

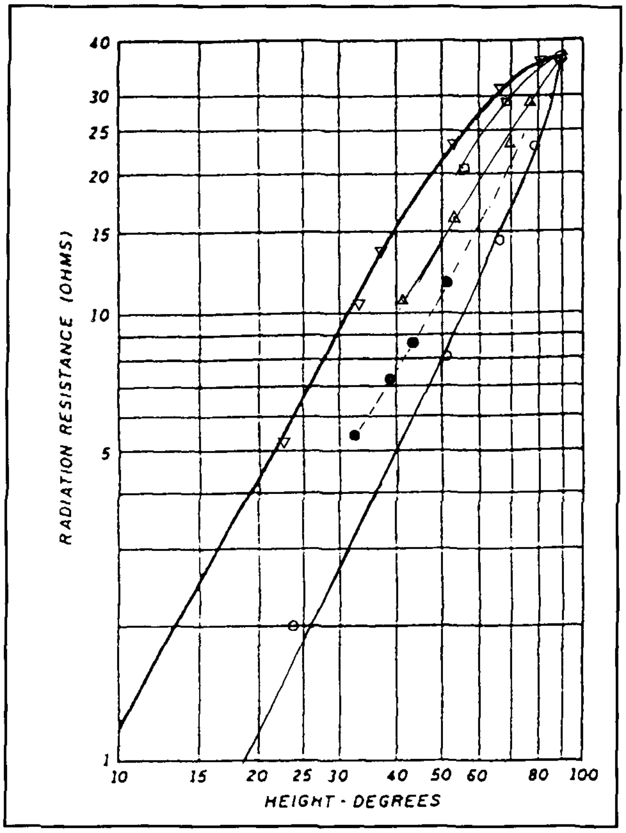

Figure 5. Using W2FMI's measurements to check the theory.

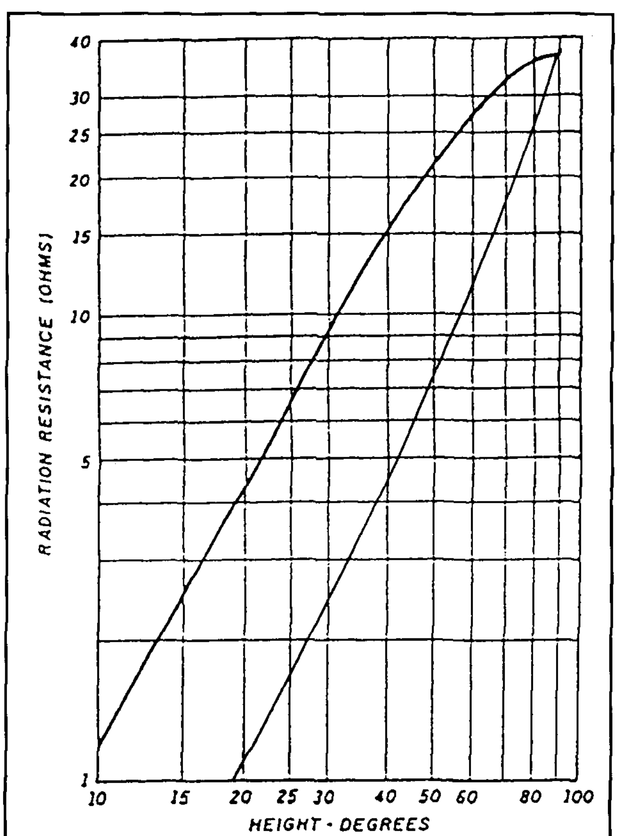

Figure 4. Combining the curves of Figures 2 and 3.

Jerry Sevick, W2FMI, performed some very worthwhile measurements covering five different designs, and published them in *QST*; they appear here, reprinted with the permission of the author (see **Figure 1**). The *calculated* radiation resistances of two of the configurations, however, additionally will be shown here. They are the derivations displayed in **Figures 2** and **3**.

These derivations assume sinusoidal current distributions on a thin vertical element. The answers are correct, as long as other aspects of the antenna do not distort them. An example would be a departure from the absolutely flat shape (a drastic "drooping") of a top-hat, for example. There, the current under that hat would be distorted slightly by the out-of-phase, but partially vertically polarized, field. For rather small top-hats, it usually will be of small concern—but remember that it *is* there. A hat composed of exactly horizontal elements would present no problem at all. The foregoing admonitions result from the method of the derivations, as explained above.

I developed the derivations (in the first two figures) in 1973. In every case in which I actually required an estimate of the radiation resistance of a somewhat complicated vertical, these derivations have worked exceedingly well.

At about the same time, Jerry Sevick, W2FMI, made some very accurate measurements using *full-sized verticals*, erected over an extensive buried radial system. There were 100 quarter-wave radials, each terminated by a rod. I am still impressed by the effort and the precision of Jerry's work. *All* of the vertical variants were constructed for resonance at 7.200 MHz!

My own work regarding short vertical radiation resistances *appeared* to predict that all designs would fall somewhere between two regimes. They were predicted to fall between the low-resistance characteristic of the totally base-loaded vertical, and those of the higher resistances of the totally top-loaded designs; and, by examining **Figure 1**, it can be seen that the highest radiation resistance is that of the top-loaded vertical, and that the lowest would be that of the base-loaded variant. My combination of the curves of **Figures 2** and **3** (shown in **Figure 4**) produce an envelope to contain the limits of *all* possible Marconi configurations.

Jerry's measurements were perfect to check the theory. The points, which retained their original definitions, were transferred from Jerry's curves (linear-linear scale) to the curves of **Figure 5** (log-log scale). The resulting curves were gratifying. As predicted, the verticals *all* fell precisely where they should. Isn't it interesting that some somewhat abstract calculations performed in Arizona in 1990 agreed so very well with some actual measurements made in Northern New Jersey in 1973?

(Continued on page 102)

PRODUCT INFORMATION

Philips ECG Expands Heatsink Line

Philips ECG® has updated its semiconductor heatsink line. The newly expanded line features six new pc-board mountable heatsinks for 12 package styles ranging from TO-126 through TO-247.

The 18th Edition *Master Replacement Guide* contains mechanical drawings, dimensions, and specifications for the complete line of heatsinks. An index makes finding the right heatsink for a particular package easier.

All ECG products and literature are available through a global network of distributors. To locate the nearest distributor call toll free, 1-800-526-9354.

Vibroplex Square Racers

Vibroplex® has announced new Square Racers. A departure from the traditional Brass Racer, these keys have a heavy solid steel base that anchors the key in the operating position. The same Racer magnetic design is used on the new Racer models; there are no springs. Each key has the Vibroplex brass logo plate with a unique serial number attached to the top of each base with stainless steel pins.

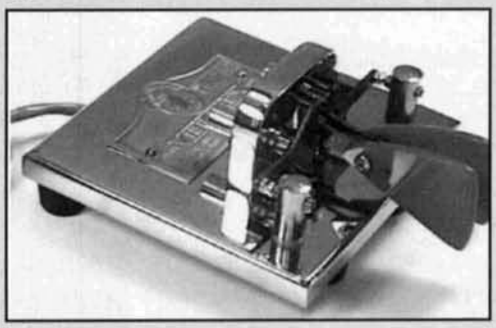

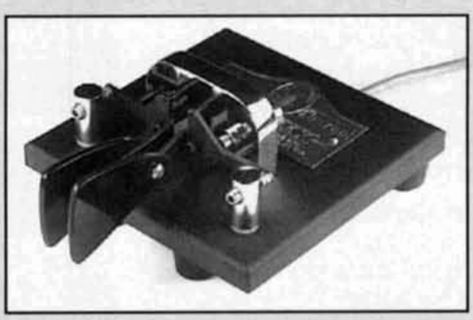

The Square Racers are available in two models. The Deluxe version has a highly polished decorative chrome base with bright chrome top parts, with red finger pieces. It retails for $134.95. The Standard version has a black textured base with decorative top parts, with black finger pieces and retails for $109.95.

Orders will be filled on a "first come-first served" basis, so early orders will receive the lowest serial numbers. To place orders, call (334) 478-8873 or Fax (334) 476-0465.

Voltronics Ultra-Miniature Surface-Mount Trimmer Caps

Voltronics offers ultra-miniature surface-mount chip size trimmer capacitors with a new range of 0.4 to 1.0 pF. The "JS" Series 2.8 mm x 2.2 mm x 1.0 mm and is the smallest trimmer of its kind. It has a self-resonant frequency of 4 GHz.

For more information, quotes, or samples contact Nicholas J. Perrella, Vice President Sales, Phone: (973) 586-8585; Fax: (973) 586-3404; E-mail: <nick@voltronicscorp.com>.

The Magellan Corp. GSC 100, Two-Way Global Messaging Device

Magellan Corporation has introduced the GSC 100 handheld satellite-based global communicator. The device provides communication from anywhere on Earth via e-mail messaging. It has received type approval from the FCC.

The GSC 100 provides integrated positioning and navigation capabilities using the global positioning system (GPS) constellation. GSC 100 users will be able to identify their position, plot and navigate a course, and communicate their position or any other information to anyone on Earth with an e-mail address, voice, or fax service.

GSC communication features include e-mail style interface for creating, editing, forwarding, copying, and deleting data messages. It can save up to 100 messages, store up to 150 addresses, and display message status with the push of a button. It displays characters in large, medium, and small type sizes and can include GPS position information in a message.

The GPS component of the GSC 100 includes the following: six graphic navigation displays; full-featured track plotter; storage of 200 user-defined waypoints; five reversible routes with up to 15 legs; five coordinate systems including LAT/LON, UTM, and OSGB; and sunrise/sunset and lunar calculations.

The GSC 100 is available from dealers. To find a dealer near you, contact Magellan at (800) 611-7955, ext. 8897. For more information about Magellan products, visit the company's Web site at: <www.magellangps.com>.

Todd Roberts, *WD4NGG*
P.O. Box 21413
Hilton Head Island, South Carolina 29925, and

Frederick H. (Fritz) Raab, *W1FR*
50 Vermont Avenue, Fort Ethan Allen
Colchester, Vermont 05446
e-mail: <f.raab@ieee.org>

CLASS-E POWER AMPLIFIER AND DIGITAL DRIVER FOR 160 METERS

Get 700 watts of CW or 250 watts of AM from $10 worth of transistors in your final amplifier

Class-E amplification is based upon a single-ended power amplifier (PA) in which the transistor is operated in switching mode. High efficiency is achieved because the drain capacitance is discharged at the time of switching, and power losses associated with charging and discharging the drain capacitance are eliminated. This property also allows class-E PAs to use relatively low-cost MOSFETs that would otherwise not be suitable for RF operation because of their large drain capacitances. As a result, the power amplifier can be both very efficient and very inexpensive.

This paper describes a 160-meter class-E PA using low-cost power-switching MOSFETs. The RF chain (**Figure 1**) consists of a digital VFO, line driver, predriver, driver, and final amplifier and is packaged in two parts. The PA has a very linear high-level amplitude-modulation characteristic, which makes it an ideal RF amplifier for a high-efficiency AM or SSB

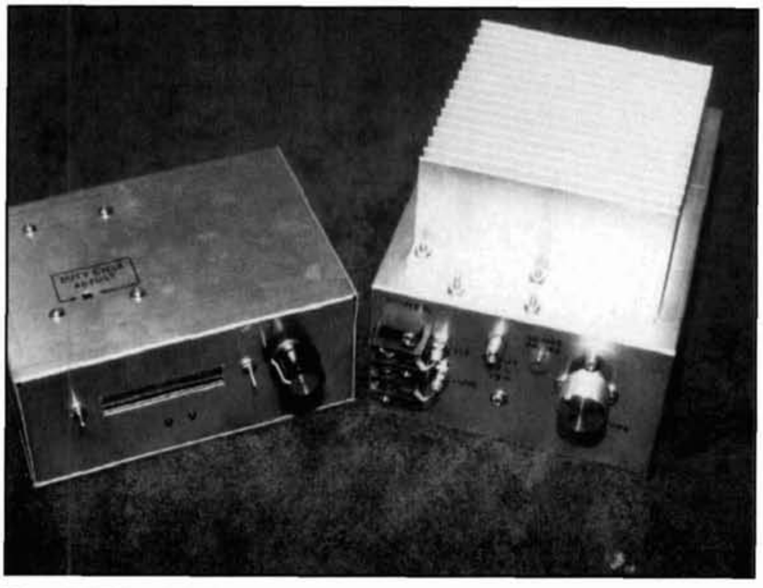

Photo A. VFO unit (left) and amplifier unit.

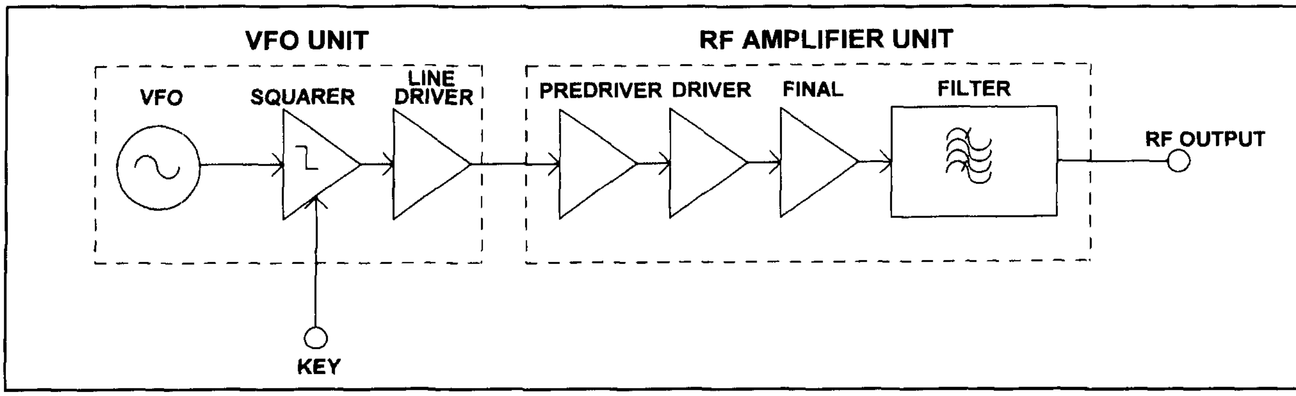

Figure 1. Block diagram.

transmitter. The companion class-S high-level amplitude modulator will be the subject of a future paper.

Class-E principles and design

High-efficiency power amplifier operation results in more power output and/or less DC-power input. Because less power is dissipated, the size of the heat sink can be reduced and/or the amplifier can be more reliable.

Other power amplifiers

Conventional power amplifiers (classes A, B, and C) use their transistors as controlled current sources.[1] Because positive drain voltage and positive drain current are present simultaneously, the efficiencies of these classes of amplification are inherently limited (50 percent for class A and 78.5 for class B with ideal transistors). While the efficiency of an ideal class-C PA can approach 100 percent, the required reduction in the conduction angle causes the peak current to become exceedingly large.

Class-D power amplifiers[1] use a pair of transistors as switches to generate a square-wave voltage. A tuned-output circuit passes only the fundamental-frequency component to the load. Ideal class-D PAs are 100-percent efficient. However, real class-D PAs suffer power losses from the on-state resistance of the MOSFETs, switching time, and the energy required to charge the drain capacitances. The capacitance-charging loss occurs because the drain capacitances aren't part of the tuned output network. Instead, they are charged through the on-state resistance of the opposite MOSFET. The stored energy is then dissipated when the MOSFETs turn on. This effect causes class-D operation to be inefficient at higher frequencies or when used with MOSFETs with large drain capacitances.

Changes in the semiconductor capacitances and the distributed nature of the "low-cost" MOSFETs result in asymmetric switching characteristics in which turn-off takes longer than turn-on.[2] In class-D operation, this results in both MOSFETs being turned on simultaneously

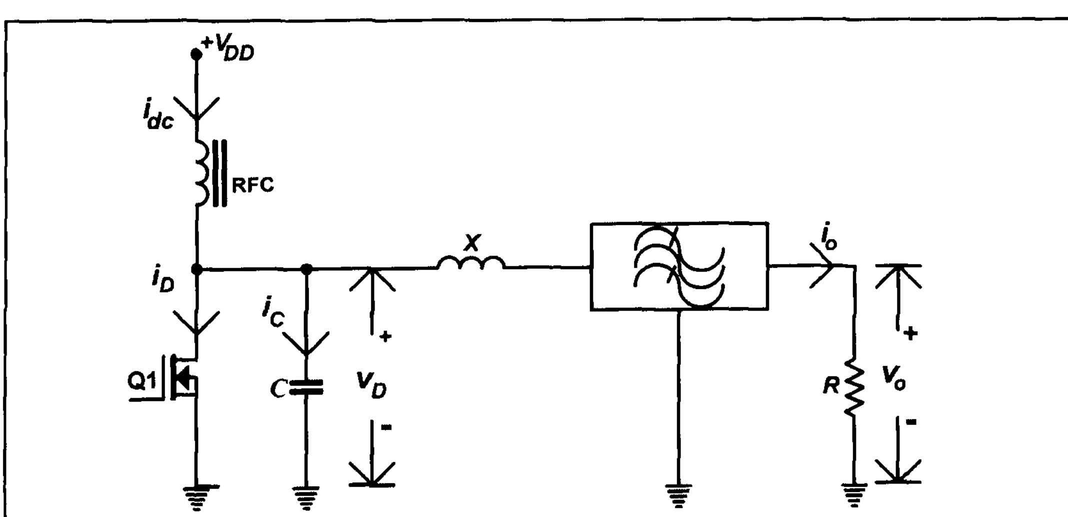

Figure 2. Simplified class-E PA.

for a period of time. This causes a brief short circuit and attendant inefficiency.

Class-E amplifiers

The class-E power amplifier[1,3] is based upon a single-ended PA topology, shown in its most basic form in **Figure 2**. The MOSFET is driven to act as a switch. Shunt capacitance C is the combination of drain capacitance and an added capacitor. The RF choke maintains a constant input of DC current. The series-tuned output filter blocks harmonic currents while passing fundamental-frequency current to the load with a residual reactance, X. The difference between the DC current from the choke and the sinusoidal output flowing to the load flows through the MOSFET when the MOSFET is turned on. When the MOSFET is turned off, the difference current charges the drain-shunt capacitance, C, creating the drain-voltage waveform.

When the MOSFET turns on, the energy stored in the shunt capacitance (because of a non-zero drain voltage) is dissipated, resulting in inefficiency. This power loss is avoided by choosing C and X so the drain voltage drops to zero at the instant the MOSFET turns on. Since drain voltage and drain current are never positive at the same time and the drain voltage is zero at turn-on, the PA is ideally 100 percent. For optimum operation, C and X are chosen so the drain voltage not only drops to zero but has zero slope at turn-on (**Figure 3**). This causes the drain current to be zero at turn-on, eliminating switching losses at this transition. It also makes the PA relatively tolerant of changes in circuit components and duty ratio.

In summary, class-E is the preferred mode of operation for PAs using low-cost MOSFETs for several reasons:[2]

- No possibility of a "short-circuit" caused by both MOSFETs being turned on simultaneously,
- Higher efficiency due to elimination of drain-capacitance losses,
- Reduced sensitivity to variations in switching time and speed, and
- Greater tolerance of circuit strays.

Design equations

The basic equation for determining the load line, R, required to deliver a specified amount of power, P_0, from a given effective supply voltage is:

$$(P_o) = 0.577 \frac{V^2_{\mathrm{eff}}}{R} \qquad (1)$$

The voltage drop across on-state resistance R_{on} of the MOSFET causes the effective supply voltage to be less than the real supply voltage, V_{DD}, by:

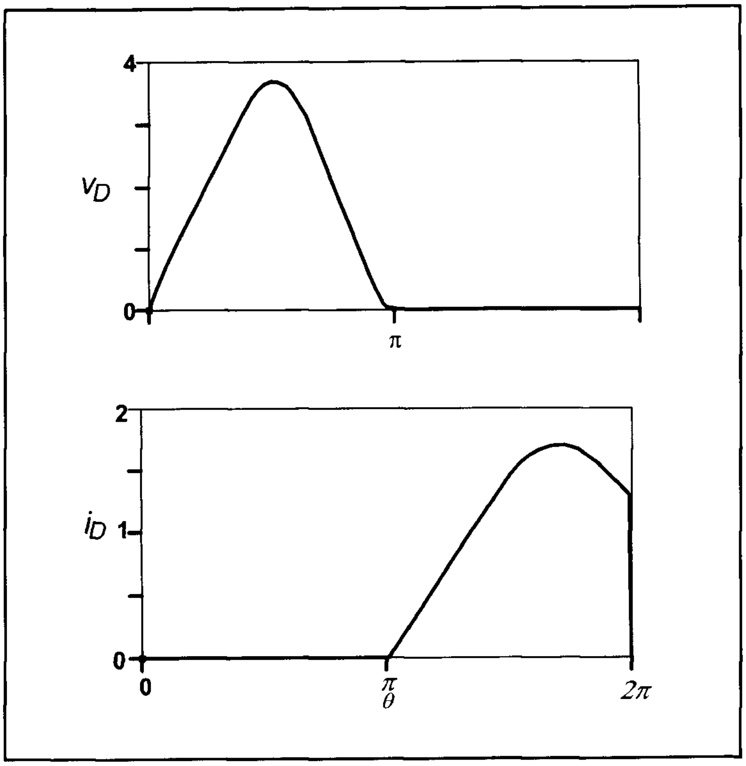

Figure 3. Waveforms in ideal class-E PA.

$$V_{\mathrm{eff}} = \frac{R}{R + 1.365R_{\mathrm{on}}} \qquad (2)$$

The value of the on-state resistance is obtained from the data sheets. Iterative use of the above two equations yields the value of R.

Once R is determined, the residual reactance, X, is given by:

$$X = 1.15\,R \qquad (3)$$

and the total shunt capacitance is given by:

$$B = 2\pi f C = \frac{0.1836}{R} \qquad (4)$$

For proper tuning, the peak drain voltage (voltage rating of the MOSFET) is:

$$V_{D\max} = 3.56\ V_{DD} \qquad (5)$$

although it can be somewhat higher if the PA is mistuned.[4] The DC-input current is:

$$I_{DC} = \frac{V_{DD}}{1.73\,R} \qquad (6)$$

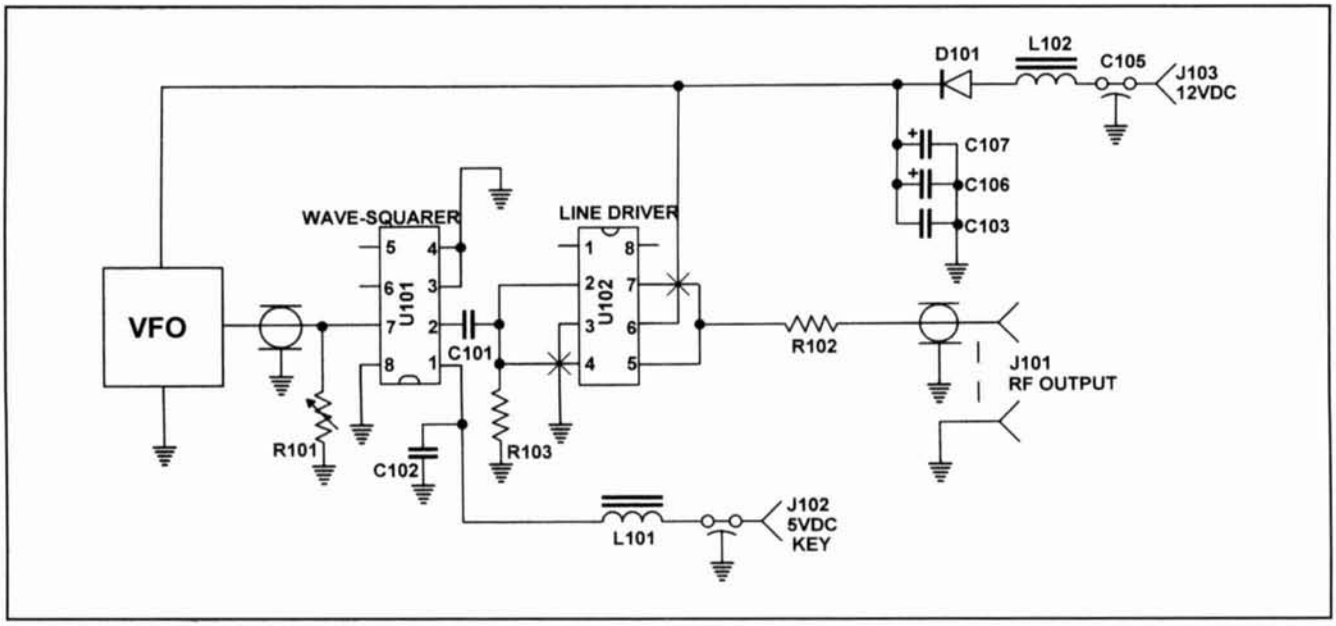

Figure 4. Circuit of VFO unit.

and the peak drain current (current rating of the MOSFET) is:

$$I_{D\max} = 2.86\ I_{DC} \quad \textbf{(7)}$$

Modulation

Class-E PAs aren't suitable as linear amplifiers because they operate in saturation and changes (unless drastic) in the amplitude of the driving signal produce little or no change in the output signal. However, their linearity for high-level amplitude modulation is generally excellent because the MOSFET is either on or off and its gain nonlinearities have little chance to affect the modulation. With the addition of a high-level class-S modulator,[5] the class-E PA can be used for AM. It can also be used for SSB with the further addition of an envelope detector through the Kahn envelope-elimination-and-restoration technique.[6,7,8]

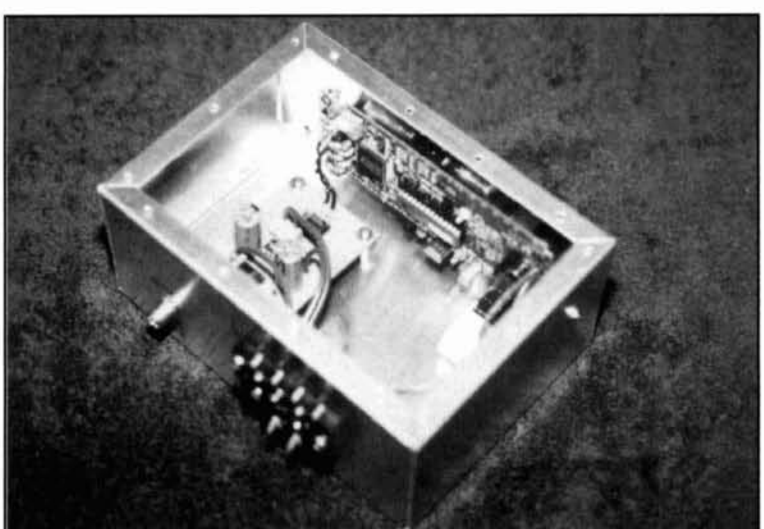

Photo B. VFO unit. VFO board is at top right, line driver at bottom left.

VFO unit

The VFO and associated circuits (**Figure 4**) are assembled in one box and powered by +12 volts at 250 mA and +5 volts at 10 mA.

VFO

The VFO A101 is a DDS (direct digital synthesis) board from S&S Engineering. It produces a sinusoidal output of 0.3 volt peak at frequencies up to 16 MHz and is operated according to instructions from S&S. Spurious products are 60 dB or more below the desired signal.

The VFO may be purchased in either assembled or kit form. Assembly requires handling and soldering a number of surface-mounted devices, so readers without experience or tools may prefer to buy the assembled version. Verify the correct polarity before applying power. Use a frequency counter to verify the frequency and an oscilloscope to verify a sinusoidal output.

Wave shaper and line driver

Because the objective is to drive a switching-mode amplifier, U101 converts the sine wave output of the VFO into a square wave. The duty ratio is controlled by varying R101. Keying for

CW operation is injected at this point by applying +5 volts through C104 and L101, which activates or deactivates U101.

The TTL-level output of U101 is boosted to a 0 to 12-volt square wave by gate driver U102. The output of U102 drives the 75-ohm line to the amplifier unit through resistor R102, which prevents damage to U102 if the output is inadvertently short circuited. This results in a square wave with voltages of 0 to 6 volts when the VFO and amplifier units are connected.

The wave shaper and line driver are assembled on a single-sided printed circuit board as shown in **Figure 5**. Remember that the square waves used in these circuits contain significant harmonics, so the construction practices required are similar to those required for a VHF amplifier. Keep the signal-carrying leads as short as possible and mount bypass capacitors as close as possible to the point being bypassed. Leave as much uninterrupted ground plane around the circuit as space permits.

Use an oscilloscope to check first the output of the VFO and then the output waveform of the line driver. Excessive ringing or rounding of the square wave indicates a problem.

For best final amplifier performance, R101 is adjusted so waveform J101 is high 60 percent of the time. The signal is again inverted in the amplifier unit, resulting in the final-amplifier MOSFETs being turned on (drain voltage low) 40 percent of the time.

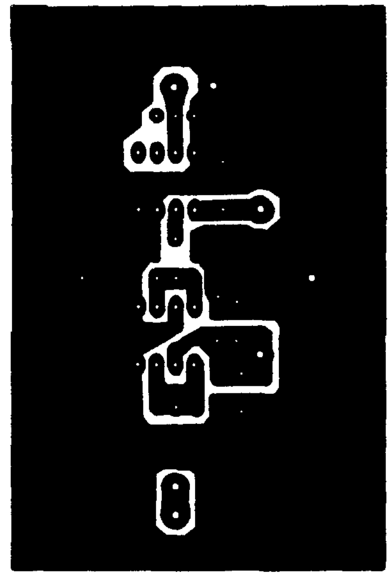

Bottom View

Figure 5. Line-driver pc board.

RF amplifier unit

The RF-amplifier unit (**Figure 6**) includes:

- driver and predriver,
- MOSFET final amplifier, and
- output network.

All are assembled in a single Bud minibox. The drivers and final amplifier (except for tuning components) are assembled on a single pc board (**Figure 7**).

Predriver and driver

Narrow-band tuned power amplifiers are traditionally driven by tuned amplifiers.[9,10] Broadband power amplifiers are typically driven by broadband, linear amplifiers. Gate-swamping resistors provide proper termination of the interstage transmission-line transformers at the cost of extra drive power.

The driver for this transmitter uses an IC and a complementary pair of MOSFETs.[11,12,13] It promotes fast switching of the final-amplifier MOSFEts by rapidly charging and discharging their gate capacitances. This driver is simple, inexpensive, and requires neither adjustment nor tuning. There's no danger of puncturing the gates with the 12-volt square-wave drive. Power is dissipated only in charging and discharging the gate capacitances.

The driver and predriver operate from +12 volts at 400 mA. The predriver is AC-coupled and biased to ground for simplicity. The predriver is DC-coupled to the driver, but the driver is AC-coupled to the final. If the VFO signal is removed or the driver fails, the final stage simply looses drive and is switched off.

Predriver U201 is an Elantec EL7104 non-inverting gate driver and accepts either TTL- or CMOS-level drive. Resistor R201 provides a matched termination for the signal from the

Table 1. Adjustment Settings for L203

Frequency, kHz	C14 ("LOAD")	C17 ("TUNE")
1820	85% meshed	100% meshed
1900	50% meshed	85% meshed
1980	15% meshed	75% meshed

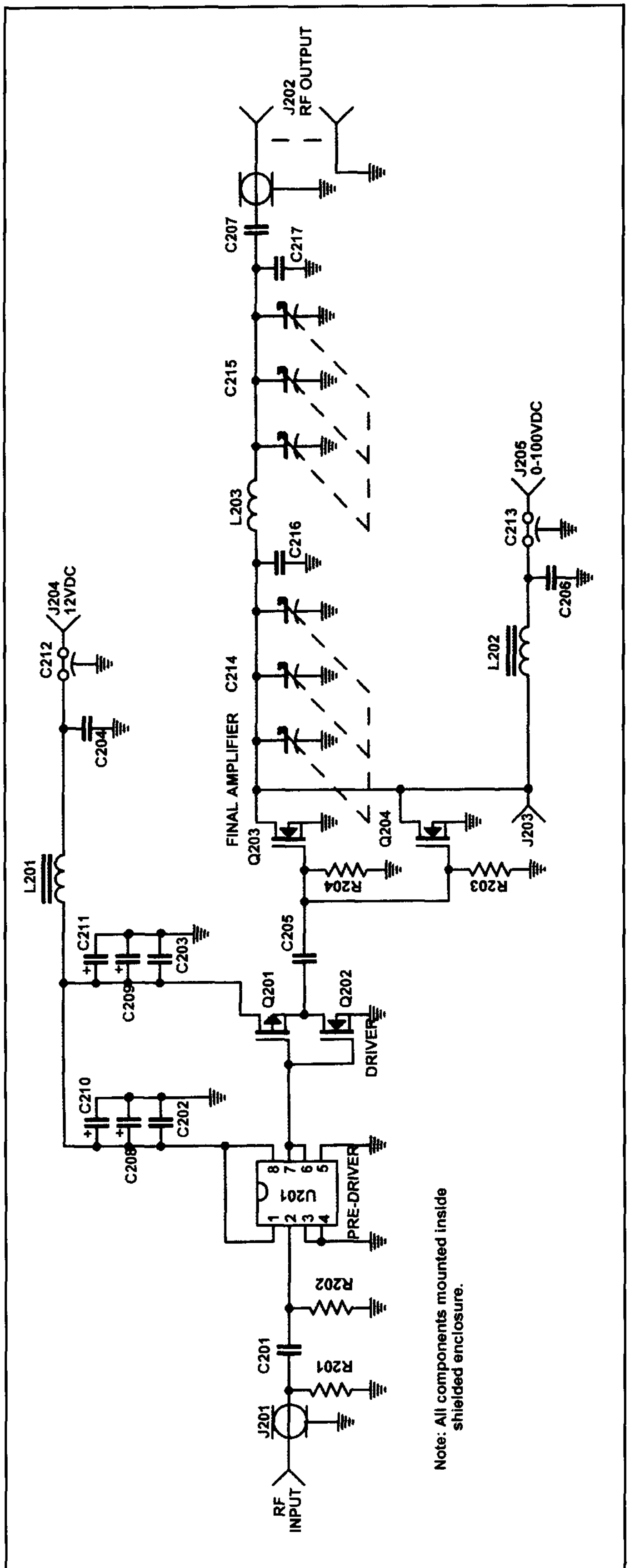

Figure 6. Circuit of RF amplifier.

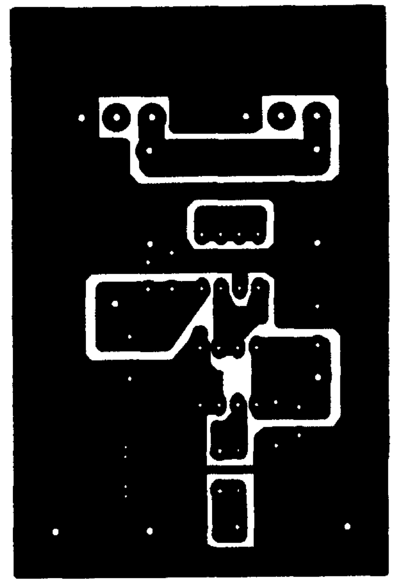

Figure 7. RF-amplifier printed circuit board.

VFO. Half-DIP IC U201 includes a Schmidt trigger that acts as a limiter and pair of complementary MOSFETs that produce a 12-volt peak square wave with rise/fall times of about 7 ns.

The driver stage (Q201-Q202) uses IRFD9120 and IRFD110 quarter-DIP MOSFETs. This complementary pair produces a 12-volt square wave with rise and fall times of about 16 and 8 ns, respectively. They are mounted close to final-amplifier MOSFETs Q203 and Q204 and connected with a chip capacitor and wide trace to minimize the inductance between them and the gates of the final MOSFETs. A low-impedance driver is essential for rapid charging or discharging of the final gate capacitance, which is, in turn, essential for fact switching.

The predriver IC and driver MOSFETs may be operated safely without heat sinks at frequencies up to 2 MHz. They can be operated at

Table 2. Parts List for VFO Unit

Reference	Description
C101-C103	0.1-µF, 100-volt monolithic ceramic
C104-C105	0.001-µF, 1000-volt feedthrough
C106	4.7-µF, 35-volt tantalum
C107	1000-µF, 35-volt electrolytic
D101	1N4001
J101	F-connector female chassis mount
L101, L102	FT-50-43 toroid with 16 turns #22-AWG enameled wire
R101	1-k trimpot
R102	50-ohm, 1-watt RC20
R103	5-ohm, 1/4-watt RC07
U101	DS8921AN RS-422 line-driver/receiver pair
U102	Elantec EL7212 inverting gate driver
A101	S&S Engineering DDS VFO (kit or assembled)
----	Printed circuit board
	Miniature coax (RG-196A/U)
	Bud aluminum minibox
	IC sockets

frequencies up to 10 MHz if clip-on heat sinks are added.[11]

Final amplifier

The final amplifier is a pair of IRFP450 MOSFETs connected in parallel. These MOSFETs are intended for low-frequency power switching and have drain ratings of 14 amps and 500 volts. Like the driver and predriver, the gates of the final amplifier are biased to ground level and the driver is AC-coupled.

Output network

The output tuning network resembles the familiar pi network used in vacuum-tube transmitters; however, it's best to think of it as two Ls. The first capacitance (C214 and C216) is adjusted to provide (in combination with drain capacitance of the MOSFETs) the desired total shunt capacitance calculated from **Reference 4.** The first part of the inductor provides the 1.15*R* reactance required for optimum class-E operation. The rest of the inductor and the second capacitance (C215 and C217) transform the 50-ohm load to the 5.5-ohm load line required for delivery of the desired power output.

The "tuning" (drain-side) capacitor comprises a fixed 0.002-µF capacitor (C216) plus a three-section "bread slicer" (C214). The "load" (output-side) capacitor comprises a fixed 0.004-µF capacitor (C217) plus another three-section bread slicer (C215). Direct current is fed through toroidal choke L202 and 1.8-µH tuning inductor L203, but blocked from the output by C207. Test point J203 allows obser-

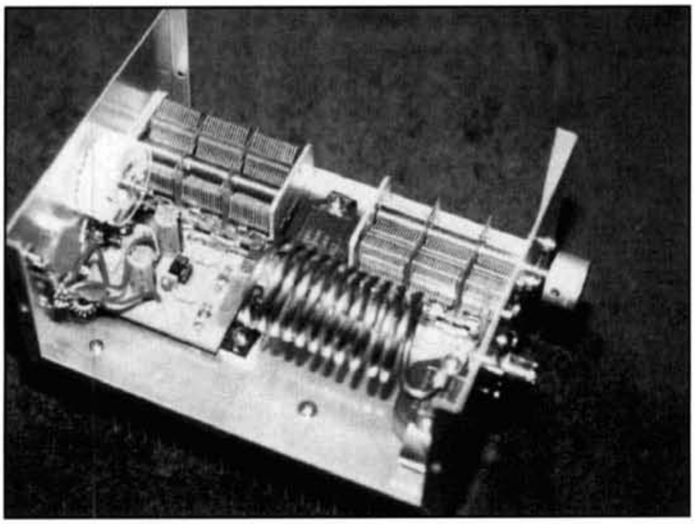

Photo C. Amplifier unit. Circuit board is at lower left, tuning inductor on right, "tune" (drain) capacitor top left, "load" (output) capacitor top right.

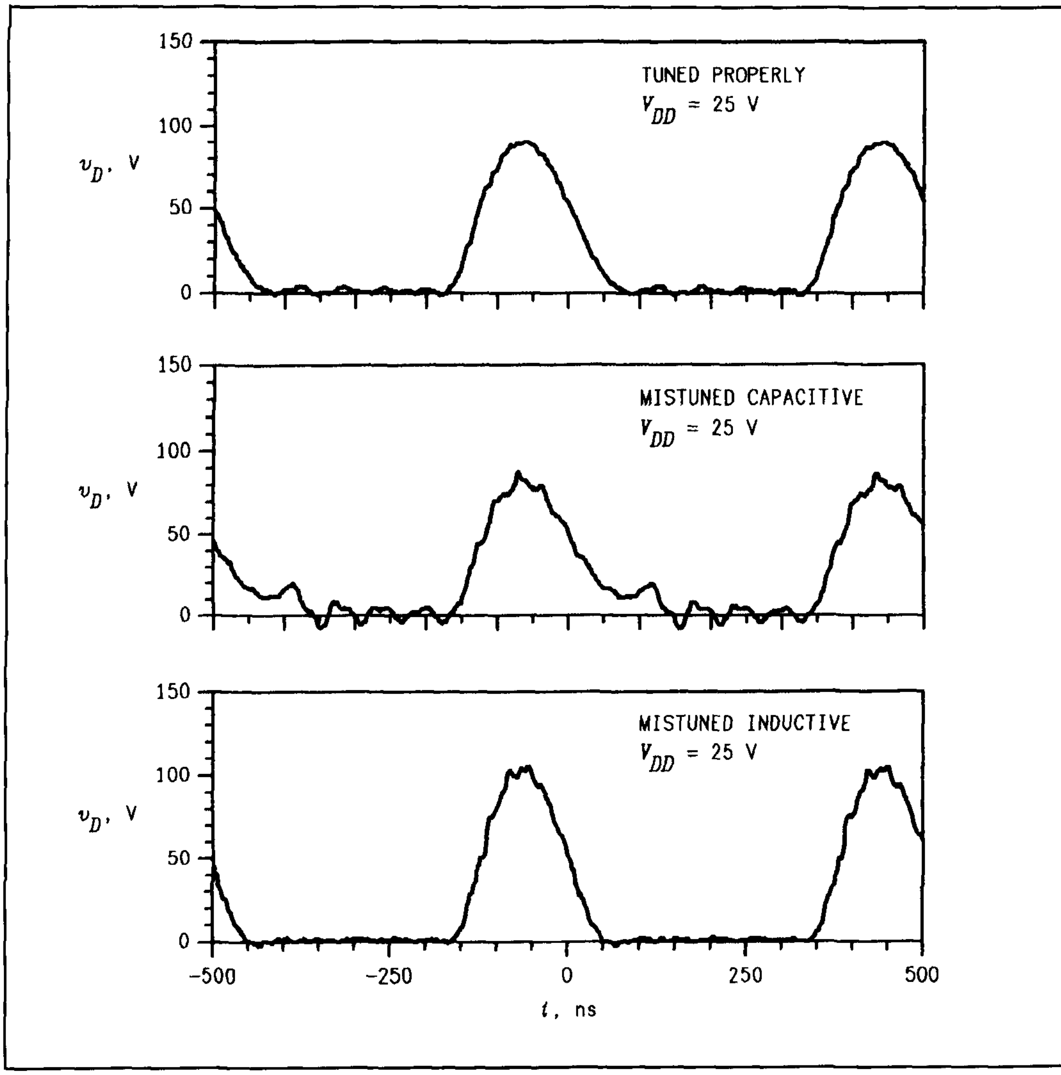

Figure 8. Observed waveforms

vation of the drain-voltage waveform while the case cover is in place.

Construction

Most components are simply mounted on the board. The final-amplifier MOSFETs Q203 and Q204 are, however, mounted on the heat sink. Their leads must be bent appropriately before being soldered to the printed circuit board. MOSFETs Q203 and 204 are insulated from the heat sink by thermal pads.

Tuner components are mounted on the Bud minibox and connected by short leads. Inductor L203 is formed by winding 11 turns of #6 AWG solid copper wire on a 1.25-inch form so the resultant length is 2.75 inches. Toroidal inductor L202 is mounted in a sandwich between two plastic disks to isolate it from the chassis. Drill the disks for #6 screws and mount the assembly against the chassis with #6-32 hardware. Choke L201 is mounted on a terminal strip.

Check-out/adjustment

Begin by verifying that the waveform from the VFO unit is present on R201 in the amplifier unit. It should be a square wave with levels of 0 and 6 volts and be high 60 percent of the time.

Next, connect +12 volts to the amplifier unit. The waveform at the output of U201 should be a square wave with levels of 0 and 12 volts. It should be high 60 percent of the time. The waveform at the driver output (Q201-Q202 connection) should also be a square wave with levels of 0 and 12 volts, but it should be high 40 percent of the time. The gate voltages on Q203 and Q204 should be square waves with levels of 0 and +12 volts. Because the predriver and driver are switching stages, there's nothing to adjust.

Now connect a dummy load and the main power supply to the amplifier unit. Increase the main supply to +10 volts. The drain waveform should be near zero 40 percent of the time.

Next, adjust L203. Expand or compress L203 so minimum output power occurs with the settings in **Table 1**. If a clear peak cannot be observed, the inductance of L203 must then be adjusted.

CAUTION

Inductor L203 is "hot." Turn off the main supply voltage before adjusting L3.

Drain-voltage waveforms are shown in **Figure 8**. When the final amplifier is correctly tuned, the drain voltage drops to zero just as the MOSFETs turn on (top waveform). If the drain-shunt capacitance is too small, the drain voltage begins to rise just before turn-on (middle waveform). Avoid this as discharge of the capacitor at turn-on wastes the energy stored in the drain-shunt capacitance. If the drain-shunt capacitance is too large, the drain voltage goes negative before turn-on (bottom waveform). The negative voltage is limited by conduction of the MOSFET intrinsic reverse-direction diode. While this doesn't degrade efficiency significantly, it should be avoided because the intrinsic diode isn't necessarily capable of handling the same current as the MOSFET itself.

Tuning for a given frequency is accomplished by first adjusting "load" for the maximum output power and the adjusting "tune" for efficiency. Tuning for maximum efficiency is somewhat tricky because maximum output power, maximum efficiency, and maximum DC-input power occur at the different drain-shunt capacitances. It's easiest to use an oscilloscope to observe the waveforms during tuning so optimum class-E operation can be verified. If a scope is not available, tuning can be accomplished by first tuning for maximum power output. The "tune" capacitance is then reduced slowly while watching the output power and input power (DC current) and calculating efficiency. When the amplifier is proper-

Table 3. Parts List for Amplifier Unit

Designator	Description
C201-C204	0.1-µF, 100-volt monolithic ceramic
C205	0.1-µF, 200-WV ATC chip capacitor, 900C104 NP200
C206-C207	0.1-µF, 1000-volt ceramic disk
C208-C209	4.7-µF, 35-volt tantalum
C210-C211	1000-µF, 35-volt electrolytic
C212-C213	0.001-µF, 1000-volt feedthrough
C214-C215	3-gang air variable, 15-535 pF per section
C216	0.002-µF, 2500-WV mica block capacitor
C217	0.004-µF, 2500-WV mica block capacitor
J201	F-connector female chassis mount
J202	S0-239 UHF female chassis mount
J203	Tip jack or scope-probe connector
J204	Terminal block
J205	Terminal block
L201	Ferroxcube FT-50-43 toroid with 16 turns AWG#22 enameled wire*
L202	Micrometals T184-2 with 24 turns AWG#18 enameled wire*
L203	Approximately 1.8-µH, see text.
	Plexiglas™ disk for mounting L2, U.S. Plastic Corp., Lima, Ohio.
Q201	IRFD9120
Q202	IRFD110
Q203-204	IRFP450
R201	75-ohm, 1-watt RC20
R202-R204	5-k ohm, 1/2-watt RC10
U201	Elantec EL7104 non-inverting gate driver

*Available through Amidon.

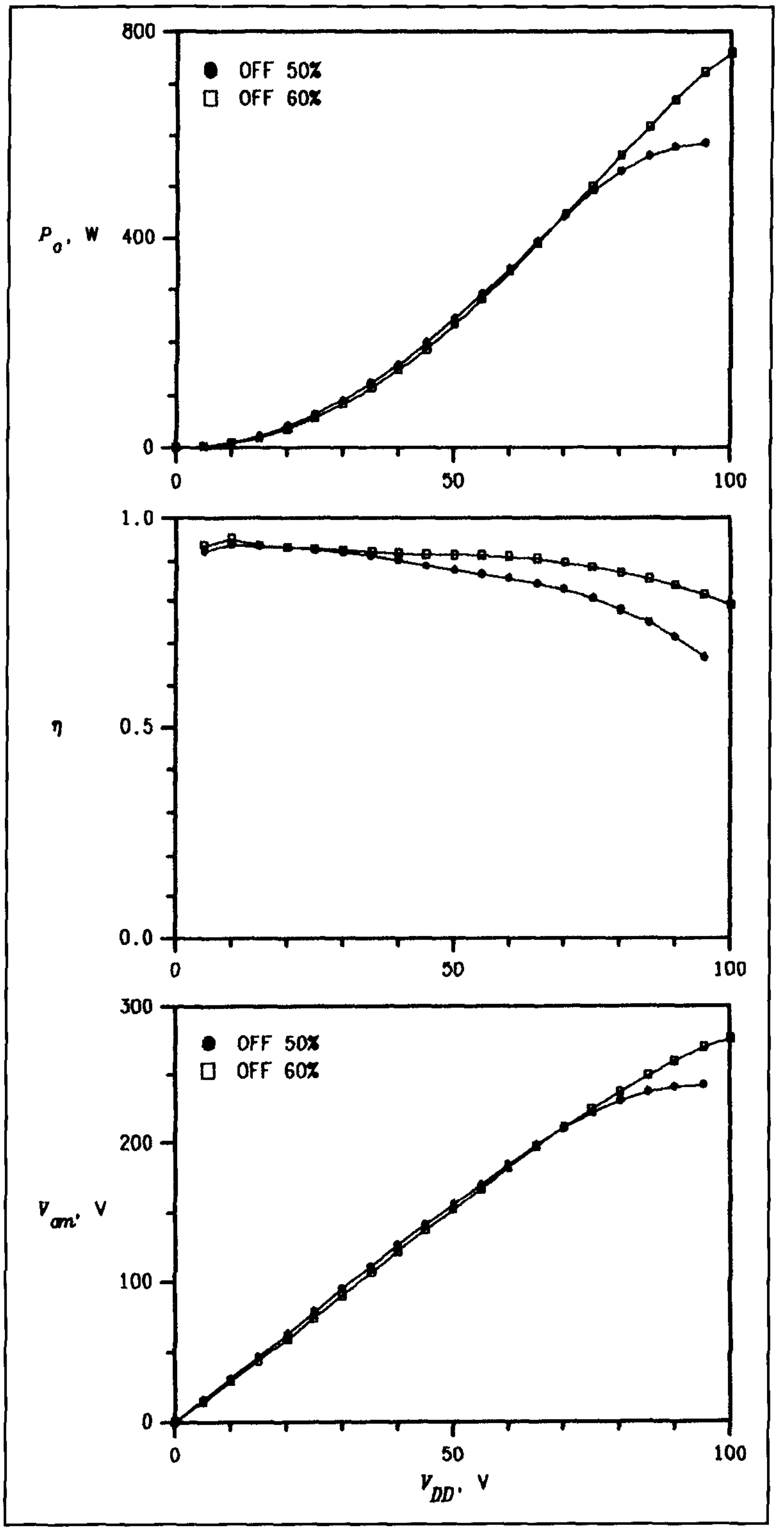

Figure 9. Measured performance.

ly tuned, it looks like an 8-ohm load to the power supply (i.e., V_{DD} = 16 volts should result in I_{DC} = 2 amps).

When retuning for a different frequency, follow the same procedure. It's best to begin retuning with a supply voltage of 25 to 50 volts. When the amplifier is properly tuned, bring the supply voltage back to its full-power value. Because the drain capacitance is voltage-variable, a slight retuning may be necessary to maximize efficiency.

Performance

The performance of the final amplifier as a function of supply voltage V_{DD} is shown in **Figure 9**. It's apparent that a 40-percent duty ratio is preferable to a 50-percent duty ratio. Output power is about 250 watts for V_{DD} = 50 volts. The efficiency remains above 90 percent for supply voltages up to 70 volts (output power up to 500 watts). The MOSFET on-state resistance increases at higher drain currents, causing the efficiency to drop gradually to about 84 percent at V_{DD} = 90 volts (output power 700 watts).

Because the final amplifier is operated in switching mode, its amplitude-modulation linearity is excellent. When operated with a 200-watt carrier and 100-percent modulation (45-volt supply voltage for no modulation, 90-volt peaks), the transfer curve (V_{om}/V_{DD}) deviates from a straight line by only 1.09 percent, which is roughly equivalent to audio distortion of 1 percent. For SSB use with a peak output supply of 90 volts (700 watts), the linearity is about 2 percent, which is equivalent to IMD products 34 dB below PEP.

The driver and VFO consume only about 8 watts (3 watts in the driver; 5 watts in the VFO). Their total power consumption is only about 1.2 percent of the peak CW output.

The second and third harmonics are 24 and 31 dB, respectively, below the fundamental at the output of the pi network. These levels are satisfactory if the amplifier is connected to an antenna (e.g., vertical) through a tuner. However, if the antenna (e.g., a dipole) doesn't require a tuner, an additional low-pass filter should be inserted between the amplifier unit and the antenna. The fourth and higher-order harmonics are more than 56 dB below the fundamental.

A year of extensive on-the-air use shows the transmitter can be reliably operated at up to 250-watt carrier level for AM and up 700 watts for CW. A class-S (switching-mode) modulator is used to produce AM; on-the-air reports of the modulation quality are excellent.

Conclusions

The transmitter described above is simple and efficient. It produces excellent amplitude-modulation linearity when used with a class-S modulator (to be described in a future paper).

The use of low-cost components and simple construction techniques puts it within reach of the average experimenter. We find it's very satisfying to produce 700 watts of CW or 250 watts of AM from $10 worth of transistors in the final amplifiers, and we hope other hams will try building similar amplifiers. ■

REFERENCES

1. H.L. Krauss, C.W. Bostian, and F.H. Raab, *Solid State Radio Engineering*, Wiley, New York, 1980.
2. F.H. Raab, "Low-cost High-efficiency HF Power Amplifiers," *Proceedings* Nordic HF '98, Faro, Sweden, pages 2.2.1–2.2.10, August 11–13, 1998.
3. N.O. Sokal and A.D. Sokal, "Class E—A New Class of High Efficiency Tuned Single-ended Switching Power Amplifiers," *IEEE J. Solid-State Circuits*, Vol. SC-10, No. 3, pages 168–176, June 1975.
4. F.H. Raab, "Effects of Circuit Variations on the Class E Tuned Power Amplifier," *IEEE J. Solid-State Circuits*, Vol. SC-13, No. 2, pages 239–247, April 1978.
5. F.H. Raab and D.J. Rupp, "Class-S High-efficiency Amplitude Modulator," *RF Design*, Vol. 17, No. 5, pages 70–74, May 1994.
6. L.R. Kahn, "Single Sideband Transmission By Envelope Elimination and Restoration," *Proceedings IRE*, Vol. 40, No. 7, pages 803–806, July 1952.
7. F.H. Raab and D.J. Rupp, "High-efficiency Single-sideband HF/VHF Transmitter Based Upon Envelope Elimination and Restoration," *Proceedings* of the Sixth International Conference on HF Radio Systems and Techniques (HF '94) (IEE CP 392), York, UK, pages 21-25, July 4–7, 1994.
8. F.H. Raab, B.E. Sigmon, R.G. Myers, and R.M. Jackson, "High-efficiency L-band Kahn-technique Transmitter," *International Microwave Symposium Digest*, Baltimore, Maryland, pages 585–588, June 9–11, 1998.
9. E. Lau, K-W. Chiu, J. Qin, J.F. Davis, K. Potter, and D. Rutledge, "High Efficiency Class-E Power Amplifiers-Part 1," *QST*, Vol. 81, No. 5, pages 39–42, May 1997.
10. E. Lau, K-W. Chiu, J. Qin, J.F. Davis, K. Potter, and D. Rutledge, "High Efficiency Class-E Power Amplifiers-Part 2," *QST*, Vol. 81, No. 6, pages 39–42, June 1997.
11. K. Dierberger, L. Max, and F.H. Raab, "Low-cost, High-efficiency 13.56-MHz Power Amplifier," presented at RF Expo East '94, Orlando, Florida, November 15–17, 1994. Available as *Application Note APT9403*, Advanced Power Technology, Bend, Oregon, November 1994.
12. K. Dierberger, F.H. Raab, B. McDonald, and L. Max, "High-efficiency Power Amplifiers for 13.56 ISM and HF Communication," *RF Design*, Vol. 18, No. 5 pages 28–36, May 1995.
13. F.H. Raab, "Simple and Inexpensive High-efficiency Power Amplifier for 160–40 Meters," *Communications Quarterly*, Winter 1996, pages 57–63.

PRODUCT INFORMATION

Antique Electronic Supply 1999 Catalog

Antique Electronic Supply has released their 1999 catalog. The catalog is mailed to all active and new customers automatically, but anyone who's interested in obtaining a free copy may do so by contacting the company directly. The 72-page catalog includes books, a line of Hammond classic 300 series power transformers, ferrite rods, inductor coils, and a line of telegraph keys.

Customers have a choice of three types of telegraph keys: straight key, iambic paddle, and a dual straight key and iambic paddle. Imported from Spain, these keys have gold-plated brass keys on olive wood bases. The handles and knobs are teakwood.

Antique Electronic Supply also offers products for all types of tube gear, including vacuum tubes, transformers, capacitors, parts, supplies, and literature.

To obtain a free catalog, contact Antique Electronic Supply at 6221 South Maple Avenue, Tempe, Arizona 85283; Phone: (602) 820-5411; Fax: (602) 820-4643. They also have a toll-free fax only number for callers from the U.S. and Canada at: (800) 706-6789. Send e-mail to: <info@tubesandmore.com>. Finally, you can browse the catalog online at <www.tubesandmore.com>.

Free Web-Based University Offers Online Course Modules

A new, free Web-based virtual university is available to engineers who wish to keep their technical skills sharp. Tech *OnLine* University (TOLU) features a course-management system that allows students to manage and track their own progress.

TOLU is composed of 30-minute interactive educational "modules." Each module typically includes one or two interactive exercises and a self-test. Courses vary in subject matter and depth, but are aimed at providing engineers with technical knowledge that can be applied to solving real-world design challenges. Each TOLU course is written by an expert in the subject matter and adapted by the company for Internet delivery. The courses are completely free, and there are plans to expand monthly in a variety of technical areas—focusing on engineering theory, existing products, and applications of emerging technologies.

Tech *OnLine* University is the newest addition to the Tech*OnLine* line of products and service. To find out more check out Tech *OnLine's* Web site at <http://www.techonline.com>.

Voltronics 1.2-pF Multi-turn Precision Trimmer Capacitor

Voltronics Corporation has a 1.2-pF multi-turn precision trimmer capacitor, the A2 series, which is only 0.240-inch long by 0.090-inch diameter. The new capacitor replaces fragile, expensive sapphire trimmers. Its capacitance range is 0.3 to 1.2 pF.

The patented solid-state dielectric design provides high reliability because plates cannot short. Tuning is linear over four full turns with positive stops at minimum and maximum capacitance.

A high-voltage option has 1250 volts DC working and 2500 volts DC withstanding.

For more information, contact Nicholas J. Perrella, Vice President, Sales, Phone: (973) 586-8585; Fax: (973) 586-3404; E-mail: <info@voltronicscorp.com>.

Rick Littlefield, *K1BQT*
109A McDaniel Shore Drive
Barrington, New Hampshire 03825

QUARTERLY COMPUTING

The Toroid Pro and Ironcore Novice programs

Who among us enjoys plowing through tedious calculations or littering the bench with "cut-and-try" debris just to wind the optimum coil? Not me! I'd prefer to get it right the first time and move on to other things. Toward that end, this edition of "Quarterly Computing" looks at two new programs that help designers find the best materials and winding data for constructing powdered-iron toroid inductors. The first is *Toroid Pro*, a comprehensive body of data aimed at the professional engineer who must consider a wide range of information when making product decisions. The second is *Ironcore Novice*, a simpler treatment targeted at experimenters and home builders. Both programs were authored in Quick Basic by John Bellora of B&E Engineering while working in cooperation with Micrometals, Inc.

Although DOS based, *Toroid* and *Ironcore* are rendered in a user-friendly, multi-color graphic format that plays well on Windows 3.1 and Windows 95. Operating documentation is minimal, mostly because little is needed to get the job done. However, *Toroid* does provide a body of supplemental application material written to help designers interpret and make best use of the data provided on the screen.

Toroid Pro

Refer to **Figure 1** for a look at *Toroid's* main screen. The program requires four basic entries: core size, core mix, wire size, and a desired inductance. It then tells you the number of turns to use. To select each data-entry box, you step sequentially across the page by clicking the on-screen arrows with a mouse, or by using the left/right keyboard arrows. To enter core and wire-size data, you use the up/down arrows to select a standard value from a list. Desired inductance is entered numerically in nH, μH, or mH—the range you choose is selected by an icon. When all four data entries are recorded, the suggested number of turns appears automatically in two boxes, one for 200-degree core coverage and the other for 360-degree coverage. Pretty simple!

However, *Toroid* doesn't stop there. While standard Micrometals core sizes and mixes are posted as a list for rapid selection, you may also manually enter custom data for options like stacked cores, "odd-ball" cores, or custom-manufactured cores. Flags at the bottom of the mix column indicate which core selections are acceptable for microwave or DC line-filter use. In the wire-size box, a secondary widow displays the maximum number of turns allowed for a given wire size (you may select either single layer or 45 percent fill using an icon). The inductance data box requires an initial numeric entry. However, once this is done, you may use the up/down arrows to change your value in predetermined increments (also icon selectable). This feature allows you to scroll through a range of inductances while watching the turns count display for a desired number of turns.

A large coil-specification box appears directly below the inductance box. This provides comprehensive core specifications for the core you've selected along with other useful specifics, such as the coil's wire length, DC resistance, self-resonant frequency (SRF) in highpass and lowpass applications, and the predicted frequency for peak Q. Below this box, the screen displays color drawings of the selected core labeled with physical dimensions.

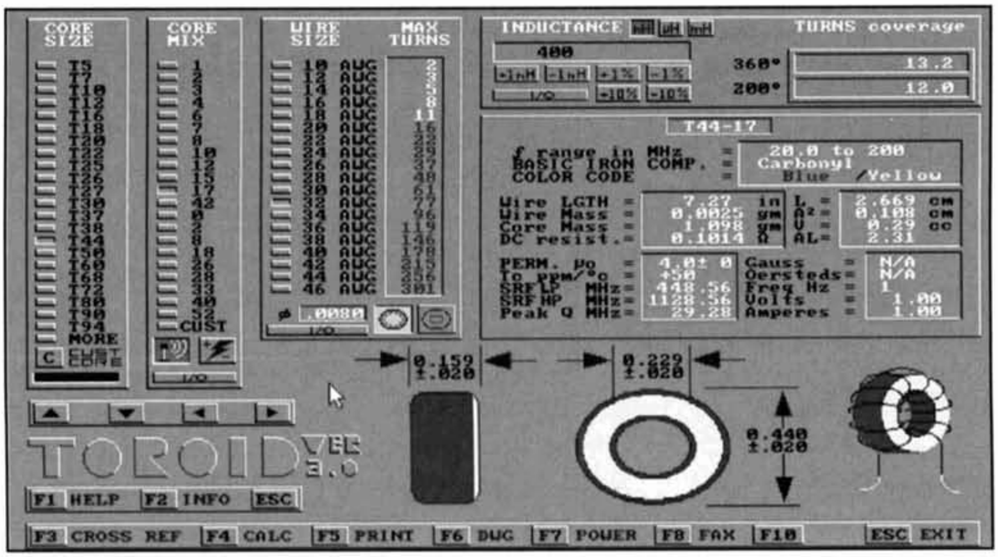

Figure 1. ***Toroid Pro*** **main screen.**

In addition to the primary on-screen data display, a number of dedicated F-keys let you gain access the program's special features and functions. For openers, there are the usual ones you'd expect like program help, program information, and screen print. In addition, you can call up and print data sheets and mechanical drawings for individual cores—a real help for preparing proposals or documenting designs. There's also an extensive cross-reference directory to help you characterize cores made by other manufacturers. You'll even find a preformatted RFQ form addressed to Micrometals to help you obtain Fax quotes. And, last but not least, there's a built-in on-screen calculator to help you crunch numbers!

Ironcore Novice

Ironcore is a less comprehensive version of *Toroid* with a simpler on-screen presentation (see **Figure 2**). For the sake of economy, many special features and data tables not essential for casual experimentation aren't included. However, despite its smaller size, *Ironcore* shares *Toroid's* predictive accuracy because both programs use the same algorithms to generate results. (Note: this is not true for earlier releases.) *Ironcore* may be simpler, but it's not any less accurate.

Like *Toroid*, *Ironcore* requires four data inputs: core size, core type, wire size, and a desired inductance. It then automatically displays turn-counts for 200 and 360-degree core coverage. Missing, however, is the stepping function that allows you scroll through higher or lower inductance values with the arrow keys. Consequently, if you want to predict how much inductance your 10-turn coil has, you'll need to input some trial values until you hit upon the right approximation. This isn't hard to do, but it's slower than scrolling. Also, some calculations such as the SRFs, frequency for maximum-Q, and DC wire resistance aren't provided. However, wire length *is* included, and this calculation is especially helpful when preparing to wind a coil with a large number of turns. Simplicity not withstanding, the "basics" are there—and *Ironcore* has the same potential to take the guesswork out of winding a coil as *Toroid*.

Putting the program to work

The first test of any new program comes when you load it into your machine and try to make it play. Although the documentation warns of a potential glitch with early Windows 95 systems, both program disks loaded into my Compaq Presario 1622 laptop and ran right away. However, because my machine runs the sometimes quarrelsome Windows 95, I discovered I'll need to install a special print driver—currently available as shareware—to print color renderings of the primary screen. This is not needed for *Toroid's* data sheet and mechanical drawing files, because these consist of simple text and line art. As I pointed out in my introduction, both programs are very simple to load up and use. This is a real plus for those of us who view the computer as a tool box rather than as an ongoing source of intellectual stimulation and challenge!

In the end, the true merit of any modeling program is its ability to predict reality. To put *Toroid* and *Ironcore* to the test, I challenged both programs to predict the inductance for nine turns of #22 wire wound on a T37-6 core. (I chose this particular problem because it falls within the boundaries of the limited demo available on the Web.) After recording the predicted results for 200 and 360-degree core coverage, I assembled the genuine articles on the bench and checked them for inductance. Lacking lab-grade equipment, my procedure consisted of measuring each coil for inductance at 5, 10, and 20 MHz on an MFJ-259B (digital) Analyzer, and then repeating the trial with an Autek RF-1 for verification. Readings from both bridges roughly agreed, so I averaged my data points to obtain a "composite" inductance value based on six trials. Here's what I found:

	200-degree Coverage	**360-degree Coverage**
Ironcore/Toroid	317 nH	297 nH
Measured	313 nH	283 nH

As anticipated, *Toroid* and *Ironcore* generated duplicated predictions. More significantly, that prediction fell remarkably close to the bench measurement—amazingly close, when you consider potential sources for error. This raises an important point about CAD simulation in general. These programs crunch inductance numbers with three-digit resolution and count windings to 1/10th of a turn, something which implies tremendous precision. However, it's not uncommon for the best modeling algorithms to vary in accuracy from one part of the simulation range to another.

In addition, real-world toroids rarely behave as well as the idealized model. That's because core permeability can vary between production lots, dimensional inaccuracies are common, some users wind coils tighter than others, and it's nearly impossible to obtain uniform turns spacing—especially when hand winding. Furthermore, external factors such as operating frequency, temperature, humidity, shielding, and the presence of external magnetic fields may alter inductance in a particular application. In other words, what you model may not always be what you get—and often through no fault of the model! It always pays to check.

Having said that, the fact remains that *Toroid* and *Ironcore both* did a great job of nailing the values of my two sample coils. Performance like that can save designers a lot of wasted time and effort!

The bottom line

Toroid and *Ironcore* were both very easy use and appear to be quite accurate. *Toroid* is aimed at the professional engineer, and is clearly the more sophisticated program of the two. *Toroid* sells for $99.95 plus $3.29 S/H and $6.00 Maryland sales tax. *Ironcore* is written for experimenters and home builders and sells for $24.95 plus $3.29 S/H and $6.00 sales tax. Both are available from B&B Engineering, 3000 Florence Road, Woodbine, Maryland 21797. You may contact B&B by phone at (410) 489-5532 or via e-mail at <Toroid.aol.com.> Also, you may download limited demos from their Web site at <http://www.members.aol.com/Toroids/johnindx.htm.> ■

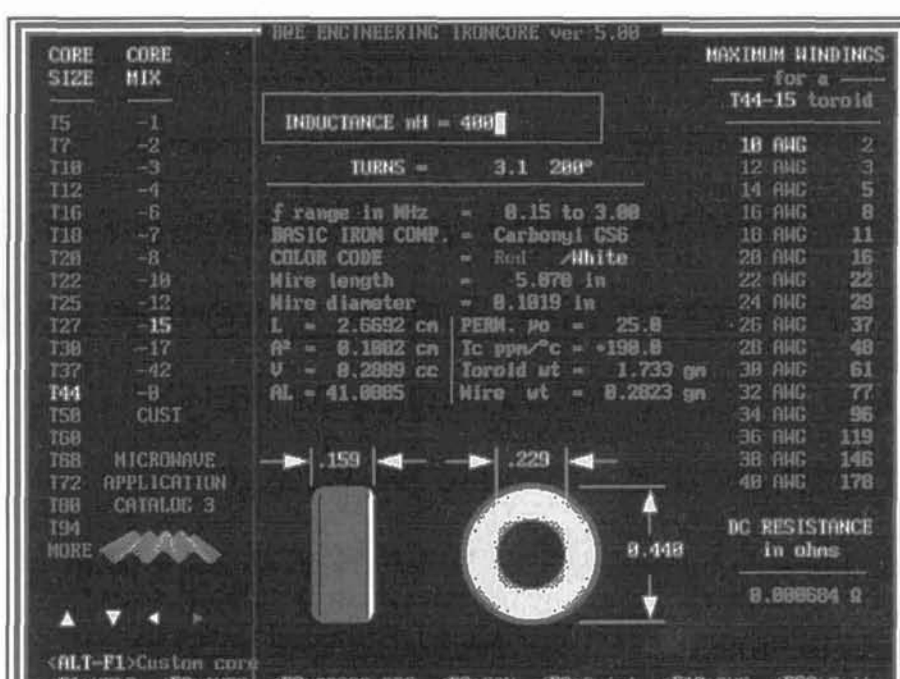

Figure 2. The *Ironcore Novice* screen.

Ian Poole, *G3YWX*
5 Meadway, Staines
Middlesex, TW18 2PW
England

A BRIEF GUIDE TO SURFACE-MOUNT TECHNOLOGY

Is this the end of ham radio construction or a brave new world?

Anyone opening a piece of modern electronic equipment these days will be confronted by a board covered in minute components. They are nothing like the leaded resistors and capacitors with which homebrewers are familiar. Instead these items are extremely small, measuring a millimeter or so in each direction. This is the result of the surface mount revolution, and it has provided many benefits to the electronics industry.

Surface-mount technology has enabled automatic assembly to be taken significantly further. It has reduced costs and increased reliability. But above all, it has taken the quest for miniaturization to another stage. To demonstrate this, it is only necessary to look inside one of the new handheld transceivers or similar piece of equipment. For the radio amateur, this trend toward miniaturization may be worrying. Is this the last nail in the coffin for home construction? Can the radio enthusiast modify or repair his rig now?

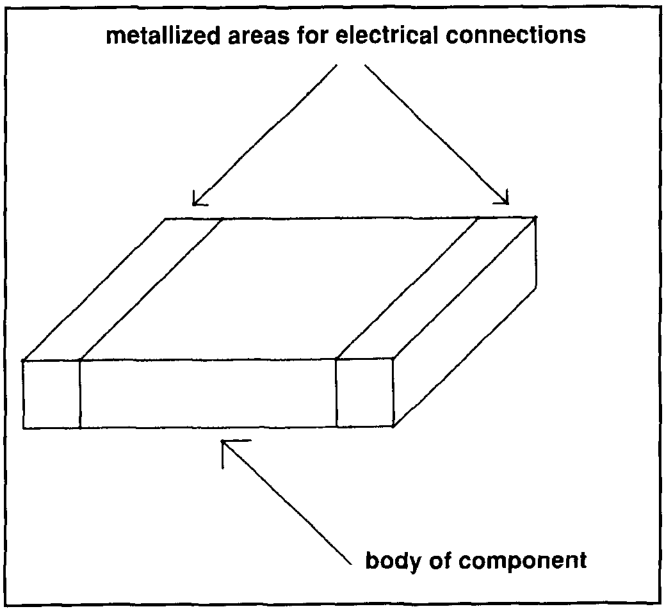

Figure 1. A passive (resistor or capacitor) surface-mount component.

Development

The idea for surface-mount technology (SMT) arose from the need to increase the level of automation in electronics manufacturing. In the 1970s, automatic pc board assembly machines were used to insert components into boards. These were very unreliable. The leads of items like resistors had to be bent or "preformed" so they would fit through the holes in the board. And, even when this had been done, the mechanical tolerances meant that they would not always fit properly.

The need for a more successful approach to automated assembly led to a reassessment of what was required. Component leads had been essential in the early days of electronics, when

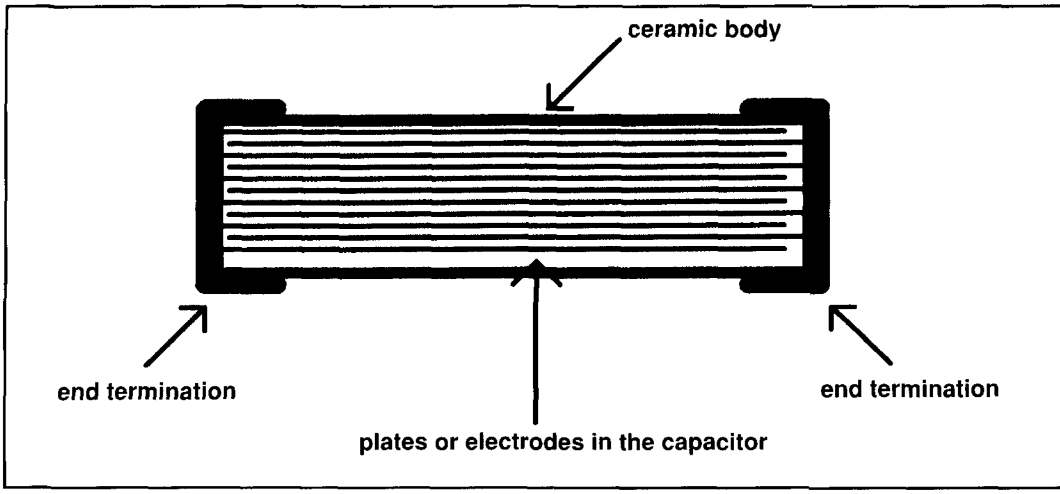

Figure 2. Internal construction of ceramic multi-layer capacitor.

components were wired between standoffs, valve bases, and tag strips. However, the revolution caused by the printed circuit board brought about a different set of requirements. As a result, the idea for leadless components which could be mounted directly onto the board was born. With such technology, the need for an intermediate lead between the component itself and the board was removed—making the component cheaper and board assembly much easier.

Its revolutionary nature meant that it took some years to catch on. In the early 1980s, manufacturers began to accept the idea, and companies using mass production techniques were the first to see the advantages. Nevertheless, there were difficulties. Initially, very few components were available, and this meant that early designs had to use a mixture of surface mount and conventional components. As the demand for the new devices started to grow, so did the selection and availability. Now many components, and particularly new ICs, can no longer be obtained in conventional packages.

Resistors and capacitors

The first devices to be converted to surface mount were the resistors and capacitors. They basically consist of a rectangular cube with areas of metallization at either end onto which the connections can be made. Package sizes are standardized for these components, and numbers like 1206 and 0805 indicate the size (**Figures 1** and **2** give the length of the components in hundreds of an inch while the second two give the width). Height is not given, and may vary from one manufacturer to the next. The same series from one manufacturer may also be of different values.

The 1206 packages, although quite small, are rarely seen these days because manufacturers have moved on to even smaller packages. They reached a peak usage in the West in the early 1990s. They were superseded by 0805 styles, which reached their peak usage around 1994. The smaller 0603 package is the most widely used in new equipment in the West, and the minute 0402 components are on the horizon. In Japan, the 0402 package is now in common use, enabling the manufacture of their matchbox-sized cellular phones. Needless to say, even smaller packages (like the 0201) are on the horizon!

Most of the capacitors used are multi-layer ceramic types and values extend to 220 nF and beyond. Their construction is like that shown in **Figure 2**, and consists of alternate plates separated by dielectric layers. The actual type of dielectric often depends upon the value and the case size. The preferred type is the COG dielectric, as this gives a capacitor that is quite stable. As more capacitance must be squeezed into a smaller space, other dielectrics are used, including X7R and Z5U. These do not offer the same stability, but are quite adequate for most decoupling applications. The end terminations are particularly important, and they now include a nickel barrier as shown.

Ceramic capacitors are the most popular by far, and are manufactured in vast quantities each day. In view of their popularity, their ranges are being extended all the time. Many ranges used to stop at values around 220 nF, although some high-value ceramic capacitors are available. Naturally, these are larger to accommodate the additional capacitance.

Other types of capacitors are available, including electrolytics. However, these are not ideal for all applications as they are generally quite tall. Additionally, the soldering process reduces their life considerably. Tantalum capacitors are often used where long-term reliability is required. They also come in packages that are larger than their small value ceramic relations. However, they last longer than electrolytics, and provide the capacitance required for many applications. Their drawback is that they are more expensive.

Resistors are similar in style to the small ceramic capacitors. They use the same package sizes, but their construction is totally different. They are formed on a ceramic base. Resistive paste is added to this to create the element, and this is covered with a protective layer. The end terminations are then added to enable contact to be made as shown in **Figure 3**.

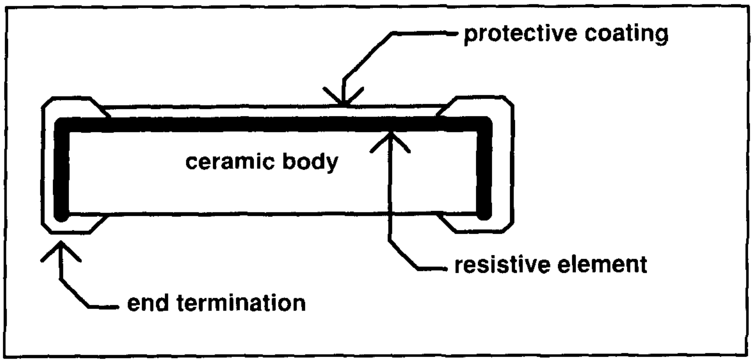

Figure 3. Construction of a resistor.

Component markings

One of the differences between surface-mount and conventional components is that it is not always possible to mark the component values onto the device because of size. This is not a major problem for manufacturers because reels of components are marked, and the machine used to place the components "knows" where to put the ones from each reel. For the home constructor, it is a bit more difficult. Home builders usually obtain components in small quantities, usually in marked bags. As a result, they should not be removed until they are required for use, and then only one at a time. If a spare part remains on the table or workbench, it's anybody's guess what it may be.

Capacitors are not marked, however some of the larger resistors may be. Three figures are used. Like the bands on a conventional resistor, the first two refer to the significant figures of the value and the third is the multiplier. For example, 473 would correspond to 47000 ohms, or 47 k.

Other passives

Although resistors and capacitors form the bulk of passive components used, a variety of other components, like small inductors, are available. These are made by a number of manufacturers and are available in a variety of values from a few nano-henries up to a hundred and more micro-henries. These inductors are widely used, especially in cellular phone applications, as well as in any radio-related product from televisions to videos and the like.

While their size is obviously important, inductors are not becoming as small as fast as capacitors and resistors are. The reason for this is simple: There is only a certain amount of wire that can be coiled into a given space. While the wire size can be reduced, the current capacity also falls, and may be too small for many applications.

Surface-mount crystals are also widely used. These items find uses as clocks in computers, are relatively common, and come in a variety of sizes. The physical size of the crystal itself means they cannot be placed in packages **of** the **same** size **that** resistors and capacitors **can occupy**. Even so, they take up significantly less space than their conventional counterparts.

Connectors are another area where the surface mount revolution is causing some changes. To prevent connectors from having to be placed and soldered separately, the industry is responding with a variety of new connector types.

Semiconductors

Transistors and diodes have been similarly affected. They cannot use the same package styles as passive components; however, they have undergone similar degrees of miniaturization. The most popular form of package is called the SOT-23 outline. Instead of having metallized areas on the side of the package, there are small leads from the package that sit on the board, as shown in **Figure 4**.

Diodes use this type of package. Even though three leads are provided (**Figure 5**), they are all

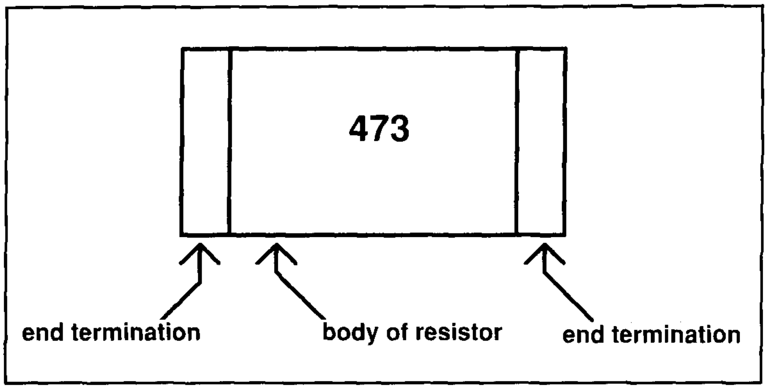

Figure 4. Component marking on a resistor.

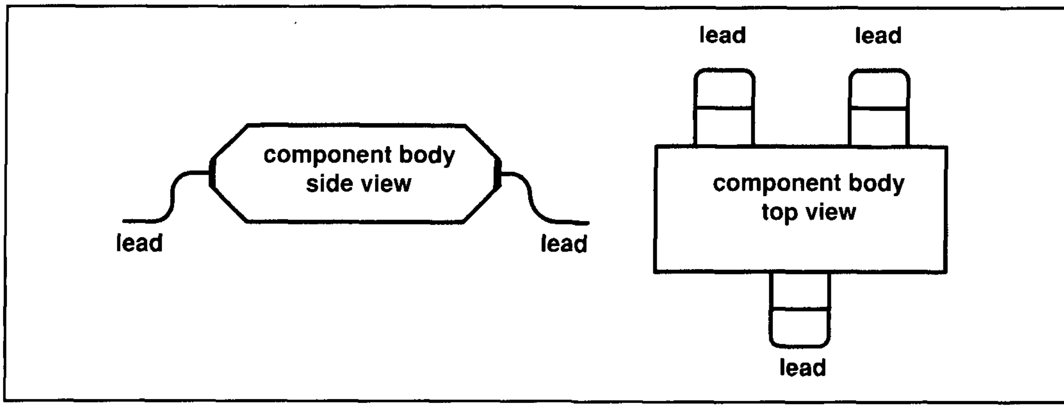

Figure 5. A transistor or diode package.

retained as the third lead provides a method of indicating the orientation. It also means that the same equipment can be used in the component manufacturing process, providing a level of standardization.

For the future, even smaller packages are emerging. One which is emerging now is the SOT-323, which is basically an even smaller version of the SOT-23.

Like resistors and capacitors, the small size of these components means they cannot have their part numbers marked on them. Fortunately, diodes and transistors can be marked more easily than resistors and capacitors. Instead of the full part number, the manufacturers place a two-letter code on the package. This code makes it possible to perform limited checks on the component. Unfortunately, these short codes are not always the same from manufacturer to manufacturer!

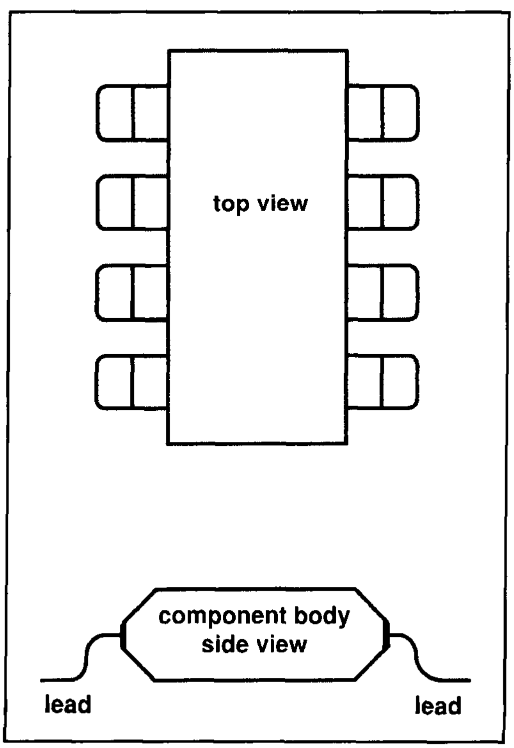

Figure 6. A gull-wing package.

ICs

Integrated circuits have been affected along with all other types of components. There are two major styles of components in widespread use that are characterized by their leads. The first is a gull-wing lead. **Figure 6** shows how the leads come out of the package in a shape similar to that of a gull's wing. Like the SOT-23, the leads and the package are formed so that when the device is placed onto the board, the leads sit on the pads.

There are a number of different packages which adopt the gull-wing style of lead. Most of the standards ICs like logic chips, op amps, and so forth use SO (small outline) packages. These have a pin spacing of 0.05 inches (compared with the DIL packages with 0.1-inch spacing). Some devices are even available in a TSOP (thin small outline package) package. This is similar to the SO package but is thinner, so it takes up even less space on the board.

For the microprocessors and other devices with large numbers of pins, a type of package called a quad flat pack (**Figure 7**) is often used. Instead of having pins on only two sides of the package, the quad flat pack has pins on all four sides. Sometimes as many as 200 or more pins are used and, to accommodate all of these pins, very narrow spacings are used—often only 0.02 inches. Naturally these pins are very fragile and, once bent out of shape, are virtually impossible to straighten to the required tolerances. This means it is very easy to damage them. As the devices are usually very expensive, this provides added incentive to treat them very carefully!

Yet another type of package is the J lead. Like the gull wing, its name describes the leads

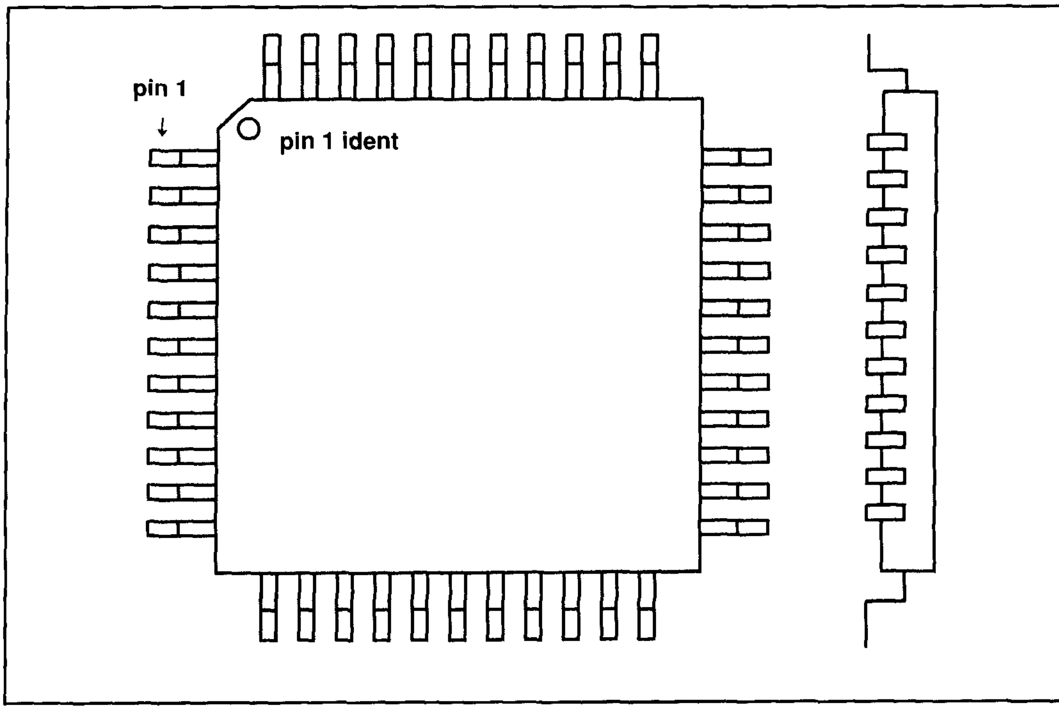

Figure 7. A quad flat pack.

on the package and are shown in **Figure 8**. This style of package is not as widely used as the gull wing, but has the advantage that it takes up less board space as the leads curl back under the main body of the chip. The other advantage is that devices with the J-lead package can be mounted in a socket. This is particularly useful when developing software. If a J-lead PROM is available, it can be socketed and the software changed as new revisions are developed, without the need for desoldering and resoldering, which quickly ruins the board.

New types of packaging are becoming available. The need for this has arisen from the increasing number of devices with very large numbers of pins. The quad flat pack is normally used for these applications. However, its drawbacks have caused further development to be undertaken. The problem with the delicacy of the pins has already been mentioned. The fine pitch of the pins also means the IC needs to be placed very accurately. The pitch also means that there are a vast number of tracks that must be routed in a very small space, which can cause problems for pc board designers. To overcome some of these problems, a new type of package is appearing. Known as ball-grid array (BGA), this package, shown in **Figure 9**, has the connections on its underside. In this way, the space under the chip is used. Also, being an array, the connections can be made larger, allowing for greater tolerances in the manufacturing process. It also allows for greater simplification of track routing.

The connections consist of small balls of solder. When the chip passes through the soldering process, the solder melts, connecting the pins to the board. While many people have fears about the process and wonder whether all the connections will be made properly, tests by a large number of manufacturers show that if the soldering process is working properly, the number of bad joints is very low. As a matter of fact, this package provides better results in the manufacturing process than other types, like the quad flat pack.

Manufacturing methods

To gain the most from surface-mount technology, manufacturers use high degrees of automation. The first stage in the board assembly process is laying solder paste down on the board. The paste has a creamy consistency and is composed of solder and any flux that may be used. It is applied to the correct areas of the board through a special screen that masks those areas not to be soldered.

Once the solder paste has been applied, the boards are passed through to a "pick and place" machine. These machines can be very expensive and can easily cost $1,000,000 or more. Reels of components are loaded onto the machine. For small components, the reels are about the size of those used on reel-to-reel audio tape machines.

The pick and place machine has a moving

Table 1.
Standard outlines for SMD passive components

Type	Size (mm)
0402	1.0 x 0.5
0603	1.6 x 0.8
0805	2.0 x 1.25
1206	3.2 x 1.6
1210	3.2 x 2.5
1812	4.5 x 3.2
2010	5.0 x 2.5
2512	6.3 x 3.1

head that picks components up from the component reels, then places them down on the board with the correct orientation and in the correct place. To operate the machines, programs are required for each board that tell the machine where to place each component. Usually, these programs are generated from the computer-aided design package used to lay out the pc board during its design. In view of the very fine pitches that components like the quad flat pack ICs possess, very high degrees of accuracy are needed. To achieve this, many of these machines have optical alignment facilities.

A great variety of components are available in reels, as shown in **Figure 10**. The obvious candidates are the resistors and capacitors, but diodes, transistors, and integrated circuits are also available in this form. ICs may also be loaded onto the machine in tubes. However, the capacity of these tubes is obviously lower than a reel and they require changing more frequently. Larger ICs are available in other forms of packaging. Again they can picked up and placed down on the board in the correct place.

Once the board has been completed, it is soldered. Nowadays, this is usually done using an infrared reflow machine (**Figure 11**). Here the board is placed on a conveyor, which passes under infrared heaters. These heat the board in stages to a point where the solder paste melts and the components are soldered.

Careful control of the machine is required as each board responds differently to the process. The amount of heat transferred, and hence the temperature of the joints, depends upon a number of variables. These include the materials on the board, the shape of the board, and the components, as well as the wavelength of the infrared radiation. In some areas, the components restrict the amount of radiation that reaches a joint: this is known as the shadow effect. Good board layout, along with the correct control of the temperature profile within the machine, is essential in minimizing this effect. To help overcome any problems, the board is usually preheated by circulating warm air in the machine prior to being exposed to the infrared radiation.

Although infrared soldering is the most common method used these days, there are others as well. Wave soldering machines were widely used at one time. Here the board is passed over a "wave of solder." This method of soldering

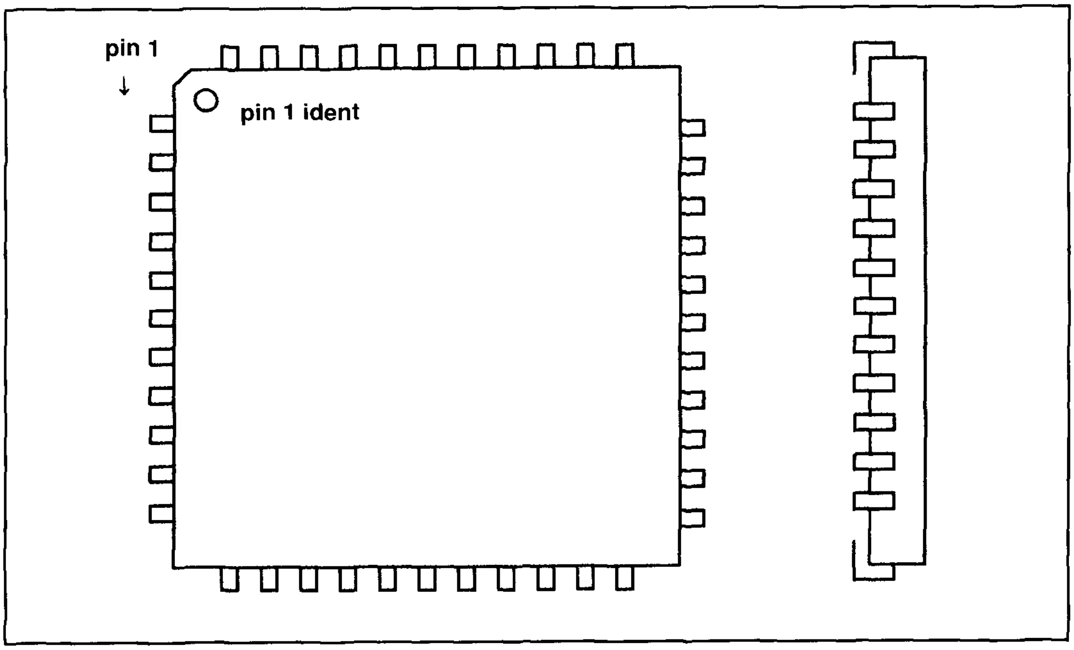

Figure 8. A J-lead package.

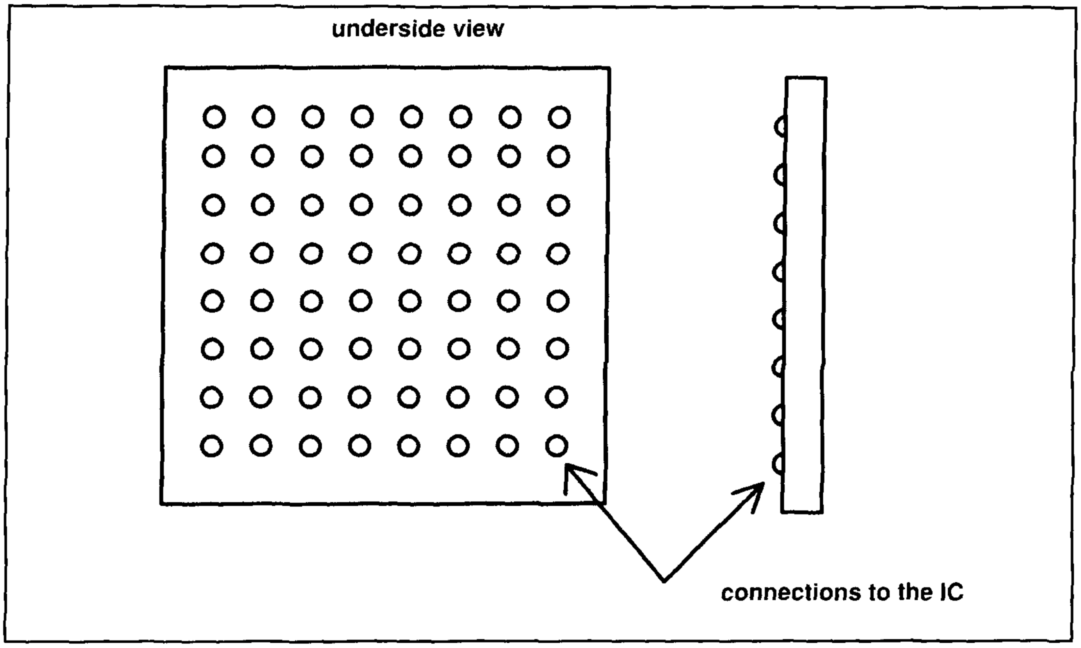

Figure 9. The ball-grid array.

can be used for conventional components as well as for surface-mount varieties, making it ideal for boards where a combination of the two types are used.

When using this method, no solder paste is applied. The components are loaded onto the board, with the surface-mount types fixed to the board with a small amount of glue that is applied to the board as part of the pick and place process. This glue keeps them in place during soldering. Usually, a special head on the pick and place machine is used to place small amounts of glue in the required places before the components are placed. Some types of glue retain their adhesion, making components difficult to remove for rework. Other types degrade after heating; i.e., once the board has been soldered.

Once the components are loaded, the board is passed through the wave soldering machine, as

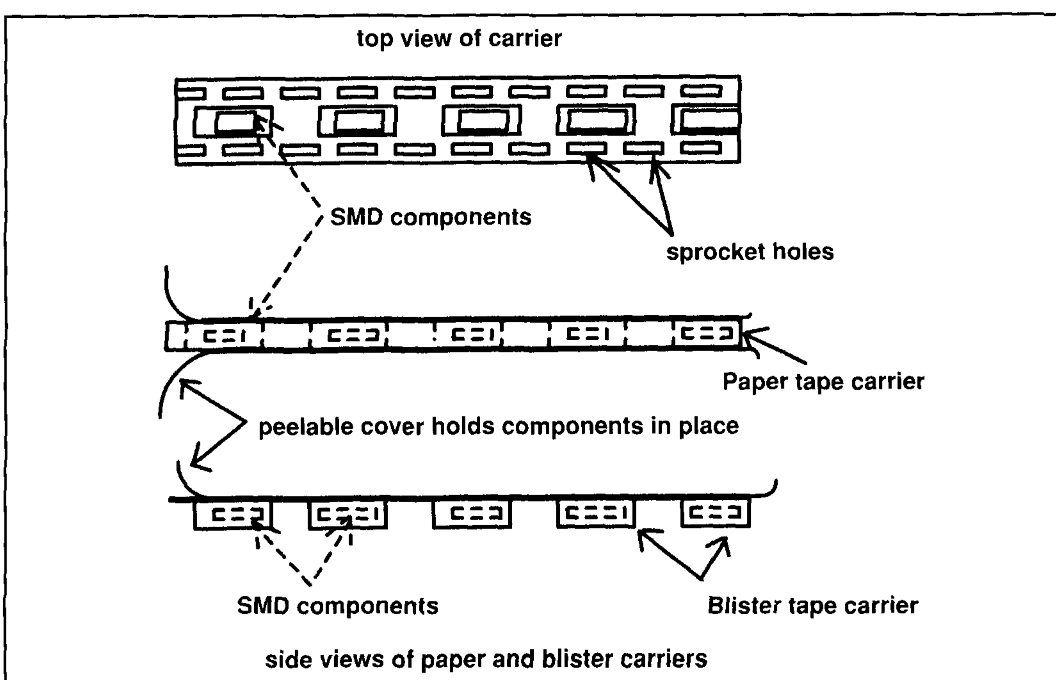

Figure 10. Component tape.

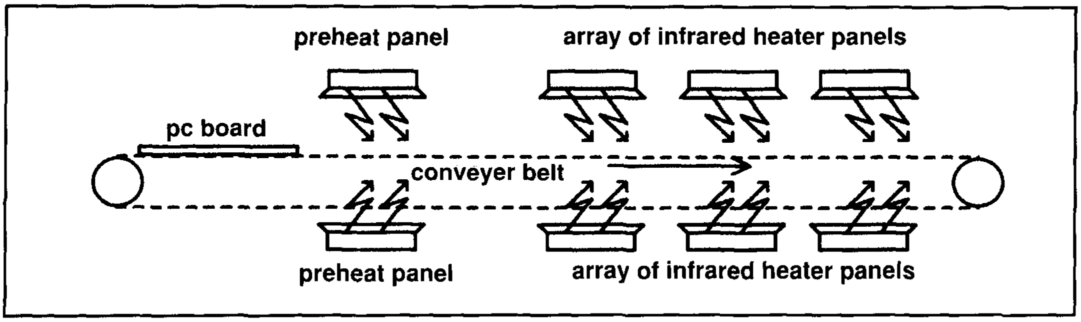

Figure 11. An infrared reflow machine.

shown in **Figure 12**. The solder is forced up to the base of the board, soldering the components in place. The height and shape of the wave is important; it must be shaped to prevent shadowing effects while not reaching areas of the board where it should remain.

In view of the requirement to hold the components in place, and the fine pitch of components being used today, wave soldering is being used far less. It was also necessary to place conventional and surface-mount devices (SMDs) on opposite sides of the board as shown. Today it is very common to place surface-mount components on both sides of the board.

Problems in manufacture

While SMT simplifies manufacture, there are a number of areas where care must be taken. It is necessary to ensure that the soldering process is tightly controlled. Too much solder can cause the occasional short circuit on the board; too little means that open circuit connections may appear. These can take a considerable time to locate if specialized inspection equipment is not used. As the soldering process is crucial to the whole operation, it is necessary to feed information from test and inspection stages back to earlier stages in manufacture to ensure that the process is controlled and optimized. After all, if the soldering process is poor, it is very difficult to rework all the joints on a board.

Another point to note is that the "via" holes which pass through the board must not be placed on a component pad. If they are, solder will flow into the hole and away from the joint, leaving the component unsoldered.

One interesting problem that was particularly prevalent in the early years of surface mount use was known as tombstoning (**Figure 13**). Caused by misalignment or poor board layout, an uneven surface tension on the smaller components, like resistors or capacitors, caused them to stand on end. For obvious reasons, this problem gained its name. Now with a greater knowledge about component pad layout and improved soldering techniques, tombstoning is far less common.

One problem that still occurs is that of boards warping. Many products still use large boards with multiple layers. These boards can experience a problem with overall flatness which is made worse when the boards are heated in the soldering process. It can be a particular problem when sections of a board require an earth plane and others do not. For example, this can

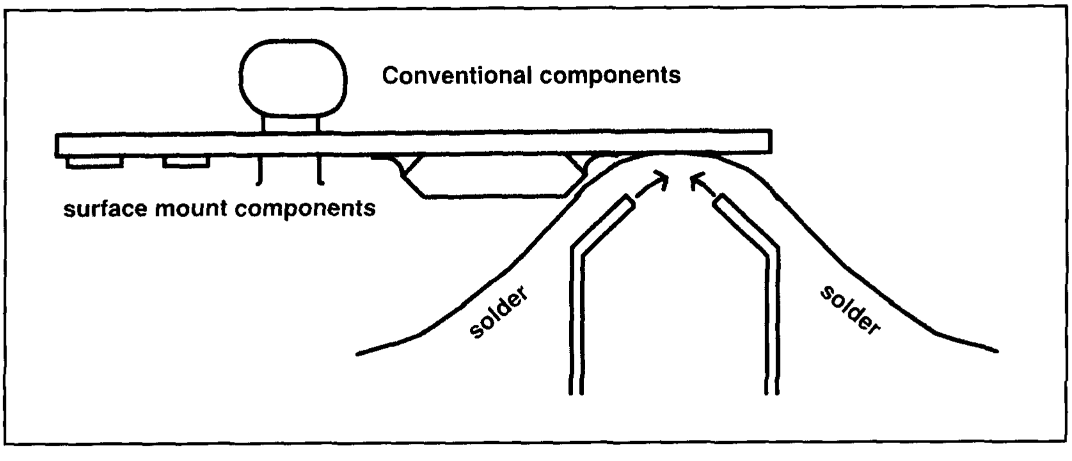

Figure 12. The principle of wave soldering.

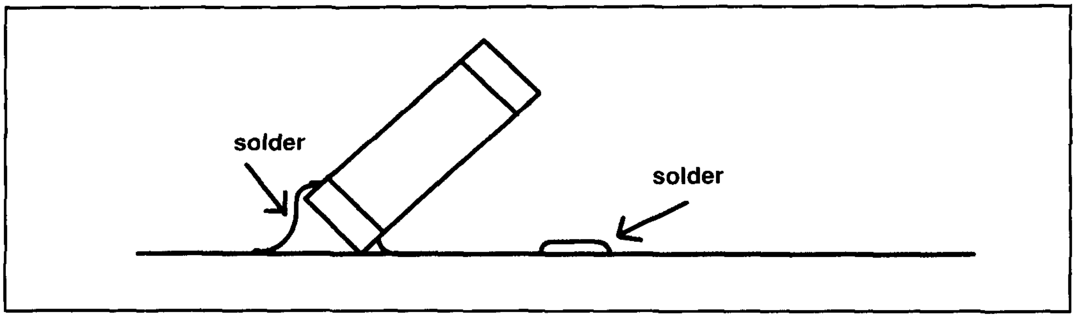

Figure 13. An example of tomb-stoning.

occur where a board has an RF and a digital area. The problem can be lessened by placing earth planes in the center of the board and trying to keep the build of the pc board itself as even as possible. Carefully controlled manufacture of the board is also required; without it, the bending on the board can cause some components, particularly ceramic capacitors, to crack. Components which fail in this way can be very difficult to trace—especially where small-value capacitors are used, because the values are almost impossible to measure in a circuit.

Naturally, there are many problems which can occur in the manufacturing process. The key to overcoming them is to closely monitor the process, and feed back information as quickly as possible to alter or correct the relevant area in the process. A fast response is crucial, particularly in areas producing large quantities of boards, otherwise large quantities of board requiring rework will be made.

AOI

To ensure that the quality of boards leaving the pc board assembly area is suitably high to pass on to the next stage of manufacture, it is often necessary to perform checks. Some years ago, an inspection check called In-Circuit Test (ICT) was widely used. This type of test used a bed of nails to connect each node on the board. The value of each component was checked to ensure that it was fitted correctly and that the value was correct. Nowadays, component density is so high that access to the components is not easy and usually ICT is not viable. Another method of board checking, called Automatic Optical Inspection (AOI), is being used more widely. Here the board is optically monitored to check for dry joints and many other problems.

SMDs and the home constructor

Although manufacturers use large and expensive machines, the radio amateur can use surface-mount components provided a little care is taken. The major problems occur when soldering the components in place. As the components do not have leads that prevent the packages themselves from becoming too hot, a little caution must be used. Ideally, low-melting-point solder should be used and the iron temperature adjusted accordingly. Heat should only be applied for a short time. Capacitors are the most vulnerable components despite improvements that have been made. In the early days of surface mount components, capacitor end caps were particularly vulnerable. If the heat was applied for too long, the silver was "leached out" of the silver palladium contact, leaving a nonconducting area and rendering the capacitor useless. Now, improvements have been made and, with a little care and practice, very few problems should be encountered.

The other point to note is that components like resistors and capacitors are not usually marked. They should only be removed from their packages when they are actually to be placed onto the board and soldered in position. Once a component is left on the work surface, there is nothing to distinguish it from any others, so a little care and order is required!

Advantages to the radio amateur

The introduction of surface-mount components may seem to be another stage in removing the radio amateur from modifying or maintaining his equipment. Equipment is undoubtedly more complicated these days and not as easy to service without the correct tools. However, there are number of advantages—particularly for the radio amateur. The main one is the improvement in performance that can be gained with RF circuits. As the components do not have leads, stray inductance from leads is almost eliminated. In addition, the circuits are much smaller, reducing stray inductance capacitance. The overall result is that circuits come far closer to the ideal, and problems with oscillation are fewer. The response of circuits is also much flatter, and they will often operate satisfactorily at higher frequencies.

Summary

While many people may believe that surface-mount components may be a retrograde step for the home enthusiast, they are firmly established in industry. Greater numbers of surface mount components are used than conventional leaded types.

Radio amateurs have a tradition of keeping up with technology and overcoming the problems. This should also apply to the surface-mount revolution. These components are here to stay and offer several advantages. Accordingly, it is worth experimenting with them, learning to live with this new technology, and making the most of it. ■

PRODUCT INFORMATION

Alinco's DJ-X10T

Alinco USA has released the DJ-X10T, a multimode 1,200-channel receiver capable of tuning from 100 kHz to 2 GHz (cellular blocked). The new receiver offers sensitivity, multimode operational versatility, three-line alphanumeric memory channel labeling, Alinco's Channel Scope™ spectrum activity display, two VFOs, selectable user configurations (beginner and expert), and more.

The 1,200 memory channels can be arranged in 30 banks of 40 channels each. In addition, the radio has two VFOs and the ability to automatically transfer frequencies from VFO to memory. Each memory can store up to three lines of text describing the channel contents.

The multi-function Channel Scope display can show up to 40 channels of activity across a wide spectrum. The user can configure the DJ-X10T in "New User" or "Expert" operating mode, and an internal "Help" feature describes radio functions and features.

The DJ-X10T has provisions for external power, external speaker, or earphone. The antenna is a standard BNC connection, allowing the use of external antenna systems. The receiver is PC programmable (RS-232); a cable and software are needed.

The unit operates on the standard rechargeable NiCd battery pack (EBP-37, 700 mAh 4.8 V), optional dry-cell battery pack, or optional external DC power and NiCd battery packs. Additional DJ-X10 features include Auto Timer On/Off, clock, cable cloning, backlit display and keys, battery save, attenuator, display contrast control, low battery alarm, and selectable lamp modes.

For more information, contact your local Alinco dealer.

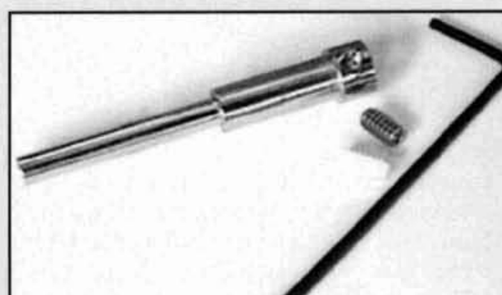

Vibroplex "Bug Tamer"

Vibroplex® has introduced the "Bug Tamer." The "Tamer" extends the pendulum and makes a dramatic reduction in the Bug's speed range with the use of your existing speed weight(s). Your Bug's speed can be adjusted down to 10 to 12 wpm, possibly slower.

Bug Tamers include the extension arm, nylon and stainless steel set screws, and Allen wrench to attach it to the pendulum of your Bug. Two versions are available: chrome version ($24.95) and brass version ($20.00). To order call (334) 478-8873 or Fax (334) 476-0465.

M.E. Gruchalla, P.E.
Member: Editorial Review Board
4816 Palo Duro, NE
Albuquerque, New Mexico 87110

COMPLEX IMPEDANCE MEASUREMENTS

Using only scalar voltage measurements

Very often in RF work, it's necessary to accurately measure the complex impedance of a network or device. For example, if the complex impedance of an antenna can be accurately measured at the desired frequency, an accurate matching network may be constructed to match the antenna to a source—minimizing time-consuming trial and error.

One classic method of measuring complex impedance is via an impedance bridge. This is a deceptively simple device, but those who have actually attempted to build a *precision* impedance bridge know it is not at all simple. Stray coupling results in unbalanced coupling to the elements of the bridge arms, which generally results in very significant errors. Another approach, which I discuss in this paper, uses simple scalar voltage measurements (basic diode RF detectors) to measure the complex impedance of almost any network. I derive this approach in detail (perhaps agonizing for some) so you can see why and how it works. There's a bit of math here, included for those purists who really want to see the "nitty gritty" of the derivation. I hope this step-by-step process will help you see more clearly why this technique works.

The "Three-Meter Method"

This complex impedance measurement method is actually quite an old technique. One of the early discussions of this approach was reported by D. Strandlund, W8CGD, in the June 1965 issue of *QST* as the "Three-Meter Method" of measurement (meaning three measurements, not a 3-meter wavelength measurement).[1] Strandlund presented a graphical method of determining the unknown impedance.

This is a reasonable method, but a bit cumbersome. A totally analytic method is much more convenient and several authors have offered useful variations. However, I have been unable to find a really comprehensive derivation. Therefore, I provide a very detailed derivation of the analytic approach for determining the complex impedance of a network by making only scalar RF voltage measurements.

A detailed derivation

The scalar measurement described here eliminates the need for precision matching of variable bridge elements and the corresponding problems associated with parasitic coupling. Also, in an impedance bridge, the variable elements must be in some way calibrated to provide a readout of their values at balance. The scalar-measurement method requires only a fixed resistor and a fixed capacitor or inductor (pure reactance). The precise value of either this resistance or reactance, but not both, must be known.

The disadvantage of this measurement approach is that several RF voltages must be measured accurately. However, in general, it's a much easier task to accurately measure RF voltages than to construct a precision-balanced RF bridge that's right on the mark. Accuracy is improved if the resistance and reactance are

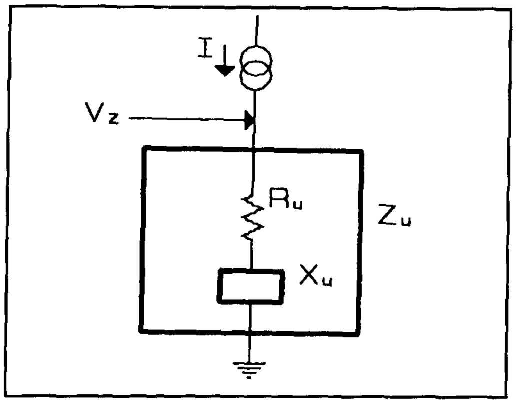

Figure 1. Basic current-source drive of unknown impedance.

near the resistance and reactance of the unknown network, but this method will work quite well when the values aren't even close. Finally, the very simple topology of this approach and the need to only measure several scalar RF voltages makes this method quite accurate because the effects of parasitic coupling are easily minimized.

A complex impedance may be represented as either a resistance in parallel with a reactance or as a resistance in series with a reactance. If you are given either of these configurations, you can easily compute the other equivalent network. For example, an antenna impedance is quite often expressed as a resistance in series with a reactance. This, perhaps, is because that configuration is somewhat logical; i.e., the resistance of the antenna conductors and feed line are in series with the capacitive coupling of the antenna to free space. However, an equivalent parallel network consisting of a resistance in parallel with a reactance may be computed.

For this derivation, I use a series network to represent the unknown complex impedance (**Figure 1**). The unknown resistance is R_u and the unknown reactance is X_u. This reactance may be either a capacitance or an inductance. A capacitive reactance will be negative and an inductive reactance positive. The unknown resistance may actually also be either positive or negative, but only a positive value has physical meaning in a passive device, such as an antenna or a matching network. I have also shown this network excited with a current source. Using a current source simplifies the arithmetic somewhat and makes the analysis a little easier to follow. In the end, this current source won't be part of the solution.

Finding the unknowns

There are two unknowns that must be found: R_u and X_u. Therefore, we must find at least two linearly independent equations to solve for these unknowns.

The voltage developed across the unknown impedance in **Figure 1** is called V_z to designate it as the voltage across the impedance of interest. By inspecting **Figure 1**, we can simply write the equation for the complex voltage V_Z.

$$V_Z = I \bullet R_u + j \bullet I - X_u \quad (1)$$

V_z in **Equation 1** isn't a scalar voltage because it has both a real and an imaginary part. What we need for this analysis is the magnitude of all the measured voltages. We can compute the magnitude of V_z by taking the square root of the sum of the squares of the real part and the imaginary part. If we simply do not take the square root of that sum, we will obtain the square of the magnitude. This square term will be much more useful in this derivation because, by using this term, we won't have to carry through a bunch of square roots.

$$|V_Z|^2 = I^2 \bullet R_u^2 + I^2 - X_u^2 \quad (2)$$

Note that the magnitude of V_z doesn't depend on the sign of either R_u or X_u. To continue, **Equation 2** gives us one of the equations we need. Now we need a second. Suppose we add a known resistance and a known reactance in series with the unknown network as shown in **Figure 2**. We don't need both of these elements if we wish only to compute the magnitude of the unknown resistance and reactance; but, since we want both the magnitude and sign of the unknown reactance (and resistance), we need these two added elements. This resistance is designated R_r and the reactance as X_r to denote these as a reference resistance and a reference reactance, respectively. The reactive element may be either a capacitor or an inductor.

We can typically expect the unknown resistance to be positive (unless we're looking at a load with some active element in it), but the reactance may be either positive (inductance) or negative (capacitance). For example, if the load we're measuring is an antenna at a frequency where the antenna is shorter than 1/4 wavelength, the reactive component of the antenna impedance will most likely be capacitive. But if the antenna is somewhat longer than 1/4 wavelength, the reactive component will likely be inductive. Therefore, it's rather important to actually obtain the sign of the reactive component in most measurements.

Because we're driving with a current source, adding these elements to the circuit doesn't affect voltage V_z developed across the unknown impedance. Therefore **Equations 1** and **2** are still valid for **Figure 2**. The voltage developed across the series combination of the unknown impedance Z_u and the reference X_r is designated V_{XZ} to indicate it is the voltage developed across reference reactance in series with an unknown impedance. We may now compute the voltage V_{XZ} by inspecting **Figure 2**.

$$V_{XZ} = I \cdot R_u + j \cdot I \cdot (X_r + X_u) \tag{3}$$

This, too, is a vector voltage. The magnitude squared of V_{XZ} is then,

$$|V_{XZ}|^2 = (I \cdot R_u)^2 + [I \cdot (X_r + X_u)]^2 \tag{4}$$

$$|V_{XZ}|^2 = I^2 \cdot R_u^2 + I^2 \cdot X_r^2 + 2 \cdot I^2 \cdot X_r \cdot X_u + I^2 \cdot X_u^2 \tag{5}$$

We can also write the equation for V_s by looking at **Figure 2**.

$$V_S = I \cdot R_r + j \cdot I \cdot X_r + I \cdot R_u + j \cdot I \cdot X_u$$

$$V_S = I \cdot (R_r + R_u) + j \cdot I \cdot (X_u + X_r) \tag{6}$$

Computing the magnitude squared of V_s,

$$|V_S|^2 = [I \cdot (R_r + R_u)]^2 + [I \cdot (X_u + X_r)]^2 \tag{7}$$

$$|V_S|^2 = I^2 \cdot R_r^2 + 2 \cdot I^2 \cdot R_r \cdot R_u + I^2 \cdot R_u^2 + [I \cdot (X_u + X_r)]^2 \tag{8}$$

We see that there is a term in common between **Equation 4** and **Equation 8**. Solving **Equation 4** for $[I \cdot (X_r + X_u)]^2$,

$$[I \cdot (X_r + X_u)]^2 = |V_{XZ}|^2 - I^2 \cdot R_u^2 \tag{9}$$

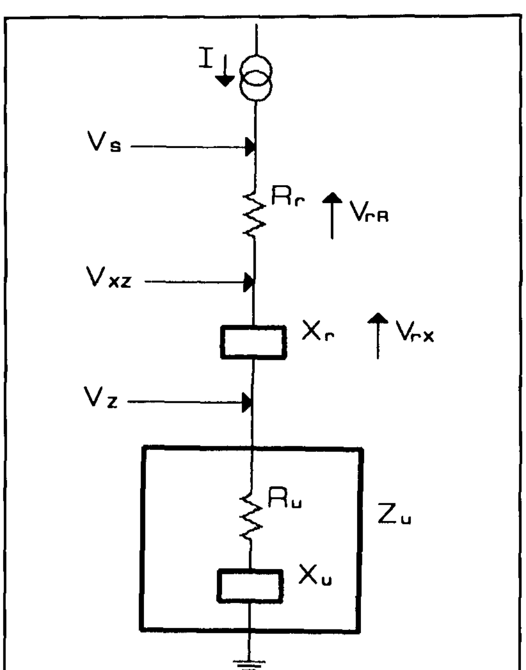

Figure 2. Unknown impedance with series reference resistance and reactance.

Substituting **Equation 9** into **Equation 8** and simplifying,

$$|V_S|^2 = I^2 \cdot R_r^2 + 2 \cdot I^2 \cdot R_r \cdot R_u + I^2 \cdot R_u^2 + |V_{XZ}|^2 - I^2 \cdot R_u^2$$

$$|V_S|^2 = I^2 \cdot R_r^2 + 2 \cdot I^2 \cdot R_r \cdot R_u + |V_{XZ}|^2 \tag{10}$$

We can now solve **Equation 10** for the unknown resistance R_u in terms of the voltage magnitudes (actually the magnitudes squared), the excitation current and the reference resistance R_r. Solving for R_u,

$$2 \cdot I^2 \cdot R_r \cdot R_u = |V_S|^2 - |V_{XZ}|^2 - I^2 \cdot R_r^2$$

$$R_u = \frac{|V_S|^2 - |V_{XZ}|^2 - I^2 \cdot R_r^2}{2 \cdot I^2 \cdot R_r} \tag{11}$$

We can make a substitution and apply a simple mathematical manipulation to simplify **Equation 11** further. First, we note that the magnitude of the term $I \cdot R_r$ is simply the magnitude of the voltage developed across the reference resistor, $|V_{rR}|$. Recall that we are measuring only voltage magnitudes so all our computations must be in terms of only these voltage magnitudes.

$$|V_{rR}| = |I \cdot R_r| \tag{12}$$

Substituting **Equation 12** into **Equation 10**,

$$R_u = \frac{|V_S|^2 - |V_{XZ}|^2 - |V_{rR}|^2}{2 \cdot I^2 \cdot R_r} \tag{13}$$

Multiply the denominator of **Equation 13** by the term R_r/R_r. Because this term is exactly equal to 1, we may make this multiplication without altering the equation. Making this mathematical manipulation and again substituting $|V_{rR}|$ as above and simplifying,

$$R_u = \frac{|V_S|^2 - |V_{XZ}|^2 - |V_{rR}|^2}{2 \cdot I^2 \cdot R_r \cdot \frac{R_r}{R_r}} = \left(\frac{|V_S|^2 - |V_{XZ}|^2 - |V_{rR}|^2}{2 \cdot I^2 \cdot R_r}\right) \cdot R_r$$

$$R_u = \left(\frac{|V_S|^2 - |V_{XZ}|^2 - |V_{rR}|^2}{2 \cdot |V_{rR}|^2}\right) \cdot R_r \tag{14}$$

Equation 14 gives the value of the resistive component of the unknown impedance in terms of just the scalar circuit voltages and the reference resistance. Both of the reactive terms have vanished from this expression. The only circuit parameter we must know in order to compute the unknown resistance is the value and sign of the reference resistor over frequency. In general, we'll always use a positive resistance so the sign is no problem. The actual value isn't too important, but its value must be known and must be constant with frequency (or at least be known accurately at each test frequency). But it's extremely important that the reference resistance have very small equivalent series inductance, very small shunt capacitance, and very low parasitic capacitance to ground or other circuit elements.

Because the term in brackets in **Equation 14** is a dimensionless ratio of voltages squared, it doesn't matter whether we use rms voltages or peak voltages as long as we use the same type of measurement for all the measurements. The peak voltage is simply the rms voltage multiplied by the $\sqrt{2}$. If each of the voltages is multiplied by a constant, such as the $\sqrt{2}$, that constant will simply divide out in each equation. Therefore, either an rms voltage detector or a peak detector may be used in this technique.

Finding the unknown resistance is only half the problem. We must now find the unknown reactance X_u of the unknown impedance. Looking back at **Equation 2** and **Equation 5**, we can see there is again a term in common. If we solve **Equation 2** for the term $I^2 \bullet R_u^2$, we can substitute the result into **Equation 5** and construct a new equation without a resistance term. Solving **Equation 2** for $I^2 \bullet R_u^2$,

$$I^2 \bullet R_u^2 = |V_Z|^2 - I^2 \bullet X_u^2 \qquad (15)$$

Substituting this into **Equation 5** and simplifying,

$$|V_{XZ}|^2 = |V_Z|^2 - I^2 \bullet X_u^2 + I^2 \bullet X_r^2 + 2 \bullet I^2 \bullet X_r \bullet X_u + I^2 \bullet X_u^2$$

$$|V_{XZ}|^2 = |V_Z|^2 + I^2 \bullet X_r^2 + 2 \bullet I^2 \bullet X_r \bullet X_u \qquad (16)$$

We can now solve **Equation 16** for the unknown reactance X_u in terms of the voltage magnitudes, the excitation current, and the reference reactance X_r. Solving,

$$2 \bullet I^2 \bullet X_r \bullet X_u = |V_{XZ}|^2 - |V_Z|^2 - I^2 \bullet X_r^2$$

$$X_u = \frac{|V_{XZ}|^2 - |V_Z|^2 - I^2 \bullet X_r^2}{2 \bullet I^2 \bullet X_r} \qquad (17)$$

This is a perfectly usable equation, but we must know the current in order to use it. We can make a substitution and apply the same type of mathematical manipulation as we did above to simplify this equation further. The voltage across the reference reactance, V_{rX} is simply,

$$V_{rX} = j \bullet I \bullet X_r$$

And the magnitude squared of the reference-reactance voltage, V_{rX}^2, is then,

$$|V_{rX}|^2 = I^2 \bullet X_r^2 \qquad (18)$$

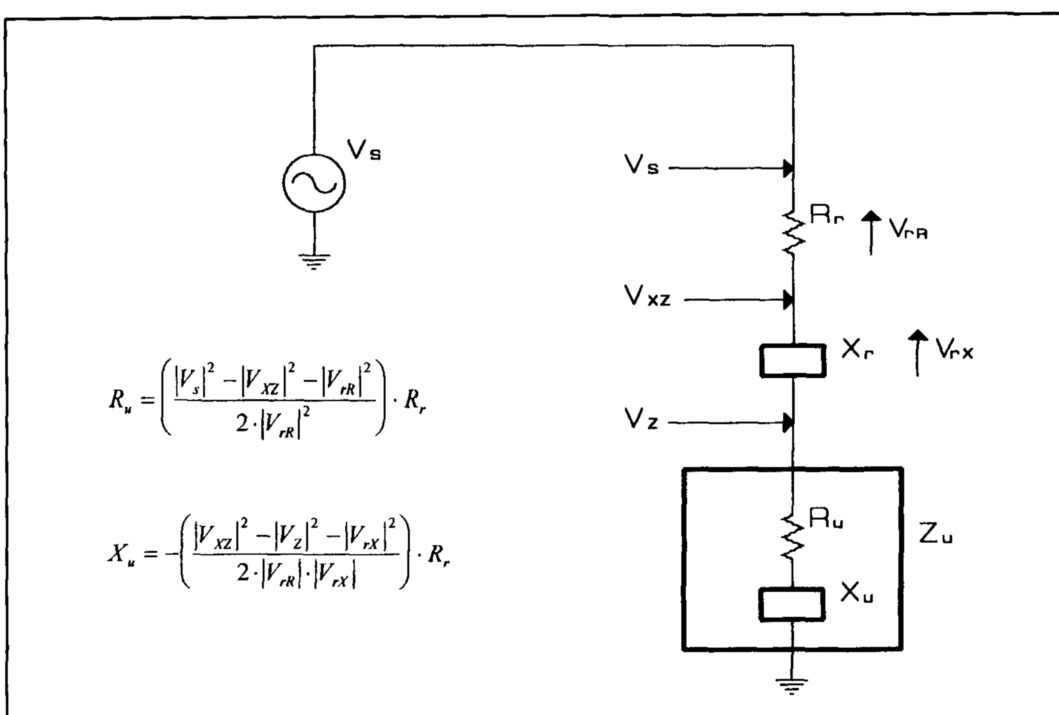

Figure 3. Complete measurement circuit.

Substituting this into **Equation 17**,

$$X_u = \frac{|V_{XZ}|^2 - |V_Z|^2 - |V_{rX}|^2}{2 \cdot I^2 \cdot X_r} \quad \textbf{(19)}$$

Now, multiply the denominator of **Equation 19** by X_r/X_r. As above, this term is exactly unity so we can do this multiplication without altering the equation. Making this mathematical manipulation, substituting the results of **Equation 18**, and simplifying,

$$X_u = \frac{|V_{XZ}|^2 - |V_Z|^2 - |V_{rX}|^2}{\dfrac{2 \cdot I^2 \cdot X_r}{X_r}} =$$

$$\frac{|V_{XZ}|^2 - |V_Z|^2 - |V_{rX}|^2}{\dfrac{2 \cdot I^2 \cdot X_r^2}{X_r}} =$$

$$\left(\frac{|V_{XZ}|^2 - |V_Z|^2 - |V_{rX}|^2}{2 \cdot V_{rX}^2}\right) \cdot X_r$$

$$X_u = \left(\frac{|V_{XZ}|^2 - |V_Z|^2 - |V_{rX}|^2}{2 \cdot |V_{XZ}|^2}\right) \cdot X_r \quad \textbf{(20)}$$

Equation 20 now gives us the value of the reactive part of the unknown impedance in terms of the squares of the magnitudes of the several circuit voltages and the known reference reactance. The resistive terms have totally vanished from this equation, just as the reactive terms vanished in the expression for the unknown resistance given by **Equation 14** above.

In actual practice, there's a somewhat annoying problem with using **Equation 20** to accurately compute the unknown reactance. In order to use **Equation 20**, the reference reactance must be precisely known at the operating frequency. This isn't an easy task. And, one would expect that the reference-reactance value wouldn't be entirely constant with frequency, further complicating calculations. But, as strange as it may seem, there's a way to totally eliminate the value of the reference reactance from the computations. We still need to have a reference reactance, but we don't need to know its actual value. We only need to know if it's capacitive or inductive.

Although it's difficult to find a reactive component that exhibits a constant value over a wide frequency range, we can find resistors that have very good frequency characteristics. So, if we can measure the several network voltages accurately, we can at least compute the resistive component of the unknown impedance accurately using **Equation 14** and the accurately known value of the reference resistance. Now, if we know the precise value of the reference resistance, and if we can accurately measure the voltage magnitude $|V_{rR}|$ across the reference resistance, we can accurately compute the magnitude of the current flowing through the entire series circuit. This current is simply,

$$|I| = \left|\frac{V_{rR}}{R_r}\right| \quad \textbf{(21)}$$

The current given by **Equation 21** is a magnitude because we measure only the magnitude of the resistor voltage. Looking back at **Equation 18**, we see that the magnitude of the voltage across the reference reactance is simply the product of the reference reactance and the current. Because we can accurately measure the network voltages, and because we know the reference resistance accurately, we know the current. Therefore, we can actually compute the value of the reference reactance by solving **Equation 18** for X_r.

$$|V_{rX}|^2 = I^2 \cdot X_r^2 \quad \textbf{[Equation (18)]}$$

$$|V_{rX}| = |I| \cdot |X_r| \quad \text{(note that these are all magnitudes)}$$

$$|X_r| = \frac{|V_{rX}|}{|I|} \quad \textbf{(22)}$$

Substituting **Equation 21** into **Equation 22**,

$$|X_r| = \frac{|V_{rX}|}{\dfrac{|V_{rR}|}{R_r}}$$

$$|X_r| = \frac{|V_{rX}|}{|V_{rR}|} \cdot R_r \quad \textbf{(23)}$$

Equation 23 now gives $|X_r|$ in terms of only the accurately known reference resistance and the accurately measurable voltages across the reference resistance and the reference reactance. If we look at **Equation 23** and mentally divide both sides of the equation by R_r, we see that the ratio of the reference reactance to the reference resistance is equal to the ratio of the voltage across the reference reactance to the voltage across the reference resistance. That should be obvious as these two components are driven by the same current in the series circuit. I could have simply stated this and saved a few lines of text, but hopefully the somewhat roundabout path I've used here actually shows how **Equation 23** is derived.

We still need to take care of one more detail: the sign of the reference reactance. If the reference reactance is a capacitor, then the reactance is negative. So, if we use a capacitive reactance as the reference reactance, we may rewrite **Equation 23** in terms of the actual reactance including both its magnitude and sign.

$$X_r = \frac{|V_{rX}|}{|V_{rR}|} \cdot R_r \qquad \text{for } X_r \text{ capacitive} \qquad \textbf{(24)}$$

We can now substitute **Equation 24** into **Equation 20**.

$$X_u = \left(\frac{|V_{XZ}|^2 - |V_Z|^2 - |V_{rX}|^2}{2 \cdot |V_{rX}|^2} \right) \cdot X_r =$$

$$\left(\frac{|V_{XZ}|^2 - |V_Z|^2 - |V_{rX}|^2}{2 \cdot |V_{rX}|^2} \right) \cdot$$

$$\left(- \frac{|V_{rX}|}{|V_{rR}|} \cdot R_r \right)$$

$$X_x = - \left(\frac{|V_{XZ}|^2 - |V_Z|^2 - |V_{rX}|^2}{2 \cdot |V_{rR}| \cdot |V_{rX}|} \right) \cdot R_r \qquad \textbf{(25)}$$

Equation 25 now gives the unknown reactance in terms of only the measured voltages, which we assume we can measure accurately, and the value of the reference resistance, which we assume is well-behaved and accurately known over frequency.

The reference reactance has only two critical requirements. First, it must be a low-loss element. It must have an equivalent series resistance that's very small compared to the reactive component of the reference reactance. In other words, it must be a "high-Q" component. The second requirement of the reference reactance is that we must definitely know whether it is inductive or capacitive. But we don't have to know the value accurately, or even at all, just whether it is inductive or capacitive.

Specifically, if we choose to use a capacitor as the reference reactance, it's not important if that capacitor has some series inductance as long as the total reactance is always capacitive at all test frequencies. However, we would like the value of the reference reactance to be somewhere near the value of the unknown reactance because that will result in the best accuracy in the computations.

Equations 14 and **25** now allow us to compute the resistive and reactive parts of the unknown impedance knowing only the value of the reference resistance and accurately measuring the five network voltages. In **Figure 2**, the voltage V_s is simply the voltage developed across the entire network consisting of the

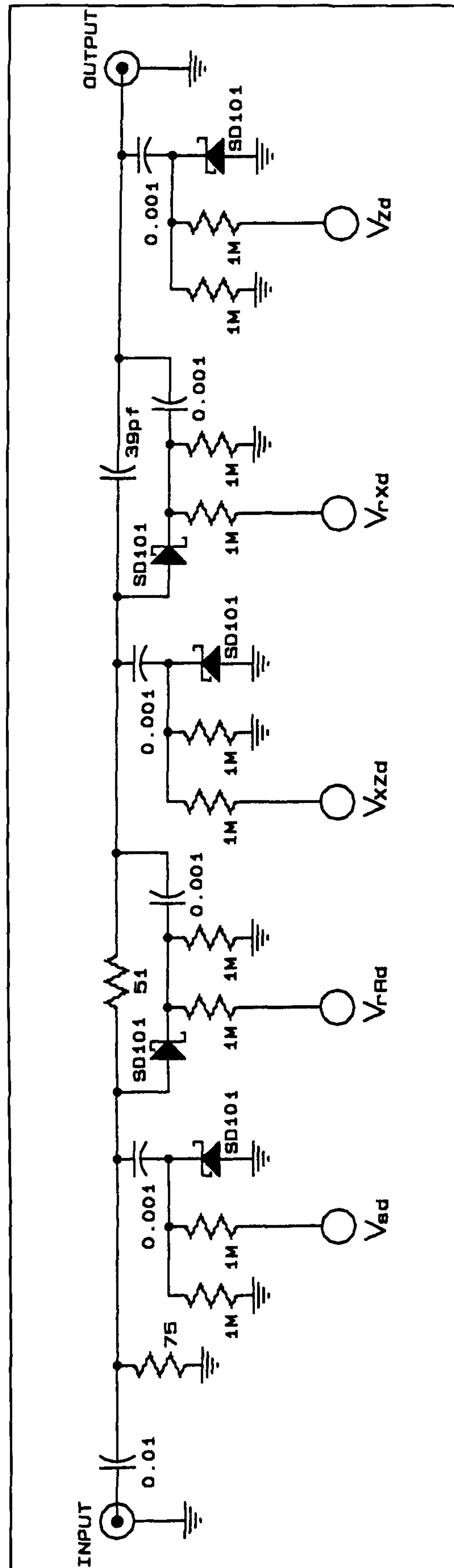

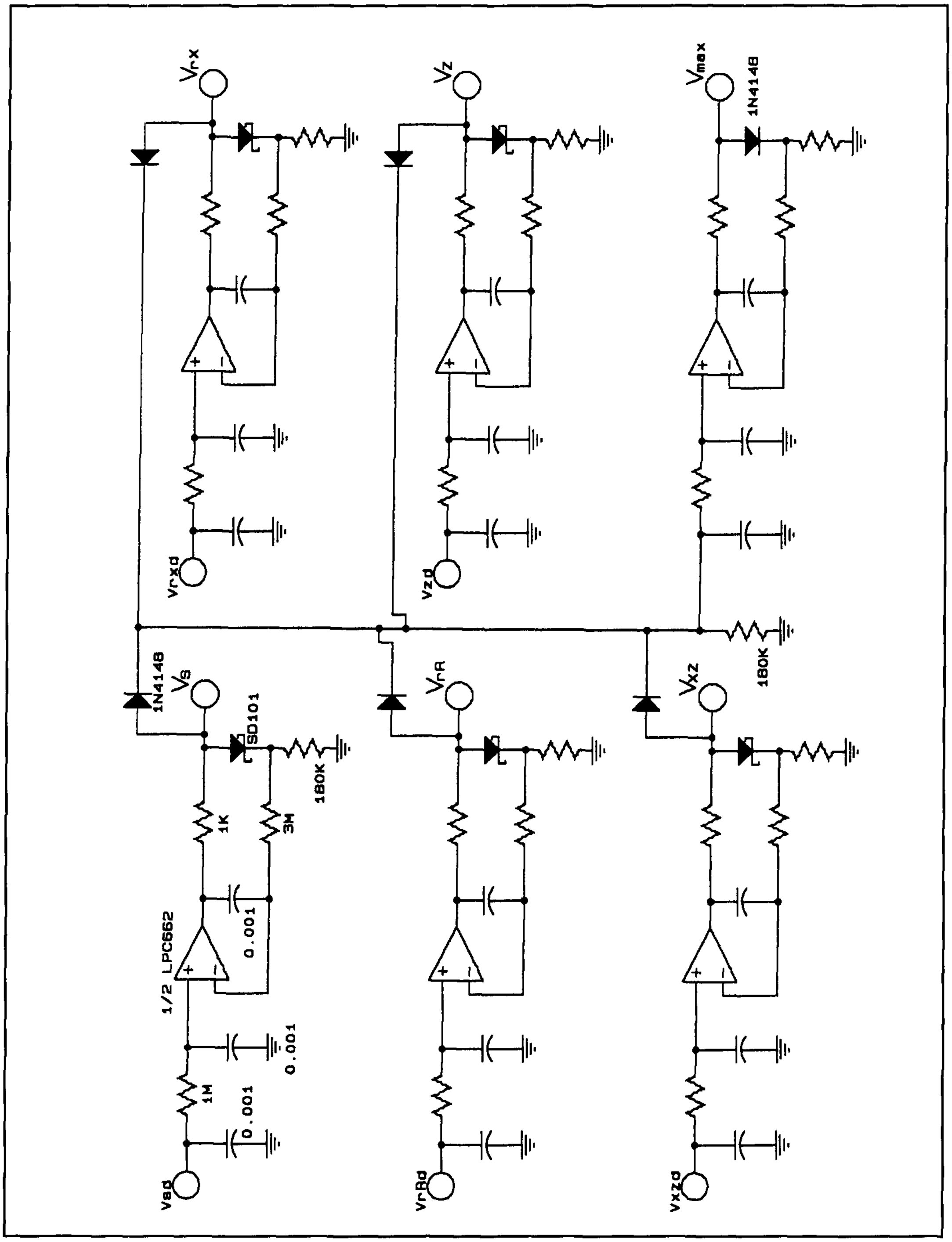

Figure 4. (A) Complex impedance measurement, detector. (B) Complex impedance measurement, analog.

unknown impedance, the reference resistance, and reference reactance. And, since the actual network current doesn't appear in either of the equations for the unknown impedance element values, we no longer need any reference to the network current. We may then draw a final schematic for the entire measurement circuit in terms of a driving voltage source, the reference resistance and reference reactance, and the unknown impedance. This is shown in **Figure 3**.

Begging the question

This now begs the question of why W8CGD termed this the "Three-Meter Method," since we actually must measure five voltages. Suppose we accurately know the reference resistance and reactance used in the network. Then, to compute the resistive and reactive components of the unknown impedance, we would need only measure the voltage across the unknown impedance, the voltage across the series combination of the unknown impedance, plus the known reference reactance and the voltage across the entire network. Only three measurements would be needed. W8CGD used these three voltages in a graphical technique to find the unknown values. So it is truly a "three-meter method."

If we wish to solve the problem totally analytically, that is without using graphs, we need to know the current accurately. That requires another measurement. We could measure the current directly with a current transformer or some other RF current-measurement means. But, since we already have a known series resistance—the reference resistance—all we need to do is accurately measure the voltage across that resistor and we can then accurately compute the RF current. So, four measurements would then be needed. But, we may not be able to really precisely know the value of the reference reactance at all frequencies. However, since we know the current through it, if we very accurately measure the magnitude of the voltage across it, we can then very accurately compute its magnitude at any operating frequency. So, we then need to make five RF voltage measurements.

To be consistent with W8CGD, I call this method the "Five-Measurement Method" of complex impedance measurement. And, as shown above, if we fiddle with the equations a bit, we can eliminate the reference reactance for our equations and express both the unknown resistance and the unknown reactance in terms of only the reference resistance and the five measured scalar voltages. This is summarized below.

In **Figure 3**, five scalar voltage measurements and one component measurement must be made:

1. The voltage V_z across unknown impedance;
2. The voltage V_{XZ} across the series combination of the unknown impedance and the reference reactance;
3. The voltage V_s across the entire network;
4. The voltage V_{rR} across the reference resistance;
5. The voltage V_{rX} across the reference reactance;
6. The value of the reference resistance R_r.

The source voltage, the voltage across the reference reactance and unknown impedance, and the unknown-impedance voltage are relatively easy to measure because these are all measured with respect to circuit ground. The voltages across the reference resistance and reference reactance are floating and a bit more difficult to measure.

The method shown by Peter Dodd, G3LDO, and referenced in his paper "Measuring RF Impedance Using the Three-Meter Method and a Computer" is an excellent technique where the signal levels are relatively high, such as using a transmitter as the signal source.[2] However, if you're using much lower signal levels, such as using a signal generator as the signal source, the error due to the detector-diode forward voltage drop will introduce significant errors in the computations. Because the differences of the squares of these measured values are used in the computations of **Equations 14** and **25**, even relatively small measurement errors can cause significant errors in the computer values.

G3LDO's circuit

This paper would be much too long if I were to actually address a complete construction project. But, for reference, I show in **Figure 4A** a variation of G3LDO's circuit. This is not intended to be a complete schematic for a construction project. It's simply intended as guidance for those who may wish to design a complete measurement system. Nevertheless, it is generally complete.

Figure 4A is the RF detection section and **Figure 4B** is the analog processing section. I separated these two functions to make it a bit easier to understand the operation. In **Figure 4B,** I've added detector-diode compensation to each of the detectors to linearize the detector operation and compensate for temperature variations in the detector diodes. The detector circuitry of **Figure 4A** may be used without the compensation circuitry of **Figure 4B** (this would provide a totally passive detector system), but using the compensation circuitry will provide much better accuracy with small signal levels.

Also in **Figure 4A,** I've added a series input capacitor to assure that no DC component of voltage can be conducted into the circuit from the source. If any DC were introduced by the source, the measurement of V_s and V_{rR} would be compromised. Finally, I added pull-down resistors at each detector to provide a resistive path for the bias current of each of the operational amplifiers of the linearizing circuits. Even if you choose not to use compensating circuits such as shown in **Figure 4B**, it is a good idea to keep these pull-down resistors just to handle any bias current that may be present in the voltmeter used to measure the detected voltages.

This method of detector linearization is a standard technique described by a number of references (see *The ARRL Antenna Book*,[3] 18th Edition, pages 27-9 through 27-17). Basically, this compensation circuit adds a small nonlinear voltage to the detected voltage that is a function of temperature and the average current through the detector diode. This is done by driving a DC current roughly equal to the average detector current through a compensating diode. The detector and compensating diodes in each detector circuit should be matched, but, even if they are not, as long as they are the same type of diode, the errors will be much smaller than if no compensation were used. A single compensating amplifier could be used with its input switched to each detector for each measurement. However, in my application, I intend to feed the compensated output of each measured signal to the A/D inputs of a microcontroller which performs the computations. The cost of the five operational amplifiers and the extra detector diodes is minimal, and this configuration provides a good low-impedance drive to the measuring instrument whether it be a basic voltmeter or a microcontroller.

The sixth compensating amplifier is used to determine which of the test signals is the largest. This is a simple maximum-value comparator circuit. To minimize the measurement errors, we would like the input signal level to be as high as possible without saturating any of the compensating amplifiers. Normally, we'd have to look at each output to determine which is the largest and then adjust the input drive level to set this signal level to some optimum value. This additional output signal from the maximum-value comparator allows the input drive signal level to be easily adjusted based on the largest test signal, regardless of which signal that may be (since this is a resonant circuit, the signal levels across the reactive elements could easily be much larger than the input drive signal level), without having to look at each of the test signals.

The five diodes from the five compensating amplifiers form a type of analog OR gate. Whichever of the five signals that is, the largest is the only one that passes to the input load resistor of the maximum-value compensating amplifier. This sixth amplifier simply compensates for the diode characteristic of whichever input diode is actually conducting. Because the signals will be large at this point and accuracy is not too critical, we can use simple silicon diodes for the five input diodes and the compensating diode. Of course, Schottky diodes may be used here if you wish to keep all the diodes the same, but they are not really necessary.

A test example

Now for a test example. Suppose we're setting up a whip antenna for operation at nominally 25 MHz and we have a very good ground plane for this test. Suppose the whip is basically a 102-inch length of 3/16-inch diameter stainless-steel wire with a standard screw mount on the bottom (RadioShack Model 21-903 unit). In *The ARRL Antenna Book*,[3] page 16-4, Table 1, the radiation resistance of a nominal eight-foot whip at 25 MHz is given as about 20 ohms and the capacitance about 45 pF (computed from the loading inductance). These are the values we wish to measure with our five-measurement system.

For measurement, I'll choose a 51-ohm resistor for R_r, a 39-pF capacitor for X_r, and a 1.000-volt driving source. The reactance of a capacitor is simply the negative of the reciprocal of the product of its capacitance and the angular frequency ω_0, where ω_0 is simply $2 \bullet \pi \bullet f_0$

$$X_r = -\frac{1}{\omega_0 \bullet C_r} = \frac{1}{(2 \bullet \pi \bullet f_0) \bullet C_r} \qquad \text{for } X_r \text{ a capacitor } C_r$$

$$X_r = -\frac{1}{(2 \bullet \pi \bullet 25\ \text{MHz}) \bullet 39\ pf} = -163\ \text{ohms} \tag{26}$$

With a 1.000-volt rms, 25-MHz drive voltage to the network, the following rms voltages would be measured (ideally):

V_s	1.000 volts
V_Z	457 mV
V_{XZ}	976 mV
V_{rX}	522 mV
V_{rR}	163 mV

Applying **Equations 14** and **25**, the following values of antenna resistance and capacitance are found:

$$R_u = 20.02\ \text{ohms} = R_a$$

$$X_u = -141.2\ \text{ohms}$$

$$C_a = -\frac{1}{\omega \bullet X_u} = -\frac{1}{(2 \bullet \pi \bullet f_0) \bullet X_u} = -\frac{1}{(2 \bullet \pi \bullet 25\ MHz) \bullet (-141.2\ ohms)}$$

$$C_a = 45.09\ pf$$

This shows that **Equations 14** and **25** do indeed provide very accurate results. Accuracy in the measurements is critical. For example, suppose that in the measurement of the voltage across the reference resistor, the detector output were 10 percent low, or about 150 mV. The computed value of the unknown resistance would be 28.25 ohms rather than 20 ohms. This is more than a 40-percent error. This shows why the compensating circuitry is important, particularly at the comparatively low levels of drive used in this example. But, if all the five measurements were in error by the same amount, for example 10 percent, and in the same direction, the result would be the same as multiplying all the measurements by a constant (a constant of 0.9 for a 10-percent error) and this error would divide out in the computation. Also, better accuracy would be provided if the reference values were nearer the unknown values. However, even with only approximate values, this technique provides very good results.

Closing thoughts

Now for a few closing thoughts. One point is quite important: The unknown impedance that is measured by the measurement unit is *everything* connected to the output following the reference reactance. For example, if you're measuring an antenna, and you use a 1-meter length of, say, RG-8 coax to connect from the antenna to this measurement unit, you won't get an accurate measurement of the antenna impedance because the length of coax isn't terminated in its characteristic impedance. What you'll get is a measurement of the antenna impedance combined with whatever the impedance of that length of coax looks like at the test frequency. Because the coax impedance can be precisely computed, its effect could be removed from the measured values by some computation, but a much better approach is to simply place the measurement unit directly at the antenna.

Another subtle source of error in measuring antenna characteristics is that the antenna being measured is an antenna. It's receiving RF energy while you are trying to make measurements. Because the measurement system can't distinguish between signals that you inject for measurement and any signals being received over the air, any significant RF exposure of the antenna will produce significant measurement errors. Further, the antenna is receiving over a wide frequency range. It may not be very efficient at all frequencies, but it can provide a significant signal level with a high enough field exposure.

You may check for the presence of over-the-air signals with the measurement unit itself by attaching it to the antenna to be measured with the input RF drive set to zero (or simply terminate the input port) and then observe the magnitude of the signal V_Z. In this mode, the measurement unit is simply a very broadband receiver (typically several hundred megahertz) with V_Z the detected signal. So, even though you may be making an HF measurement, nearby VHF or even UHF transmitters can very easily corrupt your results. Always check for RF before trying to make antenna measurements.

Although space does not permit much detail on actual construction, a few comments may be helpful. I recommend some type of a metal enclosure. The most important point is to keep all lead lengths short—particularly from the point in the circuit being measured to the corresponding detector capacitor and from the capacitor to the to the corresponding detector and resistors. Any inductance or stray capacitive coupling at this point will introduce errors.

It's best if each detector capacitor is soldered directly to the measured point with its lead cut to about 1/8 inch or less. Similarly, the lead length of the detector diode and the two resistors connected to the junction of the diode and the capacitor should be as short as possible. Surface-mount components would be excellent here. The "output" side of the resistors connected to the linearizing circuit is less critical because all that is of interest here is the DC value. Any stray capacitive coupling on series inductance simply adds to the filtering.

If you choose to use active compensating amplifiers similar to those shown in **Figure 4B**, the compensating circuitry may be mounted away from the RF elements. But, it's important that the temperature of the compensating diodes be the same as the detector diodes to assure accurate temperature tracking. Consequently, all the circuitry should at least be mounted in the same enclosure.

The reference resistor is perhaps the most critical component. As noted above, it must have very low equivalent series inductance and shunt capacitance, and its parasitic capacitance to other components and the enclosure must be very low. A good quality carbon-composition resistor with very short leads will work reasonably well. Wire-wound resistors can't be used as the inductance of these is much too high. Carbon-film or metal-film units may be acceptable provided they are "low-inductance" units. Some carbon-film and metal-film resistors are spiral cut to trim the resistor to value. Such trimming significantly increases the equivalent series inductance.

The low-inductance units are trimmed in a different manner to minimize the effect on equivalent series inductance. A good-quality surface-mount resistor should work quite well although power-dissipation limits may be a problem. Several resistors may be placed in parallel to reduce inductive effects and increase power-handling capability, but as more resistors are paralleled, the shunt capacitance is increased because the shunt capacitances of all the resistors in parallel will add. The resistor value isn't too critical, but it should be near the expected value of the resistance of the unknown impedance to be measured. A 50-ohm value is a good starting point.

The reference reactance is the next most critical component. In general, it's easier to find capacitors that are much more near ideal than inductors over a wide frequency range. One critical requirement of the reference reactance is that it exhibit almost no equivalent series resistance. Therefore, a capacitor is the better choice for the reference reactance. As stated above, a "small" amount of equivalent series inductance in the capacitor won't affect the measurements, but the lower the better, so keep all the leads short and make the entire RF path as short as possible.

Also, some ceramic capacitors often exhibit a number of mechanical resonances (due to piezoelectric characteristics of the ceramic dielectric) which could compromise measurements. A transmitting capacitor is a good choice as these typically have very low series resistance and inductance. A silver mica with very short leads also is a good choice. A high-quality porcelain chip capacitor would also be a good choice but these may be costly and difficult to find in small qualities. Again, the value is not too critical, but the magnitude of its reactance should be near the magnitude of the reactance of the unknown impedance to be measured. A good starting point is about 25 pF to 50 pF for antenna measurements.

The detector diodes are somewhat critical. For best results at low signal levels Schottky diodes should be used. Silicon diodes will work reasonably well at high signal levels, but the errors will be greater particularly where the signal to be detected is below a few volts. The detector diode and the diode in the corresponding compensation circuit should be matched at least for forward drop with current. But if you do not wish to go to the trouble of matching the parts, at lease use the same diode type in the compensation circuit as you use for the detector. You will have to experiment with the value of the compensating resistor in the compensating circuit (the resistor tied from the compensating-diode cathode to ground) to find the value that gives the best compensation for the diodes that you choose.

The power dissipation of the reference resistor must be maintained at a relatively low level. If you use a transmitter as the signal source, this resistor will dissipate a significant amount of power and will heat the enclosure significantly. Although the compensating circuit will correct somewhat for this increase in temperature, the correction is only approximate. Also the heating will not likely be uniform throughout the enclosure, further compromising thermal compensation. If you keep the total dissipation in the circuit below a few hundred milliwatts (~+25 dBm or less), there should be no problem. If you use a 50-ohm resistor, you could use input levels as high as about 10 to 15 Vp-p. Also, the maximum input to the compensating circuit must be within the common-mode range of the operational amplifiers. For example, if 9 volts is used for the power supply, about 5 volts peak, or about 10 volts peak-to-peak, is a good limit, or about +24 dBm in a 50-ohm system.

Finally, a word of caution concerning the various voltage levels. If the reference reactance used is a capacitor and the reactance of the unknown is also capacitive, the input voltage V_S will be the largest signal and all the other voltages will be equal to or less than V_S. However, if the unknown reactance is inductive, the voltage across the reference reactance and across the unknown impedance can be very much *greater* than the input voltage due to the voltage-multiplication effect of the series R-L-C network. Therefore, it's important that all of the five measured voltages be individually observed, and the drive level adjusted to make sure the highest of the voltages is within reasonable measurement limits. That's the purpose of the sixth amplifier in the analog section. The output of this amplifier is the largest of the five test signals.

I hope you found this interesting. If any of you are interested in the details of the actual construction of this impedance-measurement unit, drop a note to the editor. If there's enough interest to justify a another article, I could be persuaded to put together a detailed construction piece. ■

REFERENCES

1. D. Strandlund, W8CGD, "Measurement of R+jX," *QST*, June 1965.
2. Peter Dodd, G3LDO, "Measuring RF Impedance Using the Three-Meter Method and a Computer," *ARRL Antenna Compendium*, Vol. 4, Dean Straw, N6BV, Editor, American Radio Relay League, Newington, Connecticut, 1995.
3. *The ARRL Antenna Book*, 18th edition, American Radio Relay League, Newington, Connecticut, 1997 pages 27-9 through 27-17 and 16-4.

Joseph J. Carr, *K4IPV*
P.O. Box 1099
Falls Church, Virginia 22041
E-mail: <carrjj@aol.com>

JUNK SCIENCE

Meet the skeptic

The greatest contribution of western civilization to world knowledge is a process that can be called *skeptical discourse*. It forms the basis of all good scholarship, science, and systematic research. It is the method by which new knowledge is developed, validated, and spread. Skeptical discourse is the celebration of *reason* as the basis for the evolution of facts and ideas into knowledge, their refinement, and their communication to others.

Skeptical discourse is the process that underlies not only the scientific method, but also good scholarship in all disciplines. The radical paradigm shift that made the scientific method so powerful in so many different disciplines is the firm and utter demand that everyone be a confirmed skeptic. To the scientific or skeptical thinker, nothing is ever finally settled; all knowledge is held to be tentative and is subject to amendment as new facts are unearthed.

The word "skeptic" is often misused, so let's take a look at a dictionary definition of *skepticism*: "[The] doctrine that true knowledge or knowledge in a particular area is uncertain; the method of suspended judgment, systematic doubt or criticism; an attitude of doubt or incredulity." These meanings imply not someone who refuses to believe demonstrably true facts, but rather one who intentionally doubts unverified claims of facts. One who keeps an open mind to permit advocates the opportunity to present evidence that convinces him or her of their validity. The skeptic "...is one who questions the validity of a particular claim by calling for evidence to prove or disprove it."[1]

A skeptic is "...prudently cautious" about accepting alleged facts. Most of us know people who fit the following statement: "He has a mind like a steel trap...*rusted shut*." Such a person is not a skeptic, but rather a fool. To be an effective thinker requires that one first be a fierce skeptic: cautious, doubting, demanding of good evidence, but with an ever open mind.

Skeptics consider facts tentative until they can be verified and checked by *objective* means that are accessible to others. Opinions, hopes, wishes, beliefs, and desires have no place in determining the truth of facts. Innate knowledge, revealed knowledge, mysticism, and "racial memories" are disdained. The skeptic challenges everything, suspending both belief and judgment on any claimed fact until enough evidence is collected and the interpretation of the evidence is soundly debated.

When the skeptic hears that an idea is about to be offered, spear points are sharpened, swords are given a keen razor edge, and the straightest arrows are gleefully selected from the quiver. The attack comes not long after the freshly born idea emerges from hiding, and continues until either the idea is debunked or the severest critics have accepted it.

The critical horde of skeptics probes for weaknesses and jabs at error, until finally the strength of the idea is either proven, revised and improved, or overcome. This process is brutal, not always congenial, and frequently bruising to egos; but it is nonetheless the way serious advances are made in the state of knowledge. It takes a mature intellect to survive this process. But the process is what keeps crank ideas from gaining general credibility before they are well developed. It is precisely this process that advocates of junk science and bizarre or novel historical interpretations seek to short circuit.

Skeptical discourse *does not recognize any form of private knowledge*, no matter how fondly held; belief is not knowledge, even though it is often passed off as such. Such private "knowledge" may be true or false, but that is not the issue. Public knowledge is tested in the crucible of the public square. Before any idea can be accepted as "knowledge," it must be offered to others for criticism and attempted debunking. If it survives the efforts—sometimes very harsh efforts—at debunking, then the proposal enters the body of knowledge accepted by general consensus among thinking people. Knowledge is validated by the "...rolling consensus of a diverse, decentralized community of checkers."[2]

Neither the vapid New Ager, nor the slippery politico advocating some hidden agenda, nor pie-in-the-sky social utopians can substitute their alleged knowledge for the hard-headed reality of knowledge gained through hard-won common consensus by skeptical discourse. That's a principle we often seem to forget, even in universities where it should be nothing less than an article of religion.

Some rules

The method of skeptical discourse follows certain rules that greatly aid the process of ferreting out the wheat grain of truth from the chaff of all possible beliefs. These rules, while not infallible (which, indeed, no rule can be), offer a very high degree of success when allowed to operate in an environment free from coercion.

One of the principal reasons for the distinctive power of science since the 17th century is that scientific thinkers, according to philosopher of science Karl Popper,[3] do not attempt so much to prove what is true, but rather to disprove what is false. This approach is sometimes called the *Rule of Falsifiability* or, in certain specific contexts, the *Rule of the Null Hypothesis*. In other words, the proposition must be framed in a manner in which it can be shown to be false by collecting objective data.

In my book *The Art of Science*,[4] I used—as an example of the null hypothesis rule—the proposition that a dish of kerosene will catch fire when a lighted match is tossed into it. The null hypothesis is that kerosene will NOT catch fire when a lighted match is tossed into it. Even if the kerosene sometimes does not catch fire, if it catches fire even once (it will!) the proposition ("won't ignite") is falsified. We are thereafter confident in our knowledge that kerosene burns when lighted with a tossed match.

Attempting to prove the positive hypothesis can lead to error. Anyone stupid enough to try it will find that an *open* dish of kerosene will occasionally dowse the lighted match before it catches fire. Thus, if the hypothesis is that kerosene will catch fire from a tossed match, and the experiment, repeated several times in a row with the same unlikely result, shows no flame, then one might erroneously conclude that kerosene is indeed nonflammable under such circumstances. No number of successful "no flame" trials is sufficient to prove the hypothesis; but even a single case where the dish roars into flames is sufficient to disprove the null hypothesis. Such a test obeys the rule of falsifiability, so therefore can lead to new knowledge.

By the way, to keep our lawyers happy let me warn you not to actually try this "thought experiment," for the kerosene will catch fire quite spectacularly!

Rauch[5] provides two general rules for skeptical discourse: *no one has the last say*, and *no one has personal authority*. These rules seem to overlap one another a bit, but they do serve to establish a framework for determining truth.

The first rule implies that no one's ideas are exempt from criticism. No matter how wise, or prestigious, or how right one has been on other matters (or on the same matter in the past), every person's ideas are subject to the same brutal evaluation as those of other people.

The second rule is like unto the first, It establishes the principle that the source of an idea is irrelevant to its truth or falsehood. Thus, it is not pertinent whether the originator of the idea is a Nobel laureate, a college professor, or a world renowned authority on the subject: Each idea must be tested solely on its own merits.

Another rule to keep the critical horde from becoming unruly is: *The burden of proof is on the one who makes an assertion*. If you're making an assertion that you desire to be accepted as true, then it is incumbent on you to gather and present the relevant evidence that permits others to properly evaluate and arrive at a conclusion. Others have no obligation to help you prove your case, or to defend their own position to the contrary.

A trick used by some people, who are either deceitful or possessed of a mushy mind, is to make an assertion and then attempt to "prove" it by demanding that you present evidence that it is false. The advocate of a quack medical device, for example, cannot present evidence to support his spurious claims. To overcome that problem, he will present his claims and then demand you prove the claims are false. But there is a simple rule: It is always the responsibility of the person making an assertion of truth or fact to supply the evidence that supports the assertion. Once that evidence is presented, it then becomes the responsibility of others to evaluate and attempt to debunk the evidence. If, after the evidence is tested in the crucible of public debate, none can debunk it, then the skeptic will tentatively accept the truth of the assertion.

A related trick used by the mushy-minded is to frame an assertion in the form of a negative, and then demand that you prove the negative. An example is the person who asserts that ghosts exist, but when challenged demands (petulantly) you prove that ghosts *don't* exist. Such a "proof" is logically impossible so, by this left-handed method, the miscreant pretends that your inability to prove the negative is proof of the positive. Never be tempted to fall into that trap.

These rules work in two ways. In the normal sense, they prevent ideas from being accepted for incorrect reasons, such as *who* presented them. In another sense, these rules protect people and their ideas from abuse based on the identity of the presenter. Every scientific paper or article must stand solely on its own merits, rather than the views of the author.

Consider the Forrest Mims affair, for example. Mims was dismissed as editor of the "Amateur Scientist" column in *Scientific American* because he is a Christian and a Creationist, rather than an Evolutionist.[6] Although the nature of his column was such that Evolution would never be discussed (it was inappropriate for that particular space in the magazine), and the editors always had final say over what went in the magazine, anyway, they apparently did not want a Creationist to publish. When the matter hit the public, it turned out that a large number of scientists and scientific organizations, even though they profoundly disagree with Mims' Creationist views, supported him. The sole criterion for judging Mims' articles in *Scientific American* (or any place else) is their content; they must stand alone to face the skeptics of the critical horde.

The Mims affair revealed a lot of inconsistency among well-educated people who simply did not understand the consequences of their actions and opinions. To blast Mims for anything irrelevant to the specific articles he was publishing was to squelch freedom of expression. It is that freedom, which is so precious and makes progress possible. Of course, I suppose we could disbelieve gravity because Sir Isaac Newton was a bit of a mystic; or we could refuse to use electronic devices because one of the inventors of the transistor went on to espouse racist theories.

Personal integrity

A fundamental issue in skeptical discourse is the integrity of the participants. The basic assumption is that all parties want to come to the truth, and in the pursuit of truth they present, in evidence only, that which they believe is factual. People are also assumed to have the integrity to change their minds when confronted with compelling evidence that is contrary to a previously held position (no matter how much it is cherished).

Different professions apparently demand different standards of their members. A scientist, one of my college professors maintained that a good scientific paper deals honestly with the opinions of opponents. Indeed, a scientist is required by his or her own unwritten canon of ethics to present and deal with evidence that supports the opponent's position.

Of course, all is not idyllic in science. I suspect a few scientists are morally better suited to practicing law than science. The biomedical sciences were rocked by a series of scandals not long ago, when it was revealed that certain well-known researchers published papers based on cooked data. India ink and food coloring have been used to fake experimental data. I've known scientists who left the field because of discouragement over the dishonesty they found in the laboratory.

In general, however, scientists and scholars adhere to a high standard of integrity, even when the civility of their criticisms (actually "bad manners") leaves something to be desired. Scientists and scholars who are found to have intentionally deceived their colleagues are generally banned from ever again publishing in a serious journal, receiving grants, or being taken seriously for their work. It is a harsh punishment, but one that is necessary in an arena where the integrity of both the presenter of ideas and their critics is an essential element of the process. When the skeptic enters the public square, intellectual sinners and miscreants are bloodied and broken.

Conclusion

The skeptic takes no prisoners, shows no favorites, and can be brutal in the quest for truth and knowledge. Ideas have no safe conduct when traveling in the skeptic's domains! The skeptic is the scourge of fuzzy thinking, unreasonableness, and outright falsehoods. The mentally mushy either shrinks in terror or retorts with irrelevancies when confronted by the Skeptic (may he or she "...live long and prosper" to quote *Star Trek*'s Mr. Spock). ■

REFERENCES

1. Michael Shermer, *Why People Believe Weird Things*, W.H. Freeman Co., New York, 1997.
2. Jonathan Rauch, "The Truth Hurts: Touchy-Feely Torquemadas," *Reason*., Vol. 24, No. 11, April 1993, pages 20–27.
3. Karl R. Popper, *The Logic of Scientific Discovery*, Routledge, London, 1959, 1980.
4. Joseph J. Carr, *The Art of Science*, HighText Publications, San Diego California, 1992.
5. Jonathon Rauch, *Kindly Inquisitors*, University of Chicago Press, Chicago, 1993.
6. J. Bergman, "Censorship in Secular Science: The Mims Case," *Perspectives in Science and Christian Faith*, Vol. 45, No. 1, American Scientific Affiliation, March 1993, pages 37–45.

John S. (Jack) Belrose, Ph.D. Cantab, *VE2CV*
17 Rue de Tadoussac
Alymer, QC J9J 1G1, and

Larry Parker, *VE3EDY*
1847 Clarendon Drive
Sarnia, ON N7X 1G1

A TUNABLE ALL-BANDS HF CAMP/MOBILE ANTENNA

Experimentation and modeling determine radiation characteristics

For 50 years, Jack Belrose, VE2CV, has used dipole antennas for HF communications from remote sites and from RV parks and campgrounds. Initially (1940s), he used a Windom antenna—the original version with single-wire feed. This is a simple, basic antenna that's easy to construct and repair in the field because it's an all-wire antenna. Later (1970s), Jack used a center-fed dipole, with the wire dipole wound up on bobbins. By adjusting antenna length, this system could be used as a resonant half-wave dipole on any frequency (or band) of interest.

More recently, Jack used a coax-fed, off-center-fed dipole. Once again, since the wire dipole was wound on bobbins it could be optimized, in this case for three amateur bands: 80, 40, and 20 meters. His camp version was 41.5 meters long, fed 13.8 meters in from one end. A homebrew VE2CV/W2DU-type 4:1 ferrite bead over coax current balun was used.[1] The most usual arrangement was to install the dipole in a drooping configuration, as only one mast/tree was needed to support the antenna. But wire antennas for campsite use are a nuisance because the arms of the dipole must be strung across adjacent campsites and sometimes across a campground road. In this case, sufficient clearance must be allowed for the passage of large RVs or service trucks.

In 1993, VE2CV evaluated a number of commercially available compact (transmitting) loops. He acquired and evaluated several of the AMA series of loops manufactured by Christian Kärferlein, DK5CZ (see **Reference 2**). For HF Field Day, emergency communications practice, and practical demonstration setups, he has used three loops: a 3.4-meter diameter loop (AMA 7 which tunes from 1.75 to 8 MHz), a 1.7-meter diameter loop (AMA 8 which tunes from 3.4 to 15 MHz), and a 0.8-meter diameter loop (AMA 6 which tunes from 6.7 to 25 MHz). There are many versions of these loops; for example, the AMA 9 tunes from 9.8 to 29.7 MHz. VE2CV's AMA 6 has been used as a camp antenna for a number of years. More on loops later.

Vehicle mounted loops are a bit cumbersome for all but the keenest radio amateur. Nevertheless, they have been proposed for short dis-

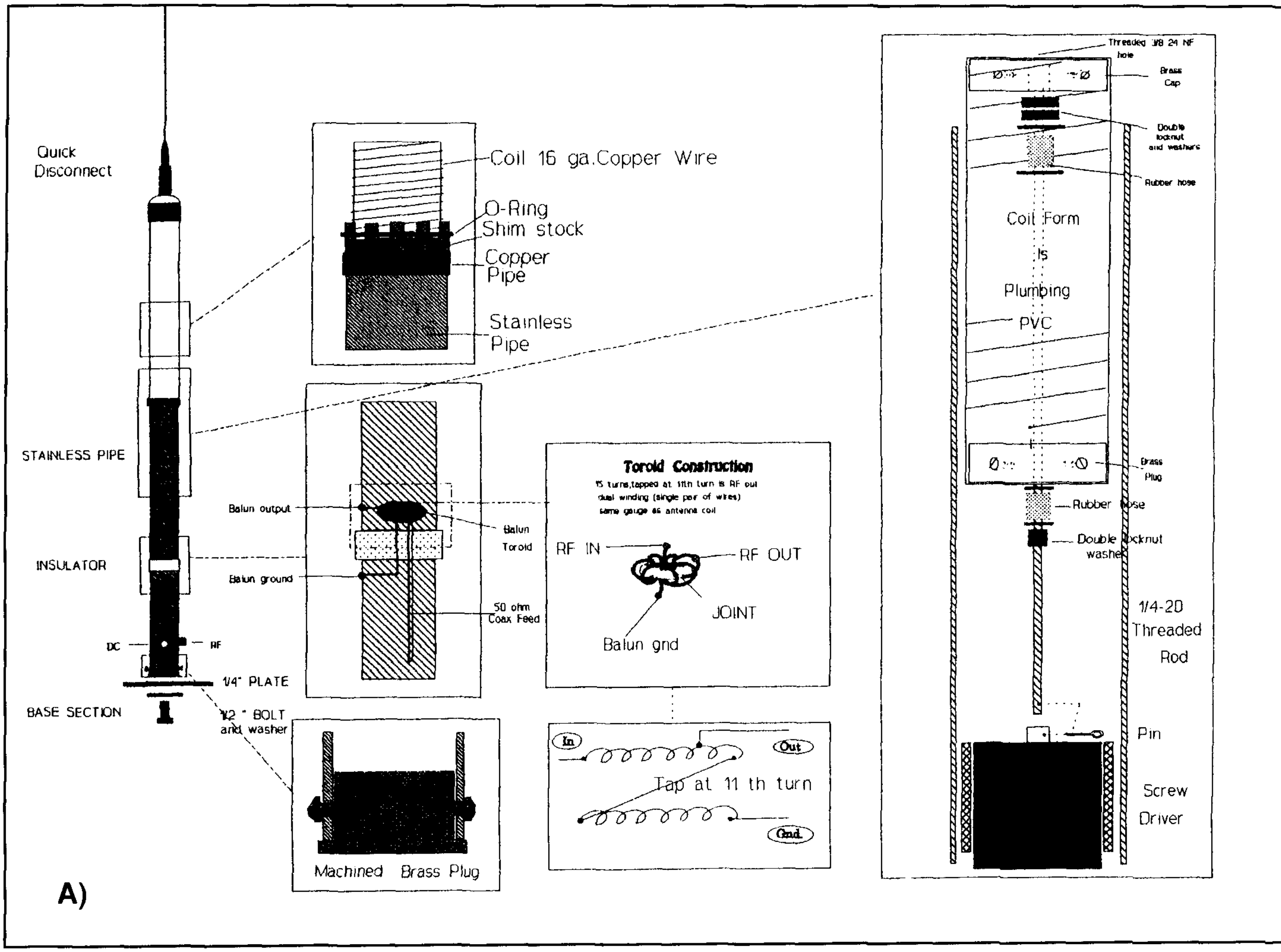

Figure 1. Sketches showing construction detail for the VE3EDY Tunable All-Bands Antenna. (A) Antenna detail. (B) The coil form.

tance—but beyond the line-of-sight communications—where the propagation mode relies on near-vertical-incidence skywaves (NVIS).[3]

The traditional HF antenna used with land vehicles is a vertical whip. The whip produces little radiation straight up, making it a relatively poor antenna for NVIS communications. A coil-loaded camp/mobile monopole is more easily transported than a loop because it breaks down into sections and can be used as a camp or mobile antenna for the 1.8 to 30-MHz band. From a campsite location it's better to go up, rather than up and out. Besides, not having to climb trees or erect a pipe mast rigid enough to support a wire dipole or a loop (even if the loop is at a low height) is a convenience. Electrically short vertical antennas are used for mobile communications, but 160/80 meter mobile antennas are rather inefficient; and while inefficiency for this application must be tolerated, a more efficient radiator is desirable for campsite use.

This article describes a mobile/transportable antenna system which we have dubbed a **T**unable **A**ll-**B**ands HF (camp/mobile) **A**ntenna (TABA). Sufficient details, construction drawings, and descriptions are included so enterprising amateurs with the necessary tools and machine shop skills can construct it. And, we present measured data to determine the radiation efficiency of the antenna for the 80-meter band, plus calculated performance for this and for several other bands.

The antenna

The antenna is a vehicle-mounted, electrically short coil-loaded HF antenna.[4,5] The loading coil is a most important consideration, as a high-Q and remote tuning ability are desirable requirements. The inductance required for the lower bands 160/80-meters can be near the self-resonant frequency for the coil, so a coil with a space between the turns must be used to reduce the coil's self-capacitance and increase its self-

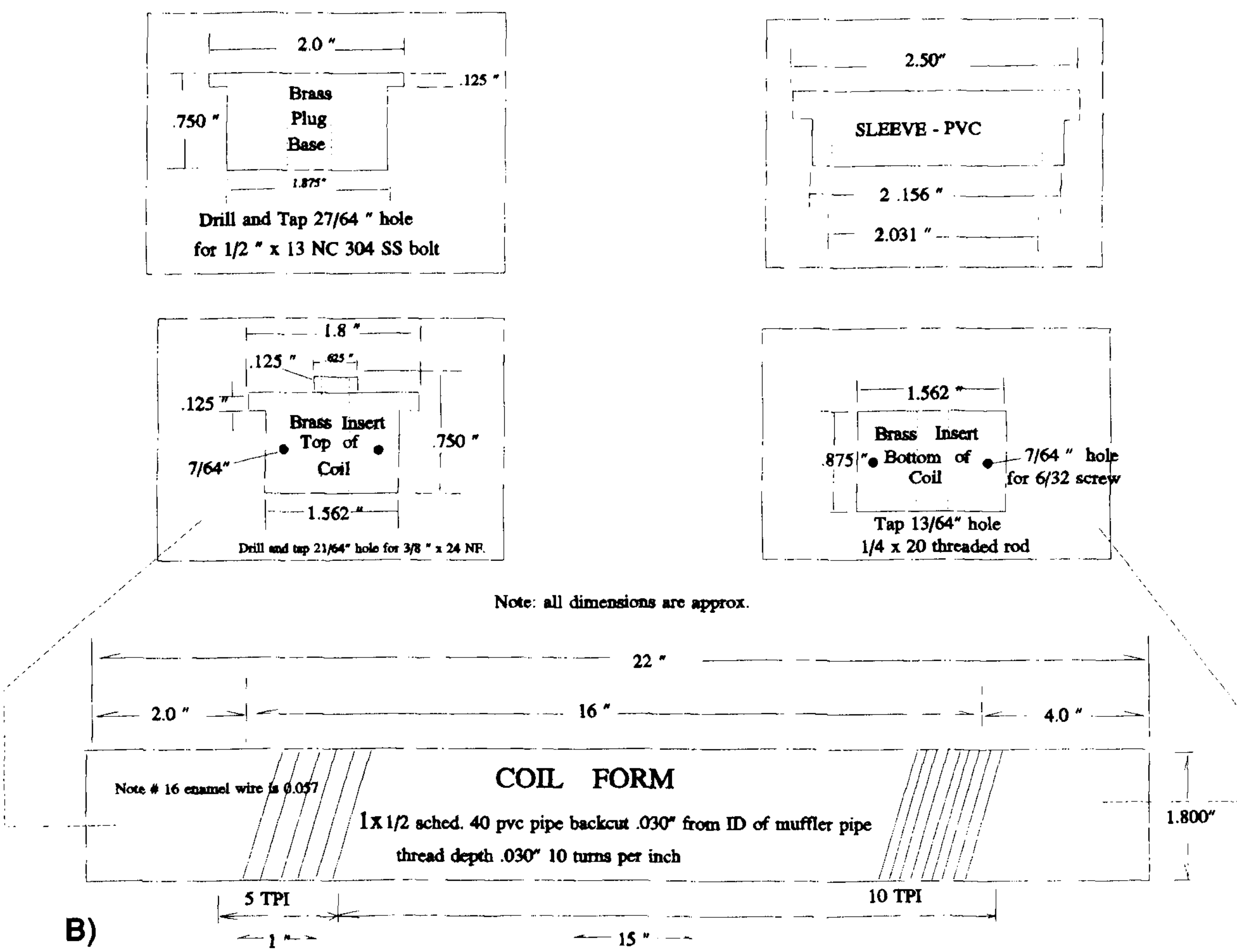

B)

resonant frequency. For typical mobile antennas, a separate coil is used for each band. But without the ability to retune, it becomes a narrow-band antenna centered on the frequency of interest. An interesting alternative to using a separate coil for each band and pruning it for the frequency of interest, was devised by D.K. Johnson, W6AAQ,[6] who described a methodology for a tunable all-band (3.5 to 30 MHz) HF mobile antenna.

This type of antenna system has attracted the interest of many U.S. and Canadian radio amateurs, and several have constructed their own versions. When the final version of our article was being drafted, Erwin David, G4LQI, drew our attention to an article[7] by Lodewijk Stuyt, PA3BTN, and Hans Spits, PDØNCF, which gives construction details for the system they built. In addition, Herb Lehman, VE3BZU, and Larry Parker, VE3EDY, have each independently developed their versions, swapping over-the-air notes, changing their design, and experimenting. Each has independently duplicated his final handiwork for use by amateur friends.

The antenna described here was fabricated by VE3EDY and its radiation characteristics were determined by VE2CV. On-the-air performance has been extensively evaluated by both of us. Two versions of the antenna have been fabricated: one that tunes to 80-meters and down and one that tunes to 160 meters and down.

The important features of the antenna are sketched in **Figures 1A** and **B**, and described below. The lower section (**Figure 1A**) is a 5-centimeter (2-inch) diameter stainless steel pipe. The series tuning/loading coil moves down into the lower mast as the frequency is increased—the coil is fully extended at the lowest frequency for the antenna. Integrity is assured by installing an O-ring, shim-stock-type of contact at the top end of the lower mast section. Although coil turns are eliminated as they go into the pipe mast, there is no current on these turns, so, in effect, they aren't there. Current flows on the outside surface of the lower mast section, on the exposed turns of the

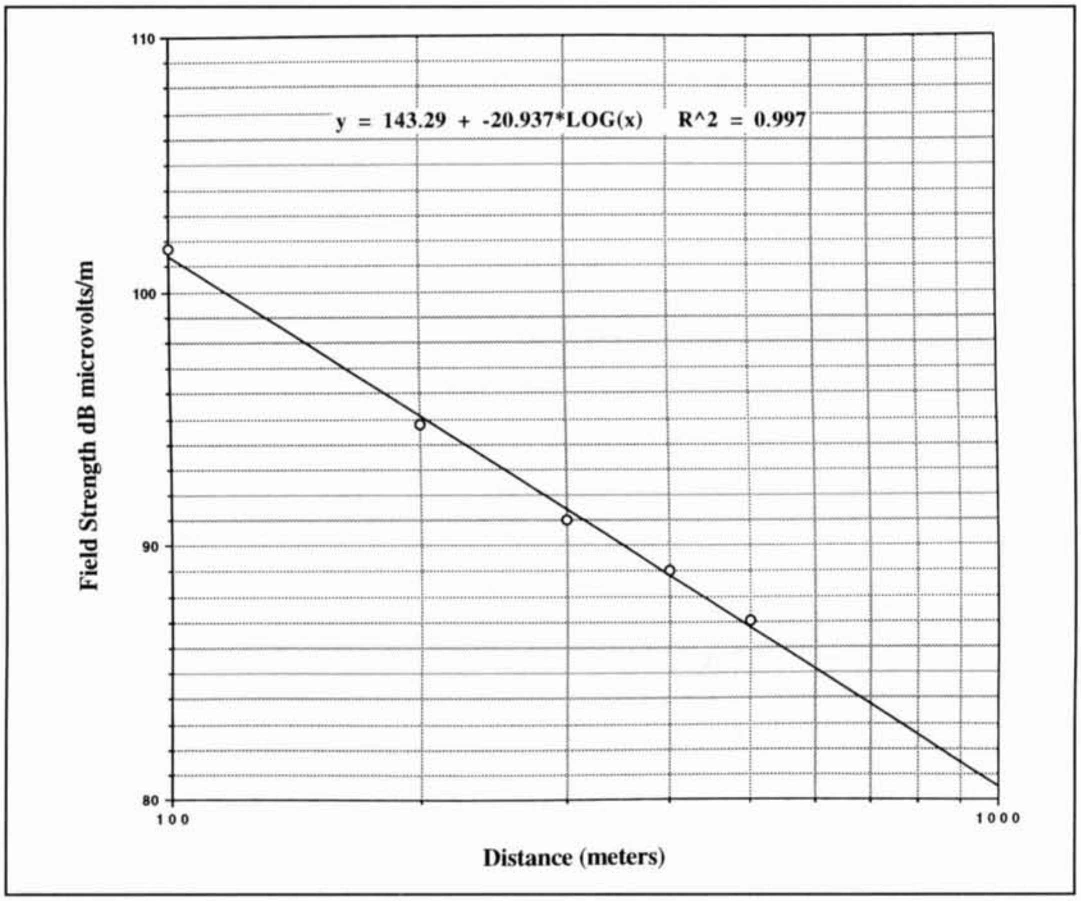

Figure 2. Measured field intensity versus distance for a 191-centimeter reference length antenna, frequency 3762 kHz, transmitter power 30 watts.

Photo A. Antenna and whip sections.

inductor, and on the top section whip. What's attractive about this antenna is that it can be remotely tuned by an internally mounted screwdriver motor. No other antenna system tuning unit is needed.

The location of the insulator, the point of feed, isn't critical. Because the antenna is grounded at its base and resonant, this only affects the tap on the toroid for optimum SWR on the bands of interest. Hence the insulator can be located above splash level for mobile use. The base of the antenna is grounded to the vehicle's frame.

The motor control, not shown, is simply a DPDT toggle switch connecting the motor to the 12-volt DC vehicle power system with a spring-return-to-center off. A series voltage dropping resistance (about 2.5 ohms, 10 watts) is needed for operation off 12 volts—so, with an added switch, the value of this resistance can be changed from fast speed (band change) to slow speed (first tune).

The top section whip is interchangeable using a quick-disconnect. Consequently, a 1.5-meter stainless steel whip can be installed for mobile use and a sectionalized 4.9-meter whip can be installed for campsite use. The top section whip used by VE2CV (as already noted) is sectionalized (four sections threaded to screw together). As a result, the whip length can be changed to suit operating conditions and band(s) of interest.

The details on the coil form (see **Figure 1B**) allow operation in the mobile configuration from 80 to 10 meters. The coil length is 55.9 centimeters (22 inches), a length needed to house the 24.4 meters of wire required to achieve the desired result. For 160-meter operation, a much longer coil with more turns is required—81.3 centimeters (32 inches)—as 48.8 meters of wire is needed to tune to 1.8 MHz. We have fabricated and evaluated the operations of both versions.

The compact stowaway feature and the ease of installation and take down is shown in **Photos A** through **C**. **Photo A** shows the antenna and whip sections lying on the ground. The bumper mount on VE2CV's GMC Yukon truck can be seen. It is a 12.7-millimeter-thick welded aluminum square-U bracket, bolted to the bumper by a factory-installed bolt that connects the bumper to the frame of the vehicle. This provides a solid, well-grounded mounting bracket, which can be easily removed if desired. **Photo B** shows VE2CV installing the full-length 4.9-meter whip. **Photo C** shows the full-length whip and a view of VE2CV's travel trailer at a state park campground.

Photo B. VE2CU installing the full-length 4.9-meter whip.

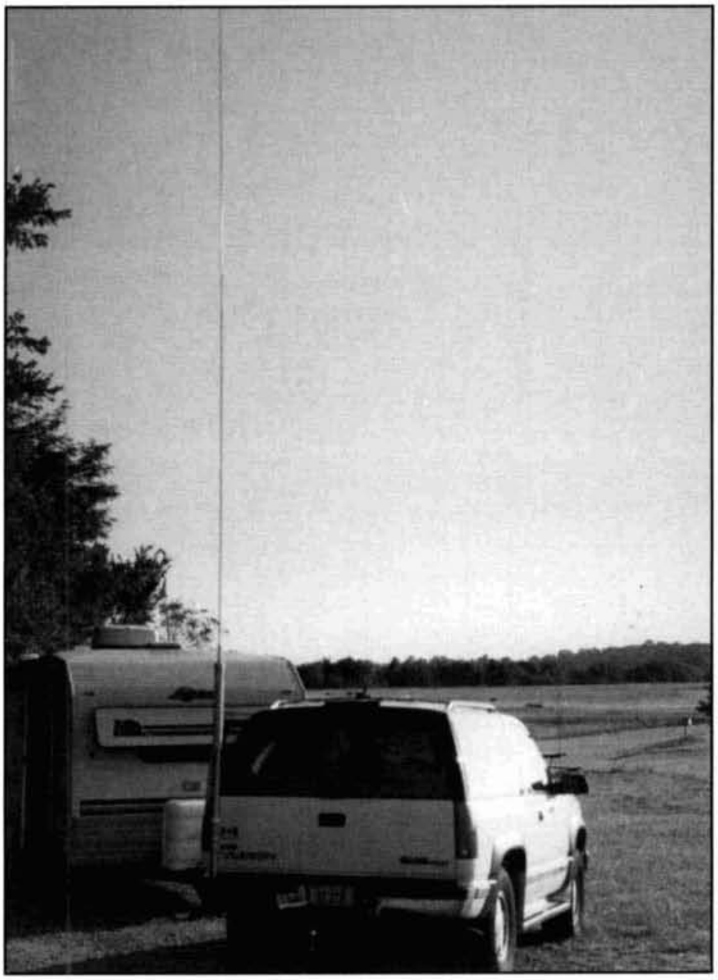

Photo C. The full-length 4.9-meter whip on the truck.

Measured performance

The TABA

To measure the radiated power for a vertical antenna, one must determine the inverse distance field strength (FS) at a distance of 1 kilometer; i.e., the field strength E_u unattenuated by ground conductivity effects.

The radiated power:

$$P_r = 1000 \left[\frac{E_u}{300} \right]^2 \text{ watts} \quad \textbf{(1)}$$

where E_u is the unattenuated (inverse distance) field strength in mV/m at 1 km, and P_r the power radiated in watts.

The Field Strength (FS) was measured using a Singer Model NM-26T FI Meter and an Electro Mechanics Company (EMCO) Passive Loop Antenna Model 6512, calibrated for FS measurement. The transmitter power was 30 watts and the frequency was 3762.5 kHz. The antenna under test, for the initial set of measurements, was the TABA base section on VE2CV's Yukon truck with one section for the top whip and a total antenna height of 191 centimeters. The FS in dBμV/m along a baseline in an open field was measured at 100, 200, 300, 400, and 500 meters distance. The results are plotted in **Figure 2**. The continuous line is the least square logarithmic fit to the data. Because the FS measured was expected to fall off faster

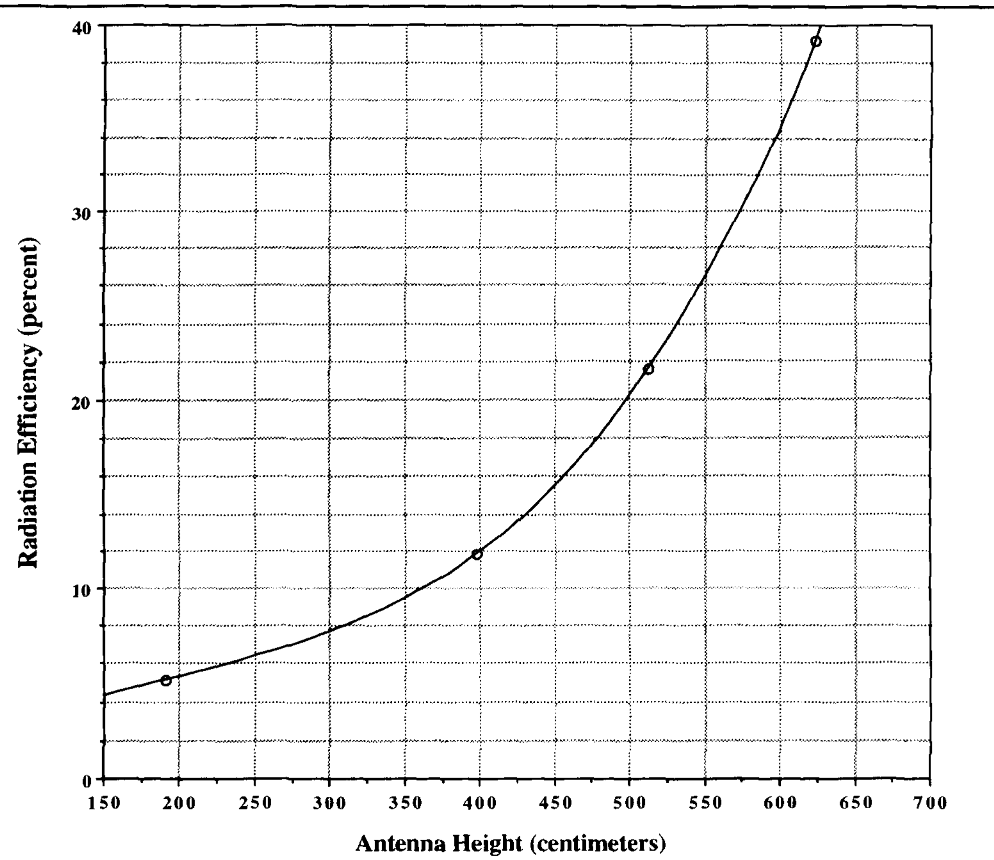

Figure 3. Measured radiation efficiency versus antenna length (or height), frequency 3762 kHz.

than the inverse distance curve even at 1 kilometer, we have determined the inverse distance field strength in the following way.

From the equation for the best fit curve to the measured data we calculated the FS at 100 meters, E(100 m) = 101.42 dBμV/m, because this value is more accurately determined than the measured value at that distance marker. Because the inverse distance curve decreases by 20 dB for each increase in distance by a factor of 10, the FS at 1000 meters is therefore Eμ = 101.42 dBμV/m - 20 dB = 81.42 dBμV/m. This value is almost exactly the same as that given by the projection of the best fit line to the data (80.5 dBμV/m at 1 kilometers). Hence, the measured FS is indeed falling off as 1/d, and the ground conductivity effect is small.

Because E_u = 81.42 dBμV/m corresponds to 11.77 mV/m, the radiated power, quite accurately determined, is 1.54 watts. Hence, for a transmitter power of 30 watts, the radiation efficiency is 5.13 percent.

The sectionalized top whip, as noted above, has four sections, each about 122 centimeters long. For each whip section length, the FS was measured at the 500-meter distance marker, and, with reference to the measured FS for initial reference antenna length, the radiation efficiency was determined. In **Figure 3**, we have graphed how the radiation efficiency increases as the length of the top section whip is changed; i.e., the overall length of the antenna is changed. The shortening of the length of the inductor as the of the top section whip is increased is included in the overall height of the antenna plotted.

The SWR measured by an MFJ-249 SWR analyzer, used to facilitate tuning the antenna, was < 1.3:1 for all antenna heights. The reflected power for 30 watts of forward power measured by a Bird Model 43 Directional Wattmeter was < 1 watt.

Comparison with a popular commercial mobile whip

We also measured the performance of a ProAm 80-meter antenna. The ProAm antenna is a helically wound mobile whip. This antenna has been reviewed for on-the-air performance by RSGB staff members.[8] It is a slim antenna and easy to mount. But because it is a single-band antenna, several must be purchased if operation on more than one band is

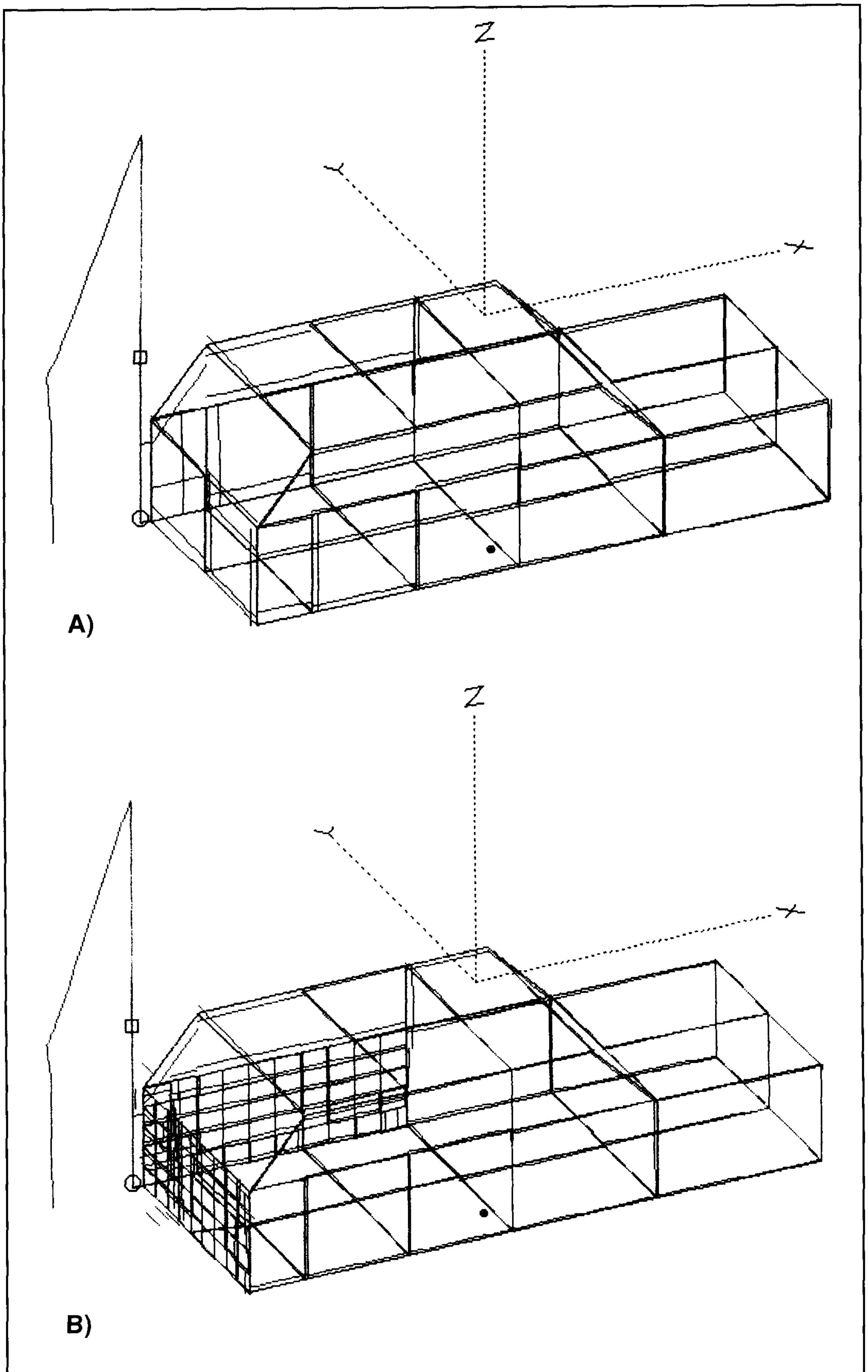

Figure 4. Two-wire grid models for a GMC Jimmy truck and current distribution on the wires for a frequency of 3.75 MHz. A) A sparse grid, and B) a detailed grid on the sides of the vehicle near the antenna.

desired. Because users have reported success with this antenna, we measured the performance of a Pro-Am 80-meter mobile antenna for comparison with our TABA mobile antenna with a top whip dimensioned for the same total antenna height (253 centimeters). The ProAm 80-meter whip was resonated and matched (see note to **Reference 8**) and the SWR was 1:1 (reflected power essentially zero). So the difference isn't due to poor matching, but is a result of antenna inefficiency.

Comparison with a compact loop

As noted at the outset, VE2CV evaluated several compact loops by numerical modeling, by experimental measurement, and by operating experience.[2] These loops were the AMA series manufactured by Christian Kärferlein, DK5CZ. The 0.8 and 1.7-meter diameter loops are transportable and, like the TABA antenna, are continuously tunable.

Since we were set up to measure the radiation efficiency of mobile antennas, we measured the radiation efficiency of an AMA 8 loop. We measured (on our calibrated test site) a radiation efficiency of 4.7 percent for this loop. The radiation resistance, according to NEC-4D (we used EZNEC pro available from Roy Lewallen, W7EL*) of an AMA 8, a 1.7-meter-diameter loop (conductor diameter 32 millimeters) at 3.852 MHz is equal to 4.356 milliohms (mΩ) (loop in free space, conductor loss zero). The conductor loss (aluminum conductor) is 41.6 mΩ. The antenna system resistance (base of loop 1.41 meters over good ground) (estimated ground at field site σ = 10mS/m; ε = 13) according to NEC-4D is R_{as} = 79.75 mΩ, so the radiation efficiency $R_r/R_{as}(100)$ is equal to 5.5 percent (difference 0.6). This is a good agreement, validating NEC-4D and revealing that the efficiency of the method of coupling to the low-impedance loop is rather good.

The TABA numerically modeled

Mobile antennas are strongly affected by the structure on which they are mounted. VE2CV had previously numerically modeled coil-loaded HF mobile antennas for the case of a rather sparse wire-grid model of a GMC Jimmy truck. **Figure 4A** shows the wire-grid model and current distribution on the wires, frequency 3.75 MHz, computed using the antenna modeling code EZNEC-4D. Notice the strong current, which is antiphased with respect to the current on the base section of the antenna, on the wire immediately in front of the antenna (representing the left rear corner of the body of the truck). This is a feature previously discussed by VE2CV.[5] At the outset, we had some concern about the sparse wire-grid model initially used. In what follows, we used a more detailed wire grid model—at least for the two sides of the vehicle close to the antenna (see **Figure 4B**). However this makes little difference in the computed resonant impedance, the reactance of the loading coil needed for resonance, and in the gain of the antenna, in spite of the much more complicated current distribution on the model with the detailed wire grid. Notice, for example (**Figure 4B**), the very strong currents at the junction between the window and the tailgate for our model. The significance of this feature is not readily assessed, because, in actuality, there's an uncertain electrical connection here (at least no solid connection), only close capacitance coupling and the contact made by the locking clips of the fold-down tailgate.

The antenna's radiation efficiency can be predicted by numerical modeling in a manner like that measured. That is, we calculate the ground wave field strength using EZNEC-4D at a distance of 100 meters. Then, by extrapolating this FS, we determine the unattenuated field E_u at 1 kilometer. For a 320-centimeter HF antenna on a GMC Jimmy over the good ground characteristics of the field site (σ = 10 mS/m, ε = 30), a transmitter power of 30 watts and a coil Q-factor of 300, the computed field strength at 100 meters (**Figure 4B**'s antenna) is 127 mV/m. Consequently, the field strength E_u at 1 kilometer is 12.7 mV/m, which compares rather well with that measured value of 15 mV/m.

The Yukon is about 11 percent larger than the Jimmy, but, according to our modeling, this factor makes little difference. The effect of the larger vehicle is (apparently) countered by the greater height of the truck, which partially shields the antenna.

In what follows, we use the model for the GMC Jimmy (**Figure 4B**). Assuming a coil Q-factor of 300 and good ground, the theoretical ground wave field strength at 100 meters for a 320-centimeter, coil-loaded mobile antenna, transmitter power 30 watts, frequency 3750 kHz (according to NEC-4), is 127 mV/m, and the ground wave field strength increases to 245 mV/m when the antenna length increases to 624 centimeters. This corresponds to a gain increase of 5.7 dB.

For an antenna 320 centimeters in height the measured radiation efficiency is 8.4 percent; for a 624-centimeter antenna, the measured radia-

*Available from Roy Lewallen, W7EL, P.O. Box 6659, Beaverton, Oregon (e-mail: <w7el@teleport.com>). Note that EZNEC pro is normally supplied with the NEC-2 engine, because NEC-4 is not available unless the user is licensed to use NEC-4.

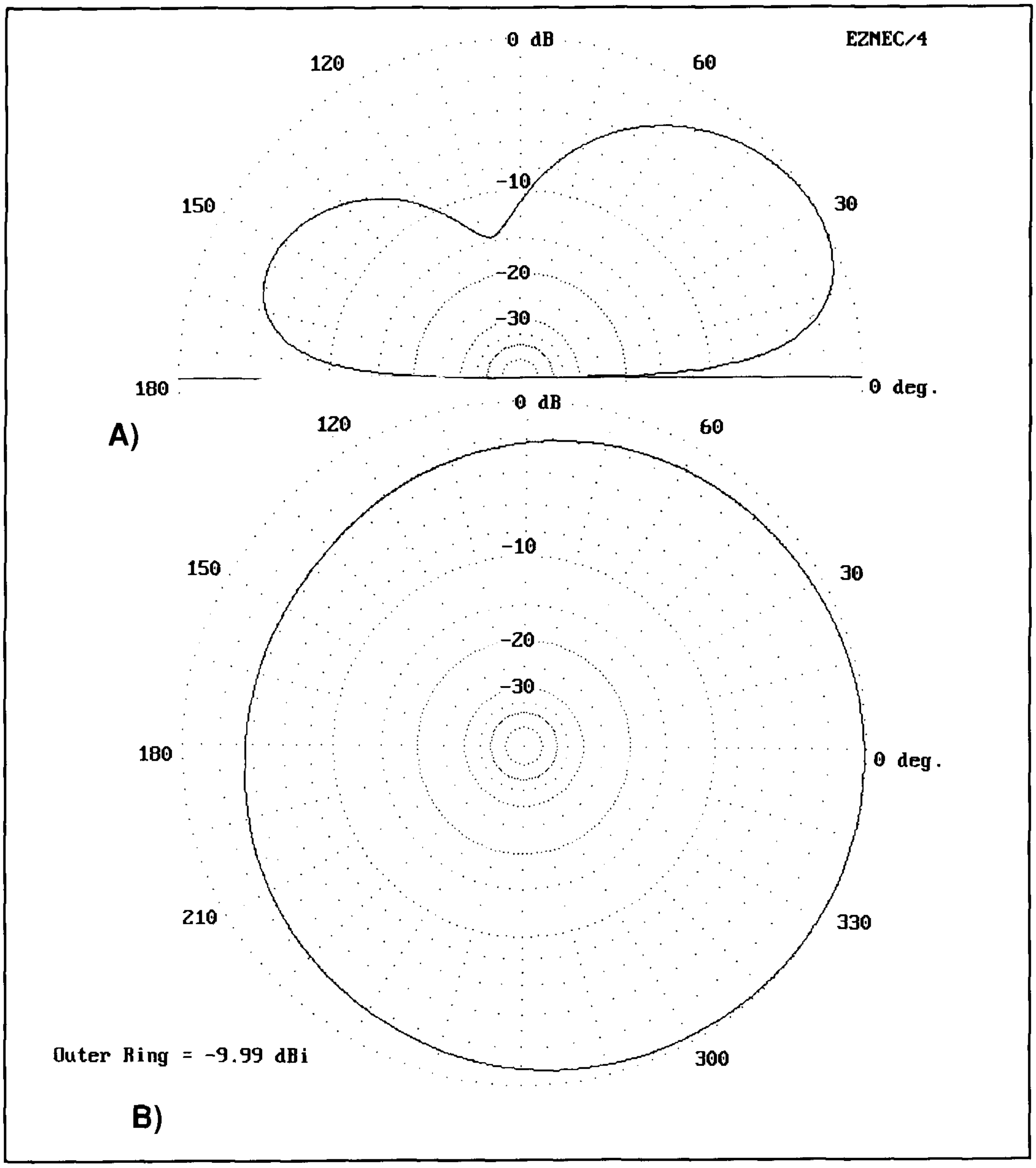

Figure 5. Predicted performance of a 320-centimeter length antenna on a Jimmy truck, average ground frequency of 3750 kHz. A) Vertical plane pattern at the azimuth of the long (diagonal) axis for the vehicle, and B) azimuthal pattern at an elevation angle of 29 degrees.

tion efficiency is 39.2 percent (see **Figure 3**). This corresponds to a power gain increase of 6.7 dB, which compares rather well with the predicted gain increase of 5.7 dB.

Continuing, with reference to earlier work in which we discussed ground loss resistance for vehicle antennas[15], it's interesting to note that to compute the same input resistance using MININEC, which assumes perfect ground beneath the vehicle as that obtained using NEC-4D for average ground, we have to include a loss resistance referenced to the base of the antenna of about 4 ohms. This is the ground-loss resistance R_g. The computed gain with this loss resistance included, according to MININEC (for average ground in front of the antenna), is approximately identical with that predicted using NEC-4D.

For measured values of commercial loading-coil Q-factors (from which we determine the coil loss resistance R_c), and for measured ground loss resistance R_g, refer to Walter Maxwell, W2DU.[9] Maxwell comments on factors contributing to coil loss and measured a loss resistance, $R_c = 8$ ohms, for a low-loss coil: a Webster KW-80 loading coil. For our example, a 320-centimeter antenna having a coil Q-factor of 300, $R_c = 6$ ohms. Maxwell also measured a ground loss resistance, $R_g = 5$ ohms, for a vehicular antenna over good ground.

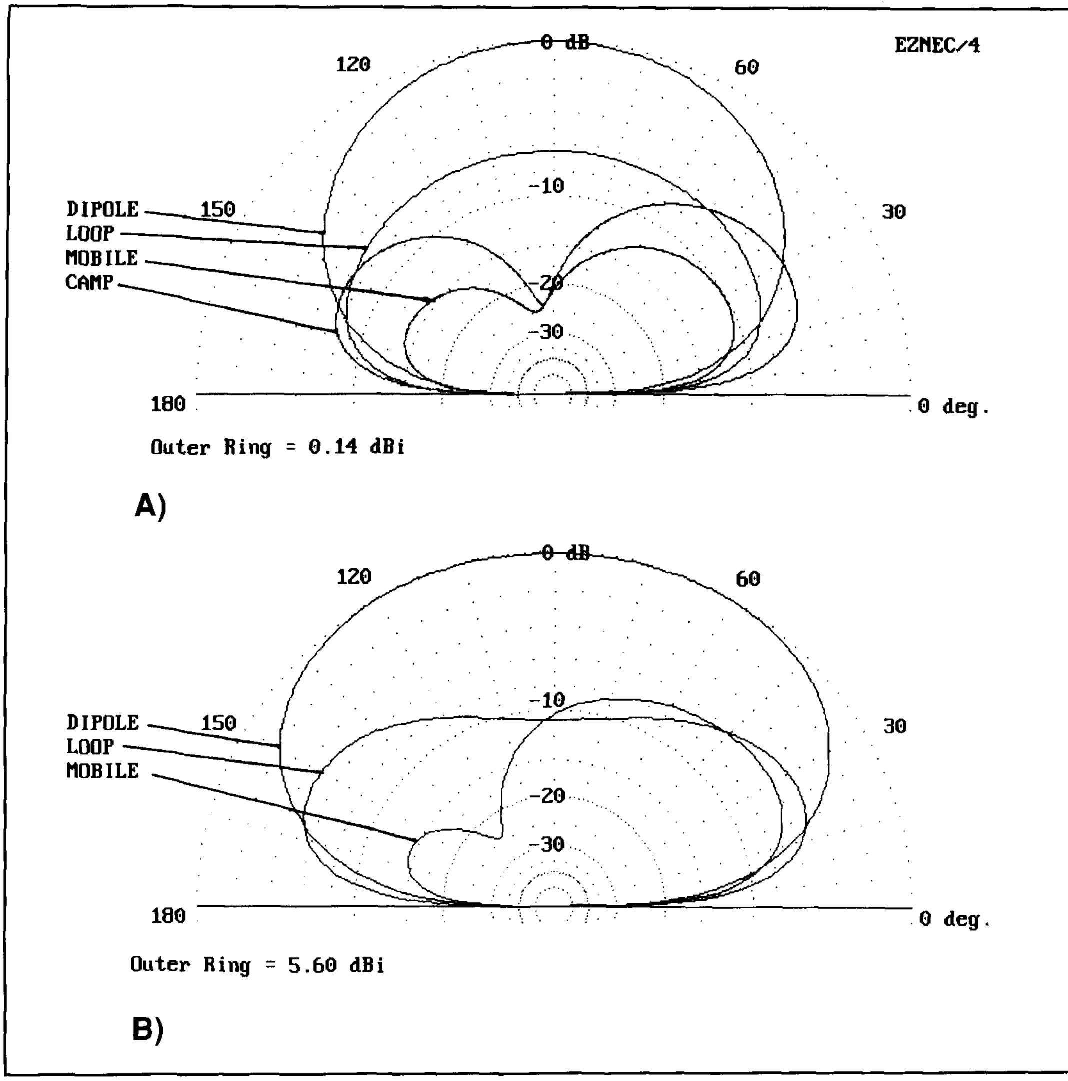

Figure 6. Predicted performance: A) for VE2CV's 80-meter mobile and camp installation, compared with a dipole at low height and a vertical 1.7-meter compact loop (see text for details), and B) for this mobile antenna on the 20-meter band, compared with a dipole (apex height and droop as for the 80-meter dipole) and a 1.7-meter compact loop.

The calculated space-wave pattern and gain (frequency 3750 kHz) for a 320-centimeter length antenna are shown, as an example, in **Figure 5**. The direction for maximum gain (as previously reported) for an antenna mounted on the left side of the rear bumper is in the direction of the right front headlight. The front/back ratio for the spacewave can be as much as 10 dB depending on frequency, antenna height, and ground conductivity. Decreasing the ground conductivity decreases the gain of the antenna system, increases the ground loss resistance, and increases the F/B ratio.

To conclude, since the antenna is, in effect, an all-bands antenna, we have computed antenna performance for a 320-centimeter antenna on a Jimmy truck for the 160 to 15-meter bands. The antenna gains (according to EZNEC-4D) for average ground ($\sigma = 5$ mS/m, $\varepsilon = 13$) at 1.9, 3.75, 7.15, 14.15, and 21.2 MHz are -17.6, -10, -4.1, -0.4, and +0.7 dBi, respectively.

Operating experience

VE2CV has used his full-length TABA (height 624 centimeters) on a travel trailer camping trip to the West Coast during the summer of 1996, the equinox of 1997, and summer equinox of 1998. He called in and received relative signal strength and reception reports from the *Sanderson Hour Group*, on 3762.5 kHz, made up of amateurs located in the Toronto, St. Catherines, and Woodstick, Ontario, areas (Bill Atcheson, VE3AUJ, usually coordinates the group). Contacts were made from numerous campgrounds on the way out and on the return trip every night or every other night (at times just after local sunset), from as far west as

Picacho Peak State Park, between Tucson and Phoenix in 1996 (from Flagstaff, Arizona, in 1997) on the way out, and from Moab, Utah, in 1997 (El Paso, Texas, in 1997) on the way back. VE2CV didn't try from points further west. Due to the difference in local times, particularly during the summer, the sun was barely set at the mobile locations at the times when these farthest west contacts were made.

A mobile-to-mobile contact between VE2CV and VE3EDY (same type of antenna at both ends) was made. Larry, VE3EDY, was in Sarnia, Ontario, and Jack, VE2CV, in Silver City, New Mexico. Larry was using a 3-meter whip for the top section at the time, which worked better than the 1.5-meter mobile in use when he first called. Transmitter power was 100 watts at both ends.

Signal reception at campsite locations is usually much better than at the base station, despite the difference in base station antenna type. This is because of the much lower radio noise levels at the campground locations. State park campgrounds are in countryside locations, and usually there are no power distribution wires overhead (see **Photos B** and **C**). In addition, the radio is battery operated. Another advantage with a vehicle-mounted antenna is that the truck could usually be turned to face in the right direction.

Concluding remarks

As noted at the outset, for operations at campsites, VE2CV has used dipole antennas for many years, and more recently compact loop antennas. In earlier years, he used a dipole at a low height, 5.5 meters, end height about 1.5 meters. In **Figure 6A**, we compared the gain for VE2CV's mobile antenna (320 centimeters length) and camp antenna (624 centimeters), for a frequency of 3.75 MHz, with a resonant dipole, and with a 1.7-meter diameter compact loop (an AMA 8). It's clear that the TABA is a very good antenna for elevation angles less than about 35 degrees.

The important features of the TABA (and the compact loop) are the ability to tune for a minimum SWR on the frequency of choice, which is particularly important for the low and top bands (80 and 160 meters) because the bandwidth is narrow. Hence, the TABA is not just a ham-band antenna, which is an important advantage since it can be used on whatever frequency is needed in the 1.8 to 30-MHz band for emergency communications—an additional antenna system unit isn't necessary. And the method of changing inductance, no taps and no shorted turns, ensures the best possible Q factor.

In **Figure 6B**, we compared the gain for this mobile antenna at 14.15 MHz and a campsite dipole (apex height and droop the same as for the 80-meter dipole). Clearly, the vertically polarized 1.7-meter loop is a better DX antenna for take-off angles <18 degrees, but the theoretical gain difference is only 1 to 2 dB (dependent on take-off angle). The TABA (mobile version) has comparable gain and is certainly easier to transport. Note: we could pick up a dB more gain easily for campsite use by lengthening the antenna a bit (VE2CV's top whip comes in four sections) since the 320-centimeter antenna is not resonant at 14.15 MHz (reactance of loading coil + j393 ohms).

For VE2CV's interest—operation from campsites principally on the 80-meter band—his TABA camp antenna is a good performer. It is perhaps surprising how well the TABA HF mobile version performs on, say, the 80-meter band, because the radiation efficiency is indeed low (8 to 9 percent). Even more of a surprise to those contacted on the 160-meter band is the performance of the mobile antenna on this band. In fact, VE2CV is continually surprised to find (since his van is always in the driveway ready to go) that he can usually hear better and even get out rather well from his mobile compared with what he can do from his base station on both the 160 and 80-meter bands.

Author notes

VE2CV works for the Communications Research Centre, Shirleys Bay, Nepean, Ontario, and is grateful for the opportunity to use instrumentation and numerical modeling codes not normally available to most radio amateurs. He acknowledges the assistance of Peter Bouliane, VE3KLO, who worked with him to make the field strength measurements for this study.

VE3EDY presently works in the petrochemical industry as an Instrumentation/Electrical/Electronics Technician. He received his amateur license in 1973. He would like to thank Jack and Peter for providing the technical assistance which as brought his antenna experimentation to fruition. ■

REFERENCES

1. J.S. Belrose, "Transforming the Balun," *QST*, June 1991, pages 30–33.
2. J.S. Belrose, "An Update on Compact Loops," *QST*, November 1993, pages 37–40.
3. B.A. Austin and K.P. Murray, "The Application of Characteristic-Mode Techniques to Vehicle-Mounted NVIS Antennas," *IEEE AP-S Magazine*, 40, February 1998, pages 7–21
4. J.S. Belrose, "Short Antennas for Mobile Operation," *QST*, September 1953, pages 30–35 and 108.
5. J.S. Belrose, "Short Coil-Loaded HF Mobile Antennas, An Update and Calculated Radiation Patterns," *ARRL Antenna Compendium*, Vol. 4, 1995, pages 83–91.
6. D.K. Johnson, *40+5 Years of HF Mobileering, Antenna Hints & Kinks*, D.K. Johnson, W6AAQ, P.O. Box 595, Esparto, California 95627-0595, USA.
7. L. Stuyt and H. Spits, "Uit en thuis met de DK3-Stuytspits," *Electron maart* 1997, pages 98–103.
8. Pro-Am Series of Mobile Antennas, Reviewed by RSGB HQ Staff, *Radio Communications*, August 1995, pages 44 and 88. See comment (by VE2CV) on matching this antenna in Pat Hawker, G3VA's "Technical Topics," *Radio Communications*, September 1996, page 72.
9. W. Maxwell, *Reflections: Transmission Lines and Antennas*, ARRL, 1990, pages 6-10 to 6-17.

Hannes Coetzee, *ZS6BZP*
P.O. Box 54098
Wierda Park
Republic of South Africa 0149
Reprinted with permission from *Electronics World*

MULTI-BAND, DIRECT-CONVERSION RECEIVER

Today's listeners ask a lot from a radio receiver. Among other things, it is expected to be able to demodulate a very weak signal—sometimes with some very strong local transmissions only a few kilohertz away. This has made the distortion free dynamic range of the receiver very important, along with selectivity and, for VHF receivers, noise figure.

For a high-frequency receiver, the distortion-free dynamic range is to a great extent determined by the mixer, or mixers, used.

Mixer using an analog switch

The heart of this direct-conversion receiver is a low-cost 74HC4066 CMOS analog switch implemented as a double-balanced mixer.[1] The switching speed of high-speed CMOS makes it possible to use this logic family right through the HF spectrum; i.e., from 3 to 30 MHz. For a summary of the receiver's capabilities, see **Table 1**; for a performance summary, see **Table 2**. Information on design improvements appears in the **Appendix**.

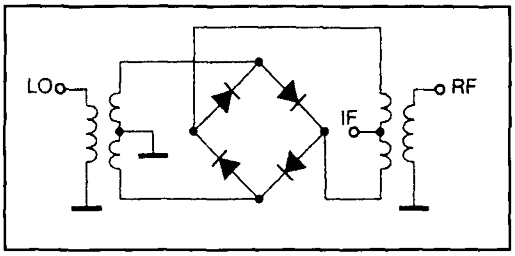

Figure 1. In the typical diode-ring mixer, the switching signal needs to be significantly higher than the signal being switched.

The switches in the 74HC4066 IC replace the diode switches found in a conventional diode-ring mixer (**Figure 1**). In the conventional normal diode mixer, local-oscillator, RF and intermediate-frequency signals are coupled

Table 1. Summary of the receiver's capabilities

Frequency coverage:	7.0-7.1 MHz (40-meter amateur band)
	14.0-14.2 MHz (20-meter amateur band)
	21.0-21.3 MHz (15-meter amateur band)
	28.0-28.4 MHz (10-meter amateur band)
RF input impedance:	50-ohm unbalanced
Detection (audio) bandwidth:	800 Hz or 2.4 kHz switchable
Audio filter type:	7th-order elliptical
Audio amplifier drive:	8-ohms or higher
Audio output power at 8 ohms:	4 watts
Power requirements:	12 volts DC

Table 2. Direct-conversion receiver performance summary

Frequency (MHz)	Bandwidth (kHz)	Minimum discernible signal (dBm)	Test-Tones spacing (kHz)	Distortion-free dynamic range (dB)
7.020	2.4	-128	20	105
14.040	2.4	-109	20	101
21.060	2.4	-112	20	100
28.080	2.4	-104	20	90

The theoretical noise floor in 2.4-kHz bandwidth is at -140.2 dBm. The measured -128-dBm minimum discernible level at a 7-MHz RF input represents a receiver noise figure of around 12 dB in 2.4 kHz bandwidth. This is made up by the mixer's 7-dB insertion loss, 1 dB through the RF band-pass filter and 3 dB contributed by the image that is also mixed down to base band. The measured and calculated values correlate fairly well for a change.

to the diode ring via two RF transformers. Two local oscillator signals that are 180 degrees out-of-phase are fed to the diode quad by the RF transformer.

Phase shift is accomplished with the aid of a radio-frequency transformer, causing two pairs of diodes to alternately conduct on the positive and negative cycles of the local-oscillator signal. The conducting diodes thus switch the RF signal to the immediate-frequency port at the rate of the local oscillator signal.

For a diode to function satisfactorily as a switch, the switching signal needs to be much more powerful than the signal being switched. For this reason, some high-level diode ring mixers make use of a +27 dBm—i.e., 500 mW—local oscillator level to provide good strong-signal handling capability.

Even then, a diode is not a perfect switch due to the transfer function of the diode not being 100 percent linear. This is one of the causes of the unwanted mixing products that become a big problem when strong signals from the antenna are present at the RF input port. With a half-watt local oscillator signal, radiation also needs some special considerations.

In the mixer to be described, the diodes are replaced with the analog switches of 74HC4066. The gates of a 74HC04 hex inverter are used to split the local-oscillator signal into two signals with a 180-degree phase difference.

The device also converts the local-oscillator signal to a square wave. Using the inverter allows one of the mixer RF transformers required by the diode-ring mixer to be replaced with an inexpensive CMOS integrated circuit. Only the RF signal needs to be transformer coupled into the mixer.

Two switches are used in parallel to reduce the on resistance $V_{cc}/2$ DC bias applied via the RF transformer (**Figure 2**). As long as the input level is high enough to activate the Schmitt trigger, the mixer is insensitive to the drive level and waveform of the local oscillator signal.

The square-wave switching signal has a not so obvious, but very useful, characteristic: the mixer responds to harmonics of the local-oscillator signal, although with reduced performance. This harmonic mixing technique is often used by microwave engineers for the

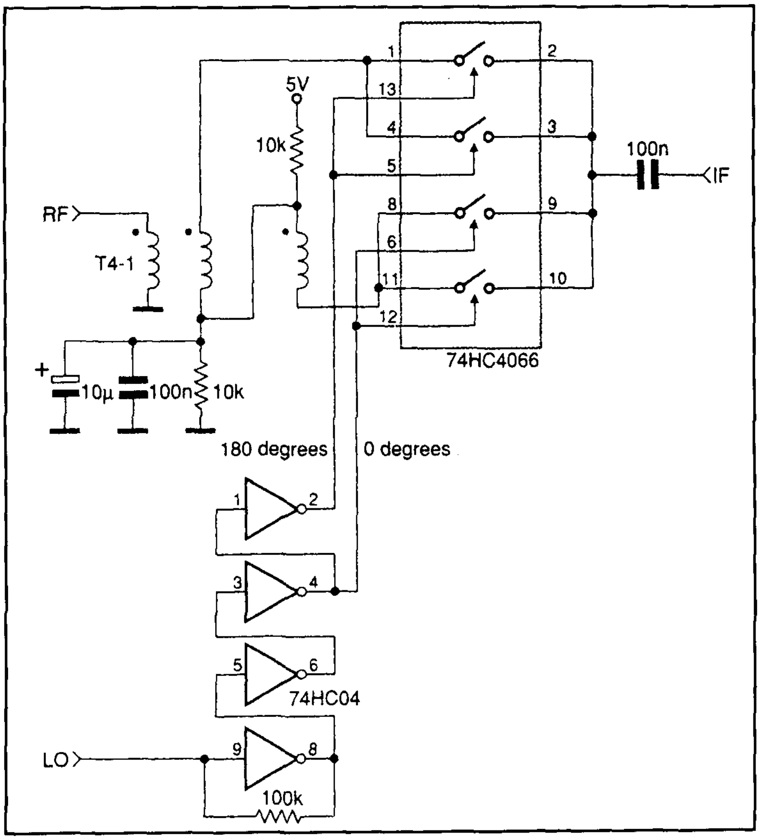

Figure 2. Replacing the diodes with CMOS switches allows a lower switching power. This configuration is much less sensitive to drive level and drive signal waveform is irrelevant.

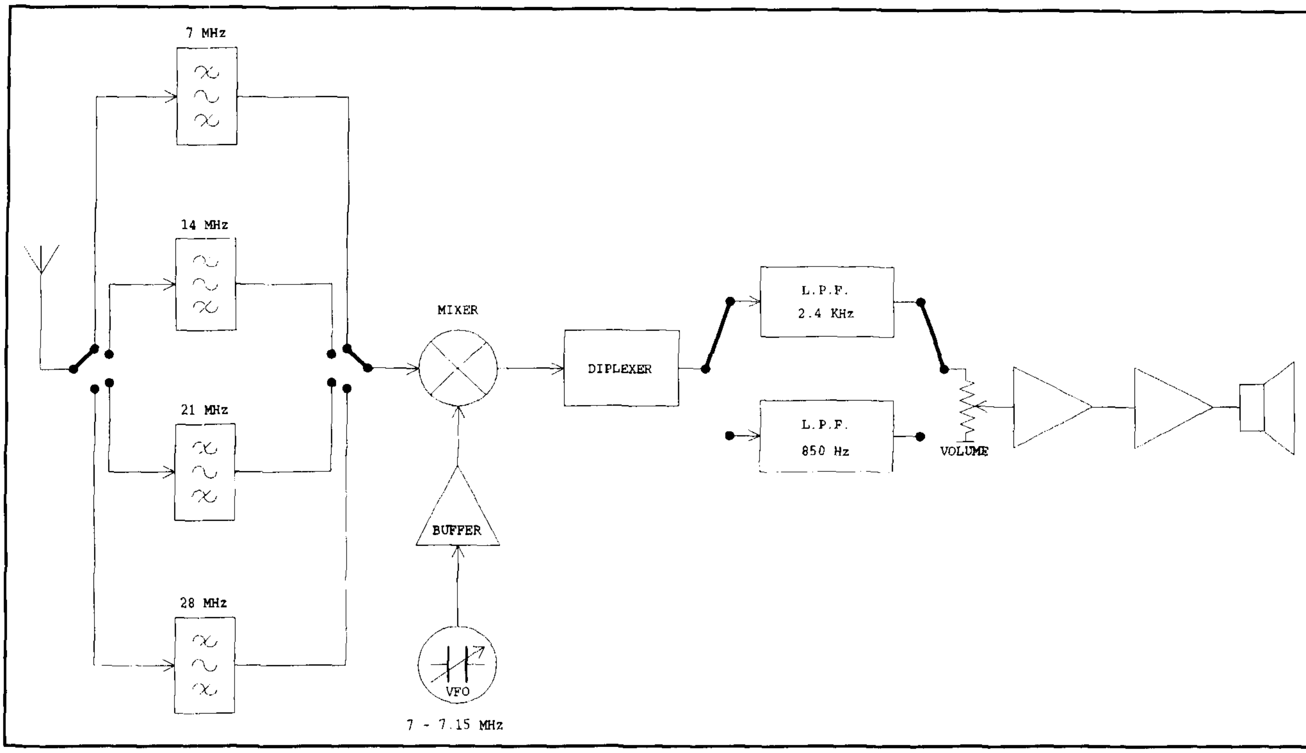

Figure 3. Four-band direct-conversion receiver blocks.

down conversion of a microwave signal to a more manageable frequency.

When the mixer is used in a direct-conversion receiver, for example at 7 MHz, signals on 14, 21, 28 MHz, etc., will also be mixed down to base band.

Fortunately, the above-mentioned frequencies are all harmonically related amateur bands. A suitable band-pass filter between the antenna and the mixer is all that is needed to select the band of interest. It is thus possible to use the same local oscillator for a multi-band, direct-conversion receiver.

But unfortunately, there are tradeoffs. The penalty for multi-band operation is increased insertion loss through the mixer and reduced dynamic range when operating on the harmonics. Fortunately though, the sensitivity can easily be improved by an RF preamplifier ahead of the mixer.

The CMOS analog switches used in the mixer are very linear when switched on and give good isolation when switched off, resulting in a mixer a with good strong signal handling capabilities. This is reflected in the very good dynamic range of the receiver.

Receiver

Shown in block form in **Figure 3** and in full in **Figure 4**, the receiver is a fairly conventional direct conversion (homodyne) design.[2,3,4]

The received signal is mixed down to base band—i.e., 300 Hz to 3 kHz—with the aid of the local oscillator running at very nearly the same frequency as the received signal. This enables Morse code continuous wave and single side-band signals to be received. Even amplitude-modulated transmissions can be demodulated if the local oscillator is tuned to the same frequency as the received signal. Note that a nasty whistle results when the local-oscillator and received frequencies differ too much, by more than about 300 Hz.

Receiver selectivity is determined by choosing either a 2.4-kHz passive low-pass filter for SSB, or passive 850-Hz low-pass filter for CW.

Audio frequency amplifiers are used to increase the signal to an adequate level for driving headphones or a loudspeaker. In this receiver, automatic gain control is not implemented to keep the design simple.

Designing the band-pass filters

The band of interest is filtered out with the aid of second-order band-pass filters preceding the mixer. If better rejection of the amateur bands is required, higher-order filters can be implemented. With the current solar cycle low of to the solar cycle, the second-order filters proved to be quite adequate.

A Butterworth response with a q0 of 14.142 was selected of Zverev[5]—the bible of filter

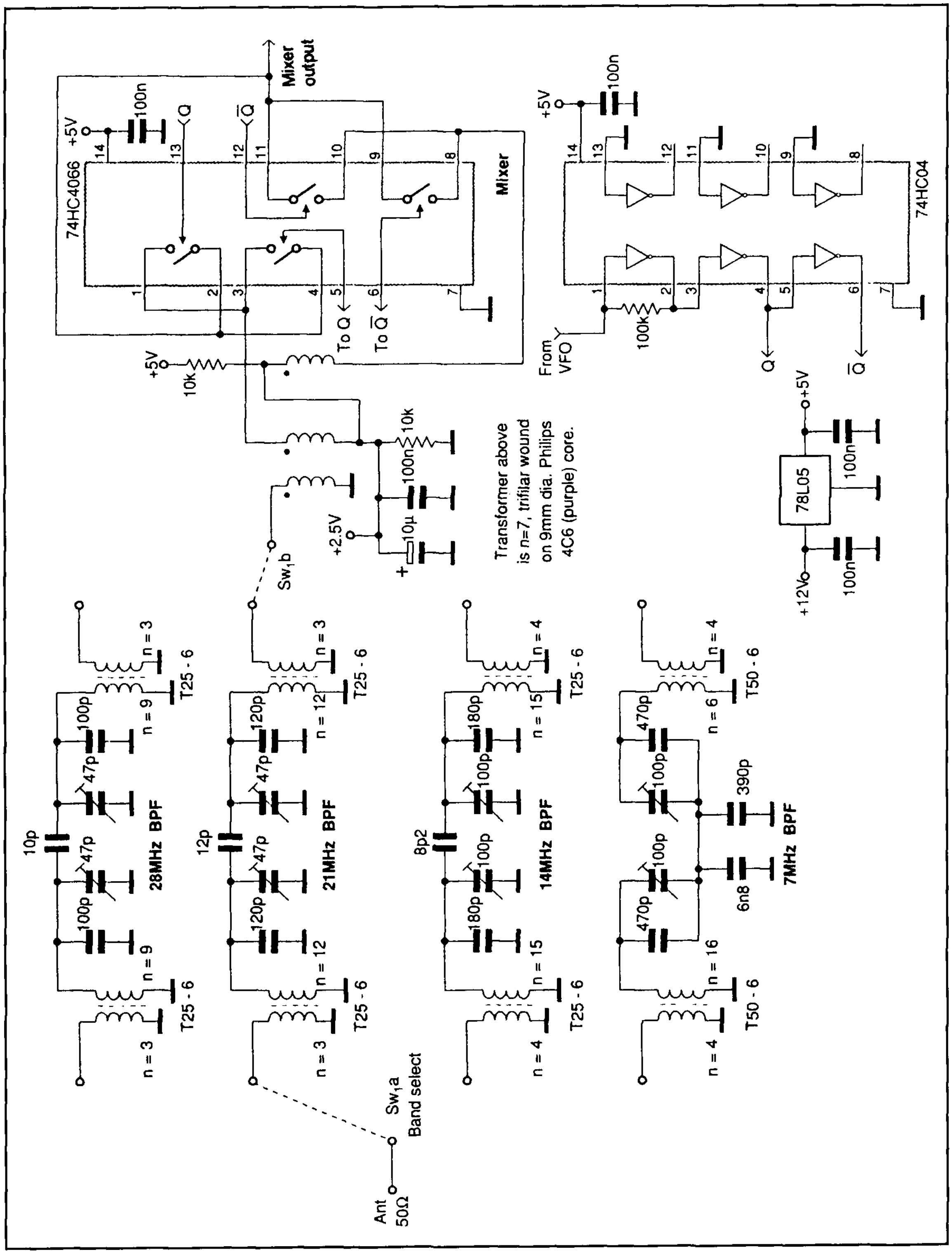

Figure 4. RF front end showing the four switch-selected band-pass filters and the mixer.

design. The theoretical insertion loss is just less than a decibel, which adds little to the noise figure of the receiver.

The inductance value used for the 7-MHz filter is 1 µH, requiring, approximately 520 pF to resonate at 7 MHz. Coupled loops are used to improve the attenuation of unwanted 14 MHz response. Coupled loops cut off at a higher rate on the high side, while coupled nodes attenuate better on the low side of the filter.

An inductor Q of 180 is realizable on an Amidon T50-6 toroid. Twenty turns provide approximately 1 µH of inductance. The loaded Q of the resonator is 15, resulting in a 3-dB filter bandwidth of 665 kHz. Note that the number of turns on a toroid is determined by the number of times that the wire passes through the hole of the toroid.

For the 14-MHz band-pass filter, use is made of Amidon T25-6 toroids. The inductor Q for an inductance of 620 nH is 170. I chose a loaded filter Q of 23, resulting in a 3-dB filter bandwidth of 853 kHz.

The 50-ohm filter termination resistance is transformed to 1490-ohms across the resonators by the transformer action between the coupling windings and those forming the inductor.

The inductance value used for the 21-MHz filter is 389 nH. Twelve turns on a T25-6 toroid provide the necessary inductance, which resonates with 148 pF. A resonator Q of 14 is realizable, which results in a 3-dB filter bandwidth of 2.1 MHz.

On 28 MHz, the inductor Q comes down to 100 for an inductance of 240 nH on a T25-6 toroid. The 3-dB bandwidth of the filter is 3.974 MHz, representing a loaded resonator Q of 10.

If you want to achieve the 1-dB theoretical insertion loss of the filters, it is vital that you only use capacitors with a low insertion loss at RF. Good choices are NPO ceramic capacitors for the fixed values and Philips trimmer capacitors for the variable types.

Local oscillator options

Many suitable designs for a variable-frequency oscillator covering approximately 7 to 7.15 MHz have been published over the years. In this receiver, a classic Hartley configuration implemented with a 2N5484 junction field-effect transformer (JFET) is used.

To ensure a clean output signal, the JFET must be prevented from operating in the pinch-off region. In a JFET with a high I_{DSS}, such as the J310, this is accomplished with a source bypassed by a suitable capacitor.

The I_{DSS} of a 2N5484 is very low and individual samples are fairly well matched. This makes the use of a source resistor to set the drain current unnecessary.

Coupling between the resonator and the amplifier (JFET), must be as light as possible to prevent degradation of the resonator's Q. This accomplished with a small value NPO capacitor.

Output is buffered by a common-gate 2N5484 JFET amplifier inductively coupled to the resonator. This effectively isolates the variable-frequency oscillator from the rest of the circuitry. Both the variable-frequency oscillator and the buffer get their DC supplies from a well-regulated, low-noise 78L08 regulator. It is good practice to build the variable-frequency oscillator and associated circuitry in a separate, shielded enclosure.

In my prototype, the span and center frequencies were adjusted using trimmer capacitors. Once the settings were correct, I replaced them with fixed-value NP0 capacitors of the same value. This greatly improved the oscillator's stability. After a 10-minute warm-up period, the drift of the oscillator was found to be low enough for monitoring SSB and CW signals. A multimeter capable of measuring capacitance is adequate for matching the fixed and variable capacitor values.

To resolve SSB and Morse code signals easily, the tuning rate must not exceed 30 kHz per revolution of the tuning knob. When the receiver is operated on one of the harmonics, at 14, 21, or 28 MHz, the tuning rate of the oscillator is also increased-four times on 28 MHz, for example. The receiver then tunes from 28.0 to 28.6 MHz.

To comply with the 30-kHz per revolution criteria on 28 MHz, the tuning rate at 7 MHz needs to be 4.25 kHz per revolution. This is difficult to implement, and a compromise might be needed. A large tuning knob helps a lot to improve matters on the higher bands.

On the prototype, a variable capacitor with a reduction gearbox was used, but this can be replaced with variable-capacitance diodes and a multi-turn potentiometer. A band-spread capacitor used in conjunction with the main capacitor is probably the best solution.

Diplexer details

It is very important that the mixer be terminated into a $50 + j0\Omega$ load from DC to at least 30 MHz[6] to prevent degradation of the mixer characteristics. This is accomplished with the aid of a low-pass, band-pass, high-pass diplexer.

Components $R_{1,2}$, C_1, C_2, C_3, T_1, $L_{1,2}$, and IC_1 form the diplexer. For frequencies from 0 to 300 Hz, the copper resistance of the primary winding of the audio transformer, T_1, of around 4 ohms, together with the 47-ohm resistor R_1, terminates the mixer.

Low-pass. The low-pass action is accomplished with two 22-µF capacitors, $C_{1,2}$, in series. These represent an unpolarized 11-µF capacitor with a reactance of 50 ohms at 300 Hz—the low-pass section's crossover frequency.

Filtering of frequencies below 300 Hz also helps to reduce microphonics. This is sometimes an annoying problem associated with direct conversion receivers.

Band-pass. The band-pass section not only terminates the mixer correctly, but also feeds the wanted received signal to the rest of the receiver chain. Generally available, low-noise

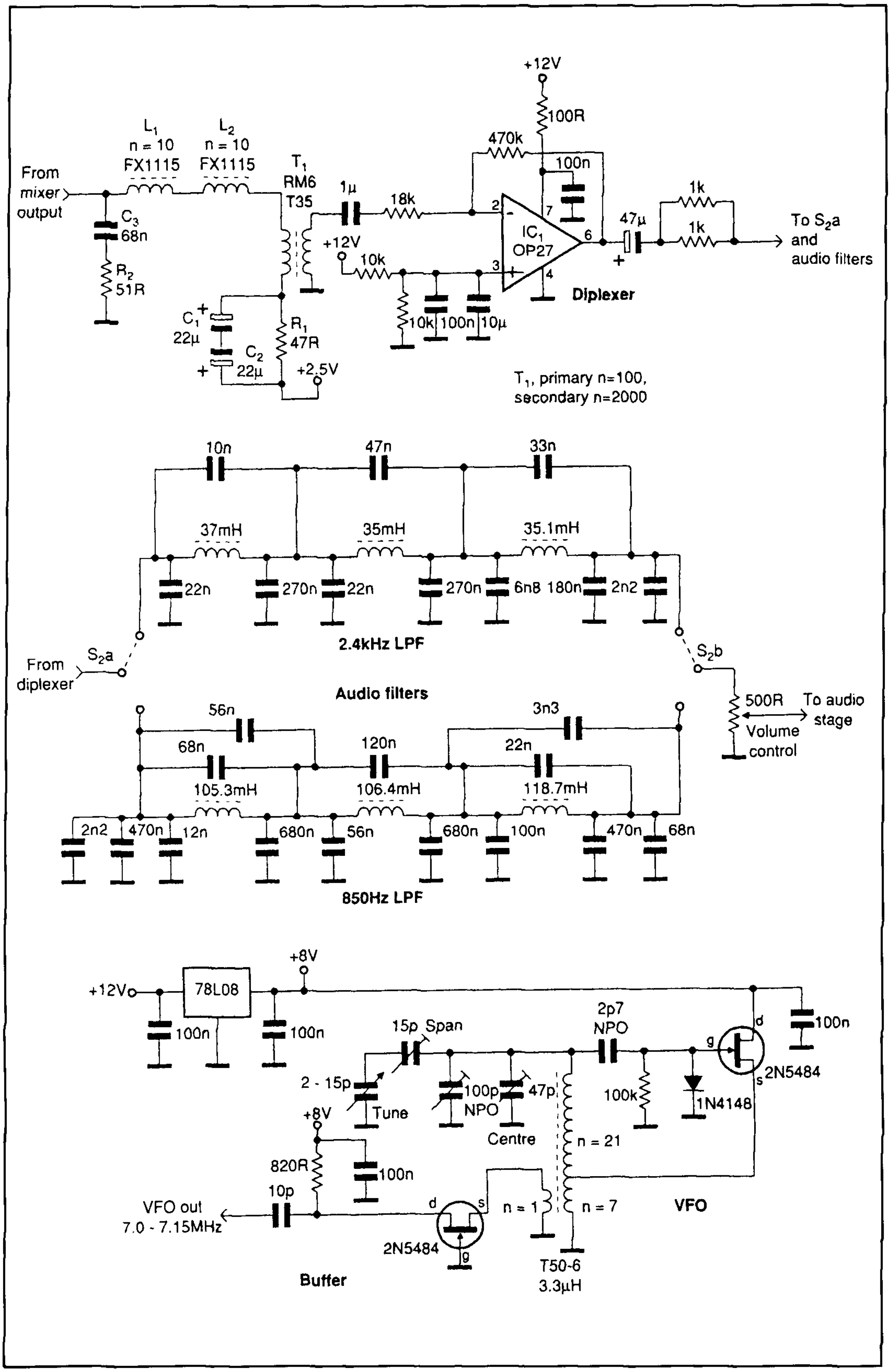

Figure 5. Diplexer presents a 500-ohm load to the front end, converts it to several kilohms ready for the op-amp filter. Two subsequent passive filters allow selection of 2.4 kHz or 850 Hz low-pass filtering of the audio signal from the op-amp. Also shown is the 7 to 7.15-MHz variable-frequency oscillator.

op-amps attain their lowest noise figures when they are fed from a source with an impedance of several kilohms.[6]

An audio transformer turns the 50-ohm impedance needed to match to the mixer into the several kilohms to suit the op-amp. This transformer has the dual advantages of voltage gain coupled with virtually no added noise. This helps to keep the overall noise figure of the receiver the same as the input stages, namely the band-pass filter and mixer.

Although winding a transformer is at the best of times a pain, the benefits really make it worth the while. The transformer is wound on an ungapped RM6 core without a mounting hole through the center. Siemens manufactures this type of core in a T35 material.

The primary consists of 100 turns while the secondary comprises 2000 turns—or as many as you can fit on. Both the primary and secondary are very carefully and patiently wound with 0.06-mm enameled copper wire. A mechanical winder will help a lot.

On the high-pass side, which lets through frequencies from 46 kHz to more than 30 MHz, the mixer is terminated as follows into 50 ohms.

The inductance of the two ferrite bead inductors in series, $L_{1,2}$, is 170 μH. Using $X_L = 2\pi FL$ shows that a load of $+j50\Omega$ is presented at 46810 Hz. A 68-nF capacitor, C_2, provides the necessary $-j50\Omega$ reactance to cancel it. In this way, from 46810 Hz up to many megahertz, 51-ohm resistor, R_2, terminates the mixer.

Low-pass filters

Seventh-order, passive elliptical low-pass filters terminated in 500 ohms provide excellent selectivity. Suitable designs have been published using off-the-shelf 33 and 100-mH inductors.[2,3] Unfortunately these components are not freely available in South Africa.

I designed 850 and 2400-Hz low-pass filters incorporating hand-wound inductors using Zverev.[5] These inductors were wound on a couple of P14/8 pot cores made from 3B7 material, which is now obsolete (try 3F3). The A_L value of this material is 350 nH/(winding).[2] The number of turns required by each inductor was calculated and the pot cores were assembled with a very small amount of epoxy used to keep the two halves together.

Fortunately many modern multimeters can measure inductance. This makes confirming the inductance values at audio frequencies a piece of cake.

High-quality capacitors are a must for this application. Polystyrene, Wima, and MKT are all suitable. Using capacitors with a tolerance of around 10 percent results in an unknown amount of ripple in the pass band of the filter. This is totally acceptable for speech and Morse code applications.

The theoretical insertion loss of an equally terminated filter is 6 dB. I measured an insertion loss of less than 7 dB on the filters used in the prototype receiver.

Although modern switched capacitor filters provide the same pass-band response as the above passive filter—and sometimes even better—the dynamic range is limited to about 85 dB. This is not enough for the main filter of a modern HF receiver.

For the narrow CW filter, I implemented a low-pass response in favor of a band-pass response. The human ear needs some background noise to aid in the decision-making process of decoding a weak Morse code signal.[9] Electronic detection on the other hand measures the energy in a certain bandwidth, which necessitates a band-pass response. The narrow CW filter also helps to reduce one of the more serious principle defects of a direct conversion receiver—namely image response.

Audio amplification

Low-noise op-amps provide the majority of gain. The low-pass filter is fed via a 500-ohm termination resistor from the op-amp stage of the diplexer.

Output of the elliptical low-pass filter feeds a non-inverting amplifier with a voltage gain of 43 dB. Input impedance of this amplifier is defined as 500 ohms by the volume potentiometer, which also terminates the filter.

A 6-volt bias voltage is applied to the input of the amplifier by the three 100-k resistors. The output of this stage feeds the power op amp output stage.

Capacitor C_p, in parallel with feed-back resistor R_p, forms a first-order low-pass filter with a 3-dB cutoff frequency of close to 2.7 kHz. This reduces the high-frequency noise generated in this stage.

Capacitor C_s in series with the voltage divider resistor R_s to ground performs two duties. First of all, it blocks DC. Second, it forms a first-order high-pass filter to reduce the effects of microphonics.

Output amplifier

A low-distortion output stage is very important to prevent weak signals from sounding fuzzy. This problem is typical of the majority of audio amplifier ICs. The class B output stage used in these ICs just isn't good enough.

I found a good compromise between current consumption and high-fidelity audio was in the TDA2030 power op amp. At 38 mA, its quies-

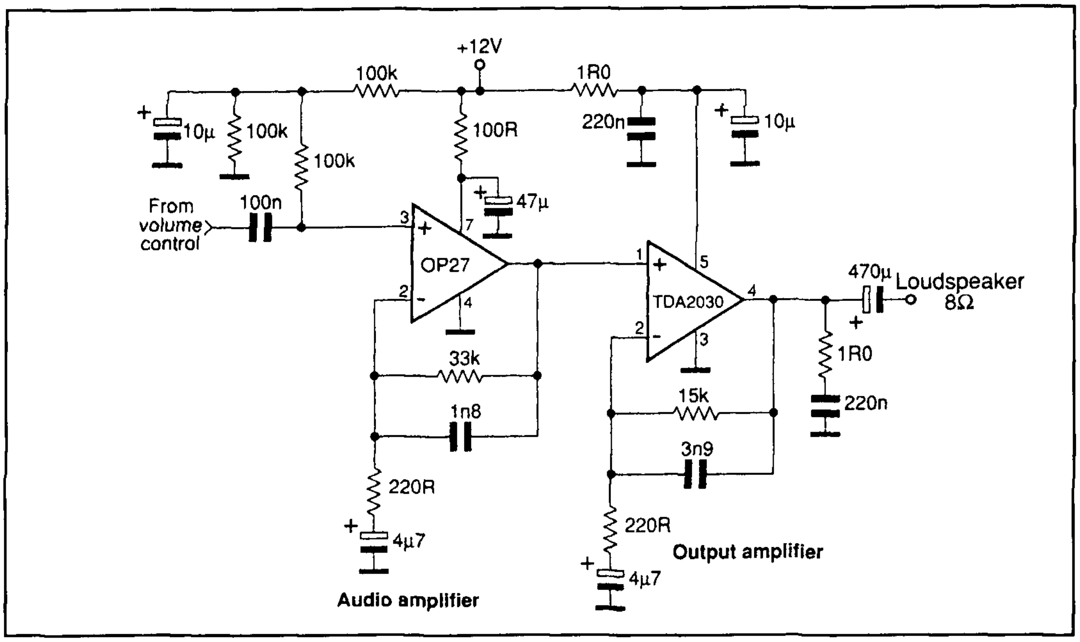

Figure 6. Band-limited audio preamp and power stage, capable of delivering 4 watts into 8 watts. Low distortion is important here if you want to be able to detect weak signals.

cent current is relatively low, yet it is capable of driving an 8-ohm loudspeaker.

The prototype receiver is frequently used at campsites for demonstrations to groups of young people interested in radio. The receiver is powered from a rechargeable sealed-gel battery, which makes the current consumption of the receiver important when a loudspeaker is used.

If you do not need to drive a loudspeaker, the output stage can be replaced with an op-amp capable of driving 600-ohm headphones. The TDA2030 is supplied in a TO220 package and will need a heat sink.

To ensure stability of the output stage and prevent any RF feedback from creating havoc, the output is terminated for high frequencies via a series connected 1-ohm resistor and 220-nF capacitor to ground.

The two resistor/capacitor pairs in the feedback path perform the same function as those in the preamplifier.

Housing the receiver in a metal enclosure avoids problems with RF pickup and emissions. I built my prototype on plain unetched pc board.

In summary

In common high-performance HF receivers, only the first mixer is a very high-performance type incorporating, for example, switched JFETs. The cost-driven assumption is made that the first intermediate-frequency filter will limit the frequencies that the following mixers are exposed to.

During a CW contest for example, there are sometimes quite a few strong signals present in the pass bands of the various IF filters. This can be the source of intermodulation distortion in following mixers in an otherwise excellent receiver.

In my direct conversion receiver, closely spaced signals are not a problem since only a single, high-performance mixer is used. Even with very closely spaced signals the spurious free dynamic range remains very good, probably only being limited by the phase noise of the local oscillator.

Although the presented receiver is fairly simple and easy to implement—especially when you make use of ready-wound inductors—the performance can rival many expensive commercial HF receivers. ■

REFERENCES

1. P.J. Coetzee, "A Low Cost, High Performance Double Balanced Mixer for HF Applications," *RF Design Magazine*, June 1995.
2. Rick Campbell, KK7B, "High-Performance Direct-Conversion Receivers," *QST*, August 1992, pages 19–28.
3. Joseph J. Carr, "Director Conversion Receivers, Parts 1 and 2," *Elector*, March 1994, pages 42–48, April 1994, pages 54–58.
4. *The ARRL Handbook for Radio Amateurs*, 1995 edition, American Radio Relay League, pages 17.19–17.22.
5. Anatol I. Zverev, *Handbook of Filter Synthesis*," John Wiley and Sons, 1967.
6. Paul E. Drexler, "Effect of Termination Mismatches on Double-Balanced Mixers," *Microwave Journal*, January 1986, pages 187–190.
7. Ulrich L. Rohde, DJ2LR, "Wideband Amplifier Summary," *Ham Radio*, November 1979, pages 34–36.
8. Alex Burwasser, N6DC, "How to Design broadband jfet amplifiers," *Ham Radio*, November 1979, pages 12–19.
9. Ron Taylor, G3AVQ, "Technical Topics: Copying Weak CW Signals," *Radio Communications*, July 1990, pages 30–31.
10. Nic Hamilton, G4TXG, "SSB: third method, fourth explanation," *Electronics World + Wireless World*, April 1993, pages 278–284.

BIBLIOGRAPHY

1. John W. Christensen, "Noise-figure curves ease the selection of low-noise op amps," *EDN*, August 1994, pages 81–84.

Appendix: Design improvements

From the performance summary of the receiver, it is clear that the sensitivity can be improved when operating on the harmonics of the local oscillator frequency; i.e., 14, 21, and 28 MHz. An RF preamplifier that can be switched in and out as needed will improve the situation quite a bit. A gain of 10 to 20 dB will probably be adequate.

It is important that such a preamplifier must not degrade the dynamic range of the receiver too much. This is accomplished with a high standing current through the preamplifier's transistor.

In general, high dynamic range and low current consumption do not go hand in hand. I suggest using a noiseless feedback design with bipolar transistors or a broadband JFET amplifier. Although I have not tried this, suitable designs can be found in **References 7** and **8**.

Dynamic range of the mixer can in most instances be improved by a few decibels by running the 74HC4066 from an 8-volt supply. For CMOS, the switching point is normally at $V_{cc}/2$, for an 8-volt supply, making it 4 volts. When run from a 5-volt supply, the 74HC04 output can swing to 4.9 volts, which is normally adequate for switching the 74HC4066. This modification will also decrease the insertion loss by nearly 0.5 dB due to the lower on resistance of the switches.

The mixer described in this article is highly suitable for implementation in a phasing or Weaver-type SSB receiver.[10] A quadrature local oscillator signal can be digitally generated with the aid of a dual D-type bistable IC. The dynamic range will be improved by 6 dB due to the 3-dB reduction in noise figure and the dividing of the RF input signal to the two mixers.

PRODUCT INFORMATION

Philips *ECG Semiconductor Master Replacement Guide*, 18th Edition

The 18th Edition *ECG® Semiconductor Master Replacement Guide* features new products, new product families, additions to existing lines, and approximately 300,000 cross references. To aid in your search, the Philips ECG Instant Cross™ program is also available in both DOS format and Microsoft Windows® 3.1 and 95.

To locate an ECG distributor near you, call toll free 1-800-526-9354.

Tetrode Boards for Control and Protection

Tetrode boards from Down East Microwave offer a new solution to the control and protection of tetrode power amplifiers. They will work with any transmitting tetrode for amateur power levels, in any power supply grounding arrangement. Two small pc boards include regulated power supplies for the screen and control grids, screen and grid current protection, TX/RX sequencing, and ALC and relay supplies.

The kit includes all components for the pc boards, a comprehensive 32-page manual, and full designer support. Experienced constructors can buy the bare boards and manual. A special mains transformer that connects directly to the boards and provides everything except the anode voltage is also available.

For details, see <http://www.ifwtech.demon.co.uk/g3sek> or contact Down East Microwave, Inc. at (908) 996-3548. Outside the U.S., contact Ian White, G3SEK, at his *Callbook* address, or e-mail: <tetrode-boards@ifwtech.demon.co.uk>.

Hands-on Guide to "Real World" Electronics

LLH Technology Publishing has published *Simple, Low-Cost Electronics Projects*. This book of do-it-yourself electronics projects written by Fred Blechman is for anyone interested in electronics. The 22 projects covered include voltmeters and multimeters, a voice-operated switch, function generator, and a telephone line analyzer.

For more information visit the company's Web site at: <www.LLH-Publishing.com>.

Robert R. Brown, *NM7M*
504 Channel View Drive
Anacortes, Washington 98221

UNUSUAL LOW-FREQUENCY SIGNAL PROPAGATION AT SUNRISE

Ap-index reaches 101 in May 1998

The electromagnetic spectrum extends from extremely low frequencies (ELF, 30 to 3000 Hz) to super high frequencies (SHF, 3000 to 30000 MHz) and various factors influence the propagation of signals across the spectrum. Those factors involve the Earth's atmosphere and ionosphere, as well as the geomagnetic field, and form a coupled system under the influence of the solar wind.[1]

The wide variety of amateur radio activities starts in the medium frequency range (MF, 300 to 3000 kHz) and extends upward. At present, there is considerable interest in the 160-meter band, particularly for DXing, and attention is

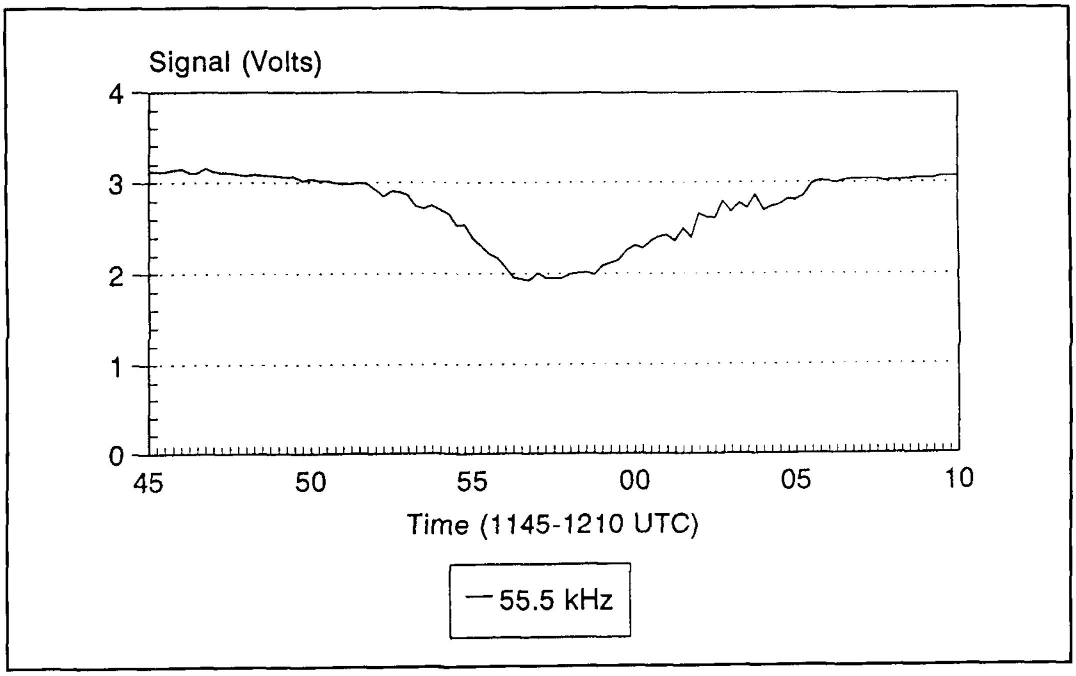

Figure 1. Sunrise profile of NPG signal strength, June 15, 1998.

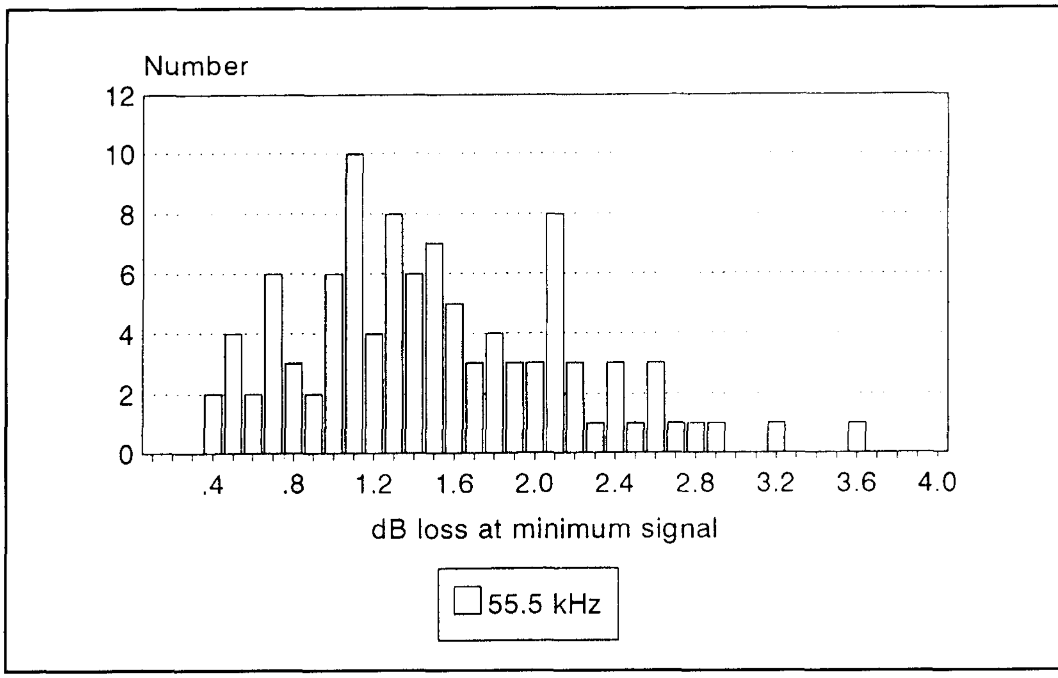

Figure 2. Number-distribution of NPG sunrise signatures, March through June, 1998.

focused on the factors which influence propagation on that band. While the usual Earth-ionosphere hops are surely in effect there, another distinct possibility is ducting of signals in the electron density valley above the nighttime *E*-region.[2]

There are other aspects of 160-meter DXing that point toward atmospheric effects influencing propagation. Those include the dawn enhancement of signals as well as a "searchlight effect" frequently observed when signals are received only from limited regions. At the moment those effects are not understood, and there is considerable interest in finding the propagation indicators which would be applicable on the 160-meter band.

To date, the best indicator seems to be magnetic K-indices for polar paths, propagation being best at times of low magnetic and auroral activity, but other determinants may exist. In that regard, another approach now involves studying signal strengths of MF broadcast stations at dawn and from other directions—say from the Orient or across the equator.[3]

The present discussion deals with signals from another part of the spectrum, in the low frequency (LF, 30 to 300 kHz) range, and on a shorter path. Signals from one LF station were monitored during both quiet and extremely disturbed conditions, and the analysis of the sunrise signal recordings during the disturbed period reflect the coupled nature of effects from the magnetosphere-thermosphere-ionosphere system. In particular, the discussion and analysis of propagation during disturbed conditions includes satellite observations of the influx of low-energy (<20 keV, or kiloelectronvolts) electrons at high latitudes and near-relativistic (>100 keV and >300 keV) electrons from the magnetosphere at middle latitudes, disturbances of the geomagnetic field, as well as ion- and neutral-chemistry processes in the lower ionosphere.

The results of the analysis point toward LF effects from the leakage of energetic electrons from the trapped radiation belt, as well as atmospheric gravity waves. There are as yet other factors which may influence the properties of the regions traversed by 160-meter signals.

Observations

The sunrise variations of LF signal strength on 55.5 kHz from NPG at Dixon, California (38.4N, 121.9W), were monitored at Guemes Island, Washington (48.5N, 122.6W), starting in February 1998. That path is 1,125 kilometers long, within 2.5 degrees of being North-South and has its midpoint just east of Cottage Grove, Oregon. The recording system was similar to that used by many others interested in low band studies. It consisted of an inductively loaded inverted-V antenna, a VLF converter with a low-pass filter, and a PLL-controlled receiver. The NPG RTTY signals were rectified, filtered, and sampled by an A/D converter every 15 seconds. The data were then fed through the RS-232 port of a computer and files were generated for each observation session.

In an effort to observe factors that influence propagation in darkness and into daylight, daily recordings of NPG were made to cover times of sunrise on the path. The sunrise signature of NPG's signals was found to be a decrease in signal strength followed by an almost full recovery to the nighttime level, as shown in **Figure 1**. That type of signature represents observation of the minimum intensity of NPG's signals from the destructive interference of its groundwave and one-hop skywaves due to the path or phase difference between the two waves which results as the reflection level is lowered at sunrise.

In connection with the question of destructive interference, note that the plural "skywaves" in the last sentence means that the received signal is the vector sum of electric field strengths of rays emitted across the antenna pattern and which reached the receiver site. This is important as sunrise affects the concave reflecting region sequentially, lowering it gradually from one end to the other (except at the equinox). In addition, that contributes to the variability of the NPG signal reduction at sunrise, as shown in **Figure 2**.

Using the greatest reduction in overall signal strength around the equinox, it is possible to make an estimate of the relative amplitudes and intensities of the first hop and groundwave from the various observations in hand. The result corresponds to an intensity ratio of about 15 dB. Support for that interpretation, using both a skywave and a groundwave at a distance of 1,125 kilometers, is obtained from methods outlined by Watt, in which a comparison was made of the groundwave and first hop skywave for 40-kHz signals from NPM in Hawaii.[4] Those calculations were based on a daytime reflecting layer at 75 kilometers, propagation to the west, and distances up to 2,000 kilometers from a 1-kW transmitter. The calculations showed a total field which was largely due to the groundwave out to 400 kilometers; beyond that, the skywave grew in importance and was dominant beyond 800 kilometers.

In the present instance, observations of signals from NPG were made at times of transition, while the reflecting layer was dropping from the nighttime level around 90 kilometers to the daytime level at about 75 km.[5] Calculations using this method, but for those two extremes, with the 40-kW transmitter at NPG, still provide both sky and groundwaves in reasonable agreement with the values cited above from experimental observations.

However, in contrast to the NPM case, where there was little ambiguity as the path was over sea water, the present case is tempered by the uncertainty in the amplitude of the groundwave. Thus, there is a need to characterize the quality of the ground material from fairly good to poor, over the 1,125-kilometer path from the Sacramento Valley in California to the San Juan Islands in Washington and during varying conditions caused by El Niño. Be that as it may, the agreement is close enough to justify further use of that interpretation, the signals coming from interference between the first hop skywaves and the groundwave at 1,125 kilometers distance. However, the presence of a second hop skywave cannot be ruled out.

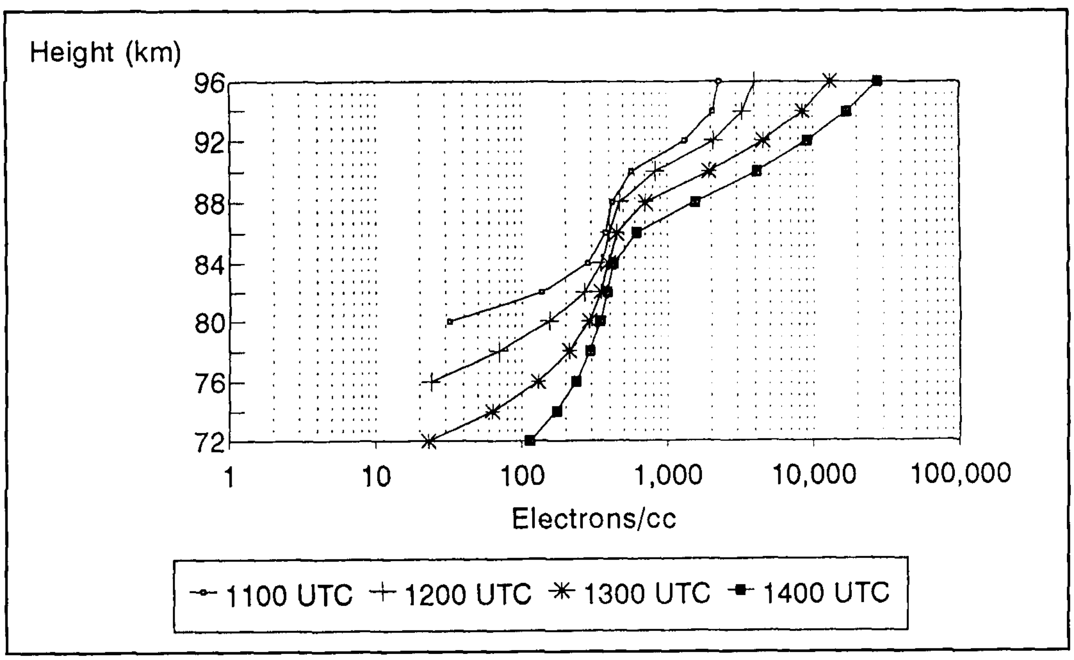

Figure 3. Electron density profiles in LF reflection region, starting before sunrise in undisturbed conditions.

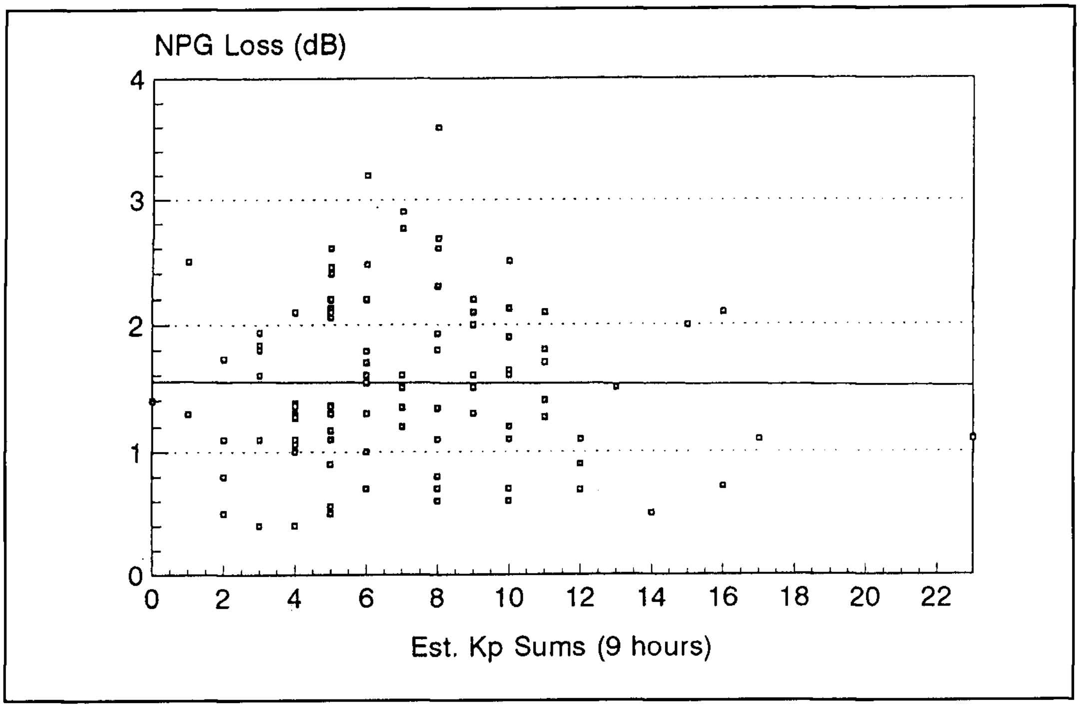

Figure 4. Point scatter-diagram for NPG signals and nine-hour Kp-sums from the records of the NOAA magnetometers.

With its steep electron density gradient, shown in **Figure 3**, the *D*-region is more metallic than ionospheric or dielectric for signals of 5.5-kilometer wavelength. And, instead of refractions, the method given by Watt uses Fresnel reflections of signals at the bottom of the D-region.[4] That being the case, signal loss is on reflection, as with the reflection of light by metals. Also, the presence of the geomagnetic field gives rise to mode conversion; i.e., the incidence of vertically polarized waves resulting in a horizontally polarized component on reflection. In addition, loss with the groundwave depends on the conducting properties of the surface. Ionospheric absorption, as in MF and HF propagation, is not considered in the LF range.

A reflecting surface which is spherically concentric with the Earth is required in this method. That is not always the case at sunrise when the terminator sweeps across the path; but for times around the equinoxes, the entire path is illuminated at about sunrise, with only small differences in solar elevation angle between the two ends. For the other seasons, the solar illumination goes from one end of the path to the other, N -> S after the spring equinox and S -> N after the fall equinox.

Daily variations

The observations from March through June 1998, show variations in the sunrise signal depression and provide data which illustrate apparent changes in the heights of the reflection region as the sun rises. The initial height results from the weak background ionization that supports the *D*- and *E*-regions at night, while the final height is that from the full solar spectrum. However, any correlation with solar activity is difficult as one variable, the background solar X-ray flux from NOAA, is an average for a full day while the sunrise signature for NPG signals is obtained in an hour, right in the middle of the UTC day.

Thus, the level of solar activity before sunrise would be expected to affect the observations, but the level after sunrise may or may not be related. The exception would be a large increase in solar activity in which the ionizing flux increases one day and remains high the next. In that case, the ionizing flux in the morning hours of the first day would probably be similar to that in the afternoon and thus support the use of the daily index for that case.

However, the X-ray data for the four-month period shows that it was in a narrow range 90 percent of the time, varying by no more than a factor of 6. If the scattered EUV and Lyman-α which support the *D*-region at night varied by the same amount, then, in equilibrium, the nighttime electron density in the upper *D*-region could vary at most by a factor of 2.5 from day to day but with essentially the same gradient.

In full solar illumination, the LF reflecting region results from the entire solar spectrum. This is quite intense, adds photo-detachment of negative ions to ionization, and brings the reflecting layer down to a level that depends not only on ionizing processes but also on the photo-chemistry of the region. Those processes are expected to show less variability as the lower region is well mixed and less subject to atmospheric irregularities than the higher scattering region at night.

Other geophysical variables, related to magnetic activity, are less direct than ionizing radiation in their influence on the *D*-region. **Figure 4** shows the distribution of NPG signal strengths during the period of interest, but the data points also include the data on the magnetic activity in the hours prior to each observation. Such a distinction is not possible with the 24-hour averages for the background solar X-ray flux.

These data points make use of three-hour K-indices from the listings of NOAA/SESC for estimated Kp/Ap values and use the sum of K-indices in the nine-hour interval before each NPG record as a measure of activity or disturbance. Details of that type of representation will be given later, but for the moment it is sufficient to note that large values of signal depression at a mid-latitude were not associated with high levels of magnetic activity. In short, large height changes at sunrise are not found at times of significant magnetic activity in the high-latitude regions.

There were occasions when small values of signal depression were noted, particularly within the period of intense geophysical disturbance in early May, which also included the presence of both solar protons and auroral/magnetic activity. Those disturbances may affect the LF reflecting regions and be lost in the statistics; that being the case, it is appropriate to review the sources of ionization and the disturbances which may have perturbed the *D*-region and signal propagation from NPG.

D-region

As the lowest-lying region of the ionosphere, the direct sources of *D*-region ionization are the most energetic and penetrating forms of radiation incident on the Earth. They are: galactic cosmic rays, largely protons with energies in excess of 1 BeV (billion electron volt), then the energetic portion of the solar X-ray spectrum below 10 Angstroms, the intense Lyman-α (1216-Angstrom) emission line of the sun, and finally the extreme ultra-violet (EUV) part of its spectrum below 1100 Angstroms.

Galactic cosmic radiation is generally considered the primary source of ionization in the lower *D*-region, up to 65 to 75 kilometers in altitude depending on the phase of the solar cycle. This is particularly true at night when direct solar UV and X-rays are not incident and only weak starlight and scattered solar UV reach the region. The mid-latitude ionization rate of galactic cosmic rays at 65 kilometers is about 0.02 to 0.05 ion pairs/cm^3/sec, the lower figure applying around solar maximum.[6]

At night, VLF and LF signals are reflected by the steep electron density gradient at the bottom of the *D*-region, shown in **Figure 3**. The curves in that figure, from the *International Reference Ionosphere*, start when the *D*-region is in the dark at 1100 UTC, and then show lowering of

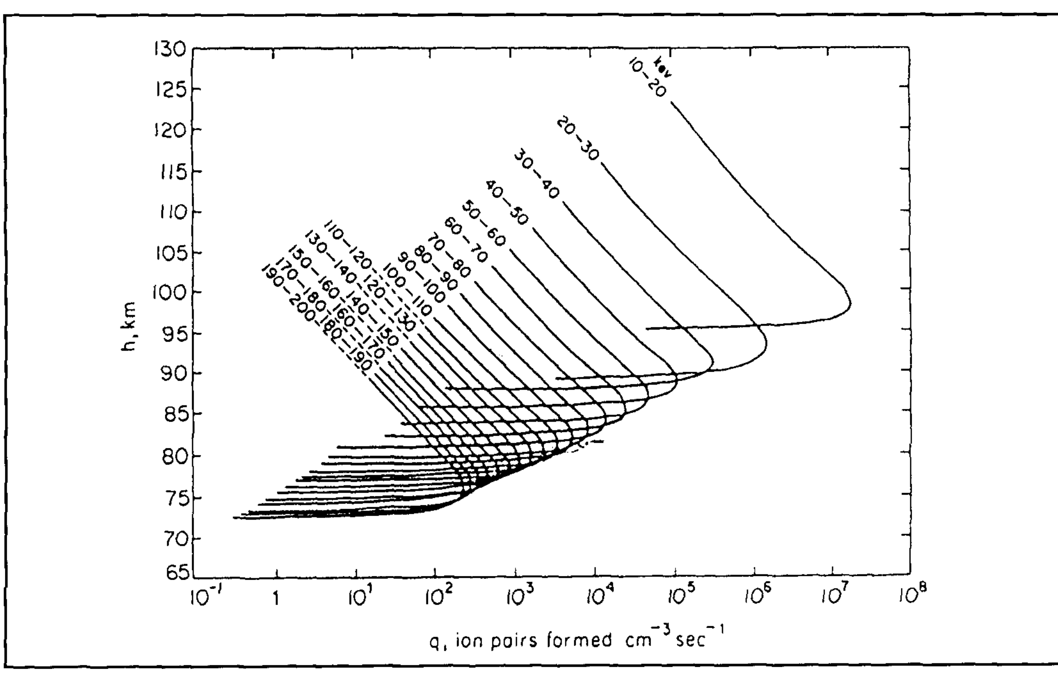

Figure 5. Ionization rate profiles for electrons of various energies.[6]

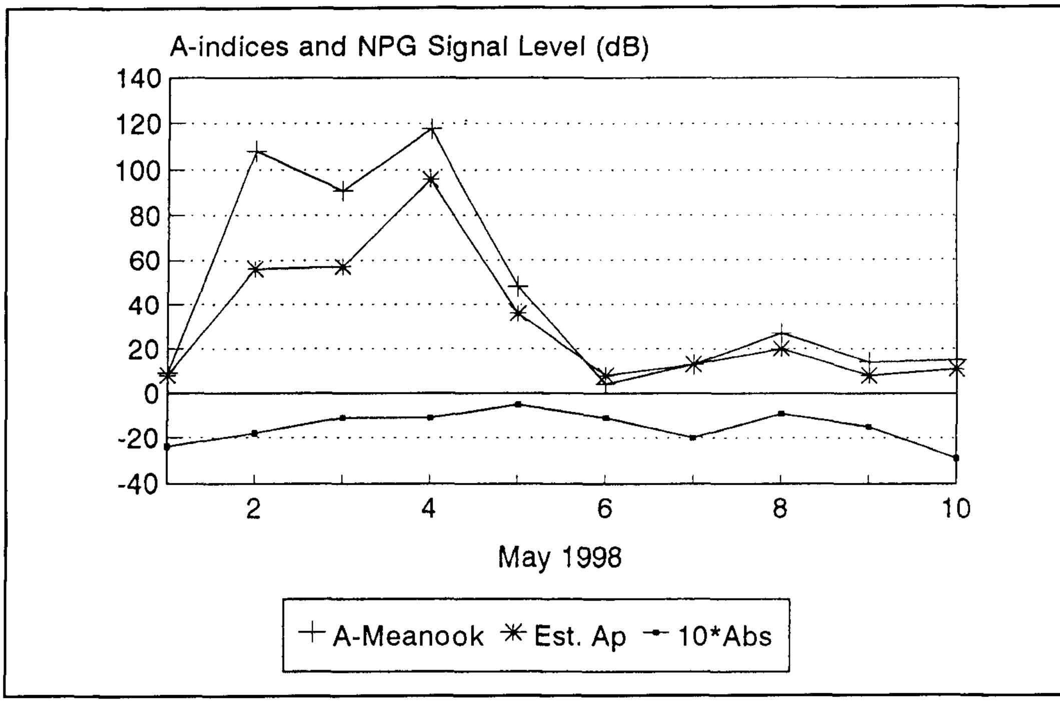

Figure 6. Magnetic A-indices and NPG signal levels for May 1 through 10.

the reflection gradient as the sun begins to rise.[7] In the absence of direct radiation by solar UV and X-rays, the gradient is due to the attachment of electrons to oxygen molecules at low altitudes, and the negative-ion to electron ratio grows to large values at low altitudes.[8] In that circumstance negative charge is lost by ion-ion recombination, but, above the gradient region, electrons are far more abundant than negative ions and are lost by dissociative recombination of positive ions with electrons.

The negative ions at the top of the *D*-region are those formed by electron attachment to atomic and molecular oxygen as well as ozone:

$O + e^- \longrightarrow O^- + \text{photon}$
$O_2 + e^- + M \longrightarrow O_2^- + M$
$O_3 + e^- \longrightarrow O^- + O_2$

where M may be O_2 or N_2. Note that molecular nitrogen does not form negative ions. Lower in the *D*-region, where heavier molecules of minor constituents (such as NO, NO_2, and CO_2) are found, it is possible that other types of negative ions may be formed (such as NO_2^-, NO_3^-, or CO_3^-) by ion-shuffling reactions with O^-, O_2^-, and O_3^-.

At night, with only galactic cosmic rays, starlight, and a weak flux of scattered sunlight, the negative ions in the *D*-region are a very weak source of electrons by photo-detachment:

$O_2^- + \text{photon} \longrightarrow O_2 + e^-$

and the release of electrons by collisional detachment

$O_2^- + M \longrightarrow O_2 + M + e^-$

does not change appreciably at night as the thermal energy of the collision partners is fairly constant. However, the associative detachment reactions:

$O^- + O \longrightarrow O_2 + e^-$
$O_2^- + O \longrightarrow O_3 + e^-$

also occur. In addition, the formation of stable negative ions of ozone occurs

$O_2^- + O_3 \longrightarrow O_3^- + O_2$

and competes with associative detachment of O_2^- in removing negative ions from the attachment/detachment cycle, making the O/O_3 ratio an important parameter in the discussion of the lower D- region.[9]

As noted above, the presence of electrons is dominant in the upper *D*-region at night as the negative-ion/electron ratio is small (above 80 to 85 kilometers altitude), because the large O/O_3 ratio favors the release of electrons from O_2^- by associative detachment. Below 80 to 85 kilometers, negative ions are dominant as the negative-ion/electron ratio is large, because the small O/O_3 ratio favors the removal of electrons at low altitudes by the formation of O_2^- and O_3^-.

It is in that transition region, where the density gradient in the electron distribution results in the reflection of low-frequency waves. With a normal sunrise, photo-detachment of negative ions and other types of direct ionization will affect the electron gradient, lowering the reflection height of low-frequency waves and changing the magnitude of the sunrise signature of NPG signals. Disturbances of the *D*-region will also affect that shift, and the question becomes which type of disturbance(s) gave rise to the observations of NPG in early May.

Disturbances

The lower ionosphere may be "illuminated" by other forms of penetrating radiation during solar and geophysical disturbances. Examples of such illumination are found in bursts of energetic solar X-rays, below 10 Angstroms wavelength, which give rise to increases in ionization over the sunlit hemisphere. Those bursts of radiation may disrupt HF communication circuits by increases in ionospheric absorption in the *D*-region, and may also produce sudden phase anomalies in VLF circuits. The latter are important for VLF applications with regard to navigation systems. In any event, the X-ray bursts are generally of short duration, lasting at most tens of minutes, are relatively infrequent, and only affect the portions of LF paths that are in daylight.

Of greater duration are the events where energetic solar protons are incident over a range of high latitudes following some solar flares. Such events, termed polar cap absorption (PCA) events, result in significant ionization increases in the lower *D*-region of the polar regions as the protons ionize heavily near the ends of their ranges. The events may last for several days and their ionospheric absorption can be quite large—up to 10 to 20 dB on 30 MHz—and can be particularly disruptive during the daytime hours for paths that cross the polar caps. However, the absorption decreases at night by about a factor of 4 because *D*-region electrons attach themselves to molecular oxygen in the absence of sunlight.

The latitude extent of solar proton bombardment during PCA events depends on the energy spectrum of the incident protons, the geomagnetic field readily allowing lower energy protons to spiral down field lines and into the polar cap. However, the field limits the access of solar protons at the lower latitudes to the small portion of the proton influx with higher energies.

To put the effects in perspective, protons in the 10-MeV (megaelectronvolt) range may reach ionospheric levels and 100-MeV protons will reach high-altitude balloons at 10-mb pressure altitude in the polar cap. Billion electron

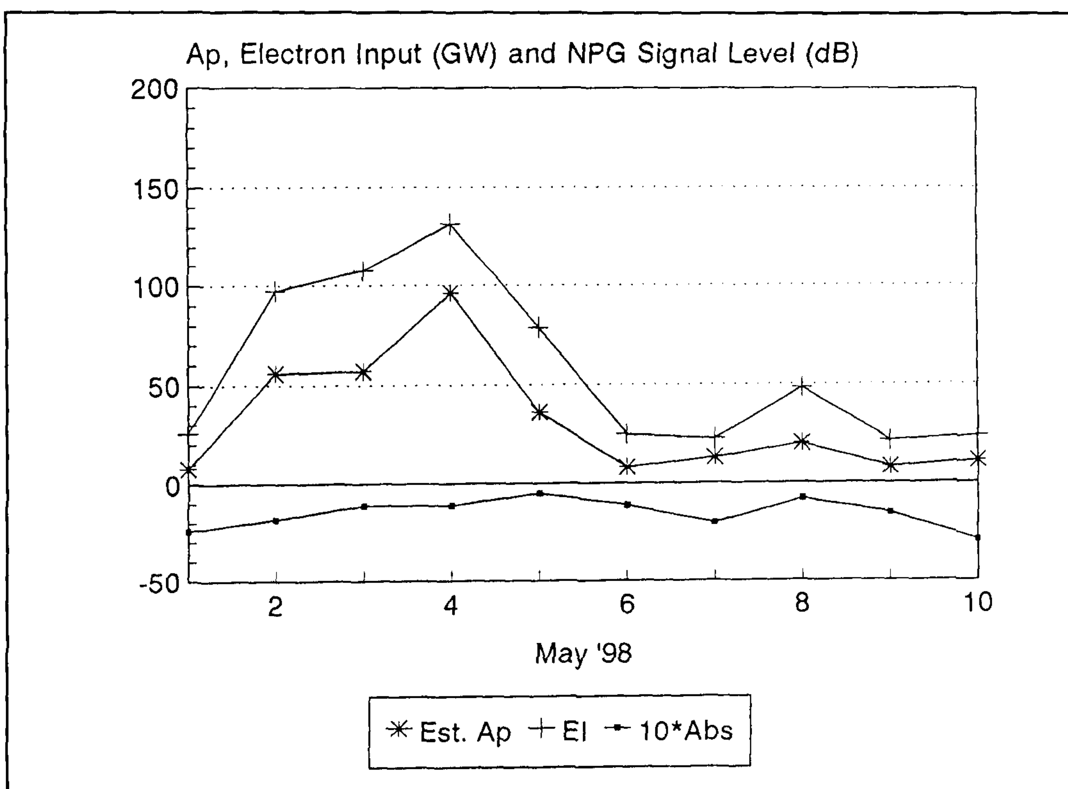

Figure 7. Estimated Ap-indices, auroral power input and NPG signal levels, May 1 through 10.

volt protons may penetrate the entire atmosphere and reach ground level at mid-latitudes, while protons above 10 BeV may penetrate to ground level at the geomagnetic equator. Although the proportions in the energy ranges vary from event to event, NOAA bulletins provide timely information on the energy spectrum of the proton influx and whether significant ionospheric absorption is noted in the polar cap at Thule, Greenland.

Some PCA events have even created an "artificial sunrise" on VLF circuits by giving rise to ionization below the nighttime gradient region and resulting in phase shifts and amplitude variations of signals. Perhaps the Great Solar Flare of February 23, 1956, was the most notable in that regard, as its radiation was energetic and intense enough to even reach ground level at the geomagnetic equator.

Other examples, less energetic but more frequent, are found at balloon altitudes. The first events of that type were observed over Minneapolis, Minnesota, and College, Arkansas, in May and July of 1959. Analysis of one proton spectrum provided ionization rates around 10 ion-pairs/cm^3/sec at 65 kilometers altitude—some 200 times the rate due to galactic cosmic rays at that altitude.[10] The most energetic event from the standpoint of energy flux was found in the series of events in August 1972, when the ionization at 65 kilometers altitude reached 60,000 ion pairs/cm^3/sec.

Needless to say, PCA events may produce an increase in ionization at low altitudes, but the extent to which they may be noted by ground-based radio observations depends on the degree to which their ionization rates exceed those of galactic cosmic radiation in the lower *D*-region and the ion-chemistry that would apply at the time in question. Thus, riometer observations of galactic radio noise passing through the ionosphere show smaller effects at night due to electron attachment in the *D*-region and rarely show effects at mid-latitudes.

Auroral/magnetic disturbances

Magnetic disturbances originate in the interaction between the solar wind and the magnetosphere. Local electrons are accelerated within the magnetosphere and then spiral down field lines to the denser portions of the atmosphere. There electrons excite atoms and molecules, giving rise to visible aurora with their characteristic spectral emissions, as well as creating intense ionization by Coulomb collisions. There is an electric field of magnetospheric origin at ionospheric heights that drives the ionization to form an electrojet current system which gives rise to disturbances in the geomagnetic field at ground level.

The magnetic disturbances associated with those events are detected by magnetometers and reported as departures from quiet-day levels of the field. Two networks collect such data from a number of stations and report disturbances as K-indices, on a quasi-logarithmic scale, in three-hour intervals.[11] Those indices are used to obtain an estimate of the global energy input into the magnetosphere from the solar wind and are used widely by the scientific community in the analysis of phenomena related to the geomagnetic field.

Most of the ionization created during auroral displays is from low energy electrons, in the tens of keV, reaching the *E*-region and is limited to altitudes between 90 and 150 kilometers, as shown in **Figure 5**.[6] Unlike ionization during PCA events, ionization in auroral events is distributed over narrow ranges in latitude and wide ranges in longitude, and the ionization results in ionospheric absorption of radio signals traversing the regions.

In the particle spectra of auroral events, there are some electrons with higher energies—up to 100 to 200 keV. They will give rise to weak X-ray fluxes that penetrate deeper in the atmosphere to produce ionization in the lower *D*-region. Balloon- and rocket-borne radiation detectors have examined these aspects of auroral events and compared them with simultaneous observations of ionospheric absorption due to the low-energy component in auroral electron fluxes.[12]

In addition to particle influxes associated in time with solar activity, there is a large reservoir of energetic electrons that have become trapped in the geomagnetic field, known as the Van Allen Radiation Belt. Those electrons can be dumped or leak out into the atmosphere. Thus, brief periods of electron precipitation at high latitudes have been observed at the sudden commencements of magnetic storms and steady leakage at lower latitudes found at magnetic anomalies, off Brazil and South Africa, where trapped electrons can spiral down and encounter the upper reaches of the atmosphere.[13]

Beyond those sources of ionization from particle influx, it should be noted that the neutral atmosphere, through the electron detachment processes discussed above in connection with the lower *D*-region, may contribute to the electron density—at least in regions where ozone is not present in significant amounts. Normally such a source would not be considered in a discussion of ionospheric disturbances, as most effects in the nighttime hours at higher latitudes are due to charged particles. However, it is possible that the transport of atomic oxygen from its reservoir at about 100 kilometers altitude could be induced and alter the rate of electron detachment from O^- and O_2- ions below the 80- to 85-kilometer level at lower latitudes. This will be discussed further, after the introduction and discussion of observational material concerning sunrise effects on low-frequency propagation.

Solar/terrestrial events in May

For the first 10 days in early May, 1998, sunrise signatures for NPG were obtained around 1230 UTC. The beginning of the month was quiet magnetically, with a planetary Ap-index of 8. The first signature record began with a decrease of -2.4 dB on May 1. In the ensuing 10-day period, the first geomagnetic storm occurred at 2158 UTC on May 1, due to an earlier event on April 29, and then declined. Another class 3B solar flare occurred at 1342 UTC on May 2, and a satellite proton event began at 1405 UTC. This was accompanied by a PCA event with 3.7 dB absorption on 30 MHz at Thule, Greenland, ending at 0310 UTC on May 4.

That flare produced a complex solar wind structure which passed the ACE spacecraft in front of the Earth at 0229 UTC on May 4. Thirty minutes later, it was observed at the Earth and gave rise to a storm's sudden commencement at 0300 UTC. Severe storm levels of magnetic activity (K = 8 and 9) were encountered in the first six hours of the storm, followed by major storm levels until 0900 UTC on May 5, and then quiet to unsettled conditions for the next two days. In that period, the LF sunrise signature decreased and reached -0.4 dB at midday UTC on May 5 and then went back toward the level of May 1.

Another major flare occurred at 0809 UTC on May 6 and was followed by a brief solar proton event, starting at 0835 UTC and ending at 1335 UTC on the same day. While both solar proton events—May 2 and May 6—involved 100-MeV protons, there is no indication that ionospheric effects reached major proportions or extended to latitudes below the auroral zones.

As for geomagnetic activity in the first 10 days of May, that is expressed in terms of A-indices derived from three-hour K-indices. Those are quasi-logarithmic averages of the departures of the geomagnetic field from quiet-day levels. The A-indices used here are from observations made in the Northern Hemisphere, as that is where the LF propagation is being studied. Those values are taken from a string of eight magnetometers running from Alaska to England and are shown in **Figure 6**, along with A-indices from the auroral zone magnetometer at Meanook, Alberta, Canada (62.5N corr, mag. lat.), and with NPG sunrise signal levels. In connection with that figure, remember that the signal level is a spot value in the interval between 1215 UTC and 1300 UTC in the first

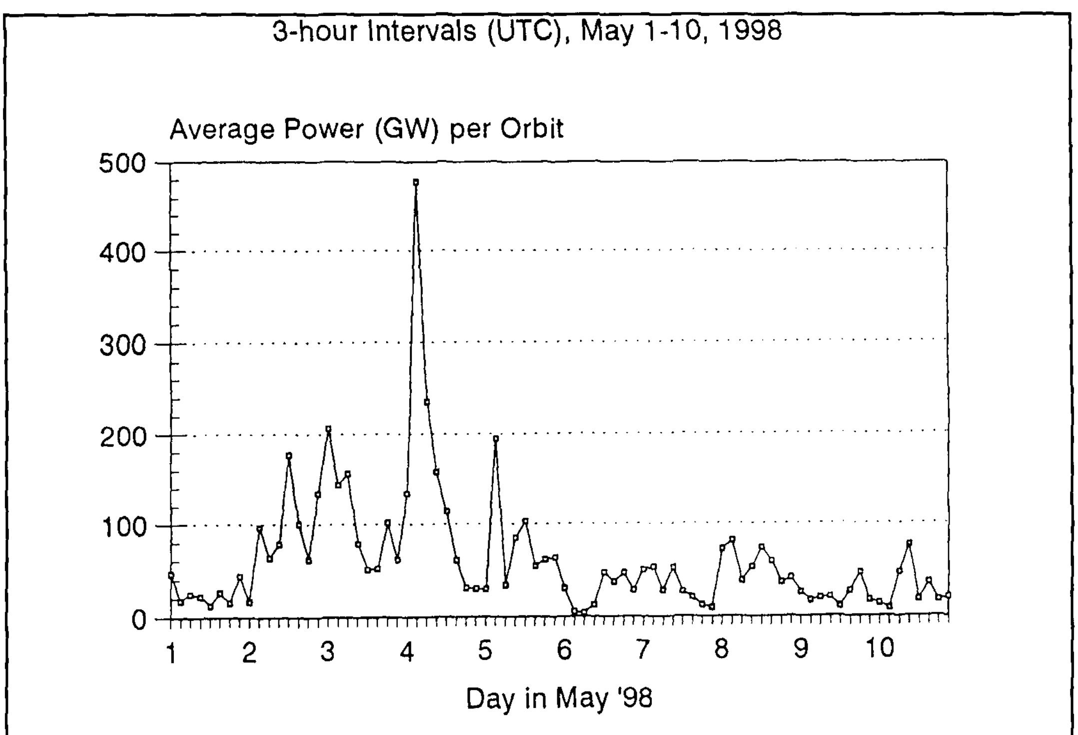

Figure 8. Average electron power input per orbit, May 1 through 10.

10 days of May, while the A-indices characterize magnetic activity at high latitudes for the full 24 hours of a day.

As noted earlier, A-indices may be used to obtain something of a qualitative estimate for the global energy input to the magnetosphere from the solar wind. Another approach, directly in terms of energy, is obtained from particle detectors aboard NOAA/TIROS satellites. The satellites carry detectors that measure the auroral electron influx from 0.2 to 20 keV on each pass across the auroral zones, and, from the statistics of a large number of observations, an estimate of the power input (given in gigawatts) to the hemispherical region poleward of 45 N latitudes can be obtained from each satellite pass.

Data from a large number of satellite passes show hemispheric power inputs for each satellite pass that ranges from less than 2.5 GW for quiet conditions (K<1) to more than 500 GW for severe storm conditions (K = 8–9). For the first 10 days of May, observations were available from passes of the NOAA 12 and 14 satellites. The lowest level of energy input was 1.5 GW at 0726 UTC on May 6, while the highest level was 478 GW on the northern pass at 0403 UTC on May 4.[14] The daily averages of electron energy input, along with the Ap-indices and NPG data, are shown in **Figure 7**.

The same satellite data, now in terms of average power input per orbit in three-hour intervals like the K-index, are shown in **Figure 8**. The very large energy flux on May 4 was on the pass at 0403 UTC, after the sudden commencement of the magnetic storm at 0300 UTC. In addition to providing data on the energy influx, the satellite data may be used to obtain a statistical view of the spatial distribution of the auroral electron influx, according to time of day and magnetic activity.

In the first geophysical activity during the first five days of May, the NPG signal strength variation decreased at sunrise, indicating that the reflecting region at the start of the sunrise sessions was decreasing in altitude throughout that period. It reached its lowest value on May 5 when the signal depression was only -0.4 dB. In that regard, **Figure 9** shows a map in azimuthal equidistant projection with the estimated locations of the auroral ovals at 1230 UTC on May 5, when the severe magnetic activity had subsided and the K index was down to 5.

That map is centered on NPG and the path of interest is to the north, ending in the Strait of Juan de Fuca. The midpoint of that path, where the reflection of 55.5-kHz signals takes place, is well below the equator-ward edge of the northern auroral oval, in British Columbia. That, plus the fact that low-energy auroral particles cannot directly reach the lower *D*-region, presents a problem in explaining the lowering of the reflection region in the first part of May when the activity was so high. In fact, the magnetic activity peaked early on May 4 with K = 9, while the NPG signal strength reached its lowest level more than a day later. Thus, the question becomes how an LF reflection region at a mid-latitude is lowered during times of magnetic activity and influx of low-energy electrons largely at auroral latitudes.

The answer is obtained, in part, by going to higher energies in the electron spectrum. Kikuchi and Evans noted VLF phase anomalies associated with the precipitation of electrons above 300 keV.[15] But, in contrast to the present observations on a short mid-latitude path, those observations were on paths longer than 7000 kilometers which crossed auroral latitudes or went through sub-auroral latitudes. Their observations of VLF phase anomalies indicated that the origin, in times of magnetic activity when sums of K-indices were high, was found first in the precipitation of energetic electrons during times when auroral electrojet current systems were present. In addition, their observations suggested precipitation of energetic electrons from the trapped electron population, but with a delayed onset relative to the magnetic activity and a longer duration.

Energetic electron data

In addition to the 0.3- to 20-keV electron detectors, NOAA satellites also carry solid-state detectors that provide flux data for electrons with energies >30 keV, >100 keV, and >300 keV. Those observations are at altitudes around 850 kilometers, and the electron fluxes measured there are from two view directions: one for electrons in the loss-cone along the field lines, which would reach the atmosphere; the other for electrons of the trapped population that were mirroring in the geomagnetic field and would not reach down to the atmosphere. For the electrons in the loss cone, their observation point at satellite altitude is mapped down field lines to the latitude and longitude at the foot of the field line where the flux would impact the 120-kilometer level of the atmosphere. For numerical calculations, the flux coming down along the field lines can be corrected to a flux incident perpendicular to the atmosphere by using the dip angle of the field line at 120 kilometers obtained from the International Geomagnetic Reference Field.[16]

Auroral electrons with energies in the tens of keV give rise to collisional ionization at heights just below the nighttime *E*-region, as shown earlier in **Figure 5**. But electrons having ener-

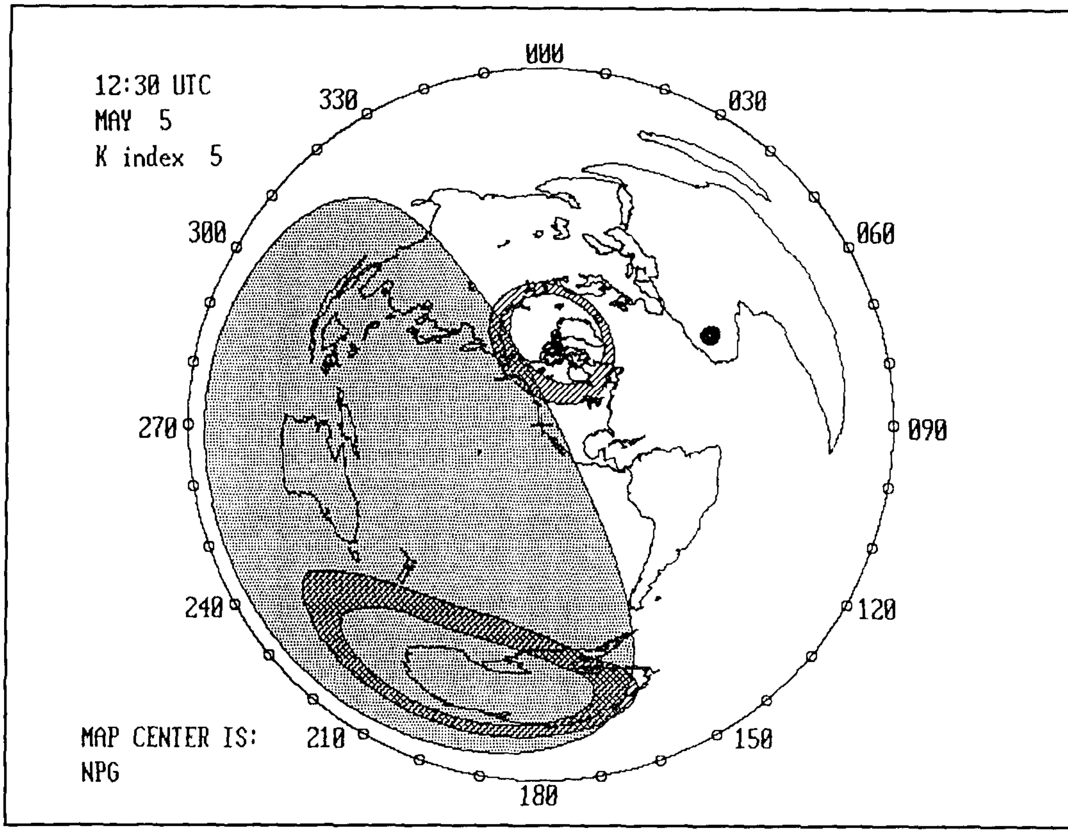

Figure 9. Azimuthal equidistant map centered on NPG for May 5.

gies around 100 keV penetrate deeper, with their collision loss peaking around 80 kilometers, while electrons with energies around 300 keV penetrate even further and their peak collision loss is below 75 kilometers. Clearly, the more energetic parts of the electron influx are of interest to questions concerning low-frequency propagation as they would penetrate into the reflecting regions.

For the first 10 days of May, an effort was made to obtain energetic electron data from passes when the satellite was in the vicinity of the midpoint of the LF path. But since the satellite is in a sun-synchronous orbit, such a demand reduced the number of passes available for data purposes to those going through the region around 1 to 3 UTC and 13 to 15 UTC—the latter closest to the sunrise observation period.

In contrast to the numerous satellite passes each day which provide energy deposition data on two northern auroral zone crossings per orbit, only 18 passes at lower latitudes were available for the LF study of the 10-day period in May. Those passes were within ±2 degrees (222 kilometers) of latitude and ±10 degrees (800 kilometers) of longitude from the midpoint of the path. Within those limits, the detector counting rate for the >300 keV-channel nearest the latitude of the midpoint of the path is given in **Figure 10** and shows a low background counting rate of about 0.4 counts/sec until after the first pass on May 6. After that, the detector rate peaked at 51 counts/sec on May 8 and then declined.

For the >30-keV and >100-keV channels, background rates were about 8 counts/sec and 4 counts/sec, respectively, and the rates corresponding to the time when the >300-keV channel peaked were 233 counts/sec and 182 counts/sec, respectively. But, like the >300-keV channel before May 6, the >30-keV and >100-keV channels did not show any counting rates significantly above background near the midpoint of the LF path in the first part of May.

While the >30-keV electrons would not penetrate into the lower *D*-region, electrons recorded on the other energy channels would, and it is interesting to find the extent to which their ionization could influence the level of the LF reflecting region before sunrise. Turning to the ionization rates shown in **Figure 5**, it is clear that the higher energy electrons lose most of their energy by collisions in the denser portions of the atmosphere, say from 150 kilometers down to about 75 kilometers. In that height range, the ionization rates of the energetic electrons rise two to three orders of magnitude, peaking near the bottom of the nighttime *D*-region, then falling to zero at the end of their physical ranges.

That being the case, one simple approach to see if the influx of energetic electrons can affect LF propagation is to determine the column rate of ionization—in ion-pairs/cm^2/sec, which they would create in the LF reflection region—and compare that with the column rate of ionization in the same region in their absence, under quiet conditions. The latter is readily calculated as the ionosphere has reached a steady-state in the hours since sunset, and equilibrium methods would apply by dawn. Thus, the lower electron density profile shown in **Figure 11**, obtained from the International Reference Ionosphere for the time and solar conditions of interest, would be an appropriate one to use.[7] The higher electron density profile in that figure is for midday and is included so, by comparison, it shows what a weak source of ionization supports the *E*- and *D*-regions at night.

To calculate the column ionization rate of the energetic electrons, say between 100 keV and 300 keV, the geometrical factor of the detector, as well as an estimate of the electron spectrum, are needed. The geometrical factor is readily available from the results of laboratory calibration and converts counting data to electrons/cm^2/sec above the energy threshold. The form of the energy spectrum was assumed to be exponential

$$J(>E) = A \exp(-E/E_0) \qquad (1)$$

for the flux of electrons with energies greater than E, and then ratios of the counting rates for >100 keV and >300 keV are used to estimate E_0. This form of electron spectrum has no particular foundation in theory but is often used when more energetic particles are involved, and, in the present instance, E_0 is about 220 keV.[17]

The next step is to calculate the energy carried in by electrons between 100 keV and 300 keV in that spectrum. Given the ionization curves in **Figure 5**, it is clear that practically all that energy would be dissipated between 75 and 150 kilometers, and, having obtained the energy flux in eV/cm^2/sec, use of the value of 34 eV for the energy to form an ion-pair in air gives the number of ion pairs/sec formed in that square-cm column, some 2.6 x 10^8 ion-pairs/cm^2/sec.[8]

For comparison, the ionization rate in the nighttime ionosphere is obtained from the lower electron density profile in **Figure 11**, say at 2.5-kilometer intervals between 75 kilometers and 150 kilometers, using the average dissociative recombination rate coefficient for the molecular ions present (NO^+ and O_2^+). Assuming ionization equilibrium, ionization production rate is then given by the rate of dissociative recombination. Correcting for the presence of negative ions at the greatest depths, that provides a profile with the greatest ionization rate around 105 kilometers and a column ionization rate of 5 x 106 ion-pairs/cm^2/sec between 75 and 150 kilometers.

Making the comparison, the influx of electrons between 100 and 300 keV coming from the trapped electron reservoir ionizes the region at a rate some 50 times greater than the normal nighttime sources of ionization: galactic cosmic rays as well as starlight and scattered solar radiation. Since the energetic electrons ionize at a greater rate near to the end of their ranges, that difference in column ionization rates would be capable of lowering the LF reflecting region. This is in contrast to electrons of lower energies, like those found at auroral latitudes, which would not be able to directly affect the LF propagation region at middle latitudes.

Before leaving this subject, the methods used above for the electrons in the 100- to 300-keV energy range were applied to those in the lower energy interval, from 30 to 100 keV. There, the column ionization rate of the incoming electrons was about 45 times greater than the normal nighttime sources of ionization. As noted earlier, electrons in that range ionize at somewhat higher altitudes and would not be expected to seriously affect the height of the LF reflection region. However, over heights in the *E*-region, they would contribute to a rather significant increase in electron density and have an effect on any 160-meter signals traversing the region.

For the electrons above 300 keV, the calculations are more approximate, as only that one integral flux value is available in contrast to two values for calculations at the lower energies. But assuming the e-folding energy, E_0, is about the same as for the 100- to 300-keV range, their column ionization rate is about 10 times greater than normal nighttime ionization sources. But those electrons would ionize down to the bottom of the *D*-region, too.

Discussion

The solar/terrestrial activity in early May of 1998, with the Ap-index reaching 101, was unusual—nothing comparable had taken place since 1992. The first six days involved a tremendous energy input in the form of auroral electron influx with a corresponding response in geomagnetic terms, as shown in **Figure 7**. In the next four days, the energy input was down by at least a factor of two. But, on both occasions, the NPG sunrise signature on the mid-latitude path reached low values, -0.4 dB on

May 5 and 8, showing a lowering in the height of the LF reflecting layer before sunrise.

Those results can be understood only for May 8 when the NOAA satellite showed energetic (>100 and >300 keV) electrons being deposited on the atmosphere over the propagation path. There was no indication of such ionization in the first five days, so the propagation effects at that time (a slow decrease in signal strength at dawn, day after day) cannot be understood in terms of any direct processes. Indirectly, there is the possibility that the effects resulted from the influence of the great energy deposition on the neutral atmosphere and the propagation of its effects to lower latitudes.

Before getting to that, it is appropriate to comment on the difference between the present observations, where the sunrise signature suggests the nighttime reflecting level was at a *lower than normal* altitude before sunrise began, and the earlier work on VLF phase anomalies for paths across auroral latitudes. First, with those long VLF signal paths, more than 7,500 kilometers, location of the satellite observations of the influx of energetic electrons was not deemed crucial. In fact, the satellite data never gave fluxes along the paths in the study. Instead, the association of VLF phase anomalies with electron influx was made in terms of the energetic electrons being able to penetrate to the reflection region and, with time, using the fact that electron influx at auroral latitudes observed by the satellites just happened to coincide in time with the phase anomalies. Other, closer associations were made between the VLF phase records and those of magnetometers along the paths.

In the present case, the association of satellite data on the influx of energetic electrons with LF signals is made from the satellite observations within a spatial window (±222 kilometers in latitude, ±800 kilometers in longitude) over the midpoint of the LF path. The times of the satellite passes were after LF observation periods by a couple hours since the satellites are sun synchronous and cross the equator at the same sub-satellite local time throughout the year. So, in the absence of data obtained more directly, say from balloon-borne X-ray detectors or rocket-borne electron detectors flown from right under the LF path, the present satellite data will have to suffice as it is about the best that can be obtained. But it is presumed to apply to the discussion around the time of sunrises on the LF path, given the duration of the geophysical activity.

Turning now to the indirect possibility of effects on the sunrise signature through the neutral atmosphere, it was mentioned earlier that ionospheric electrons in the *D*-region may become attached to oxygen molecules to form negative ions, and the ratio of negative ions to electrons is large at night—on the order of 1,000 around 70 to 75 kilometers. That situation results from the low concentration of atomic oxygen in the region, negative ions from collisional attachment surviving due to only small loss rates from associative detachment by O atoms. While that is usually the case, the day-to-day variability of the NPG signal loss in **Figure 2** suggests the role of atomic oxygen may be variable, with fluctuations in its number density resulting in variations of the height of the reflecting region before sunrise.

If that were the case, it would also be possible to have similar effects, perhaps even

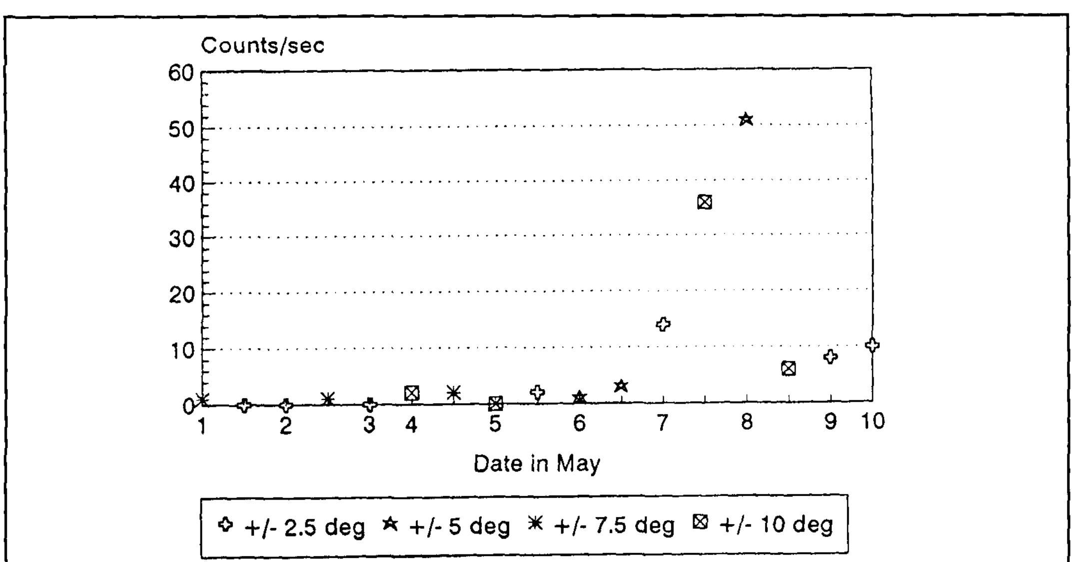

Figure 10. Counting rates of a NOAA satellite detector near the path midpoint for electrons with energies >300 keV, May 1 through 10.

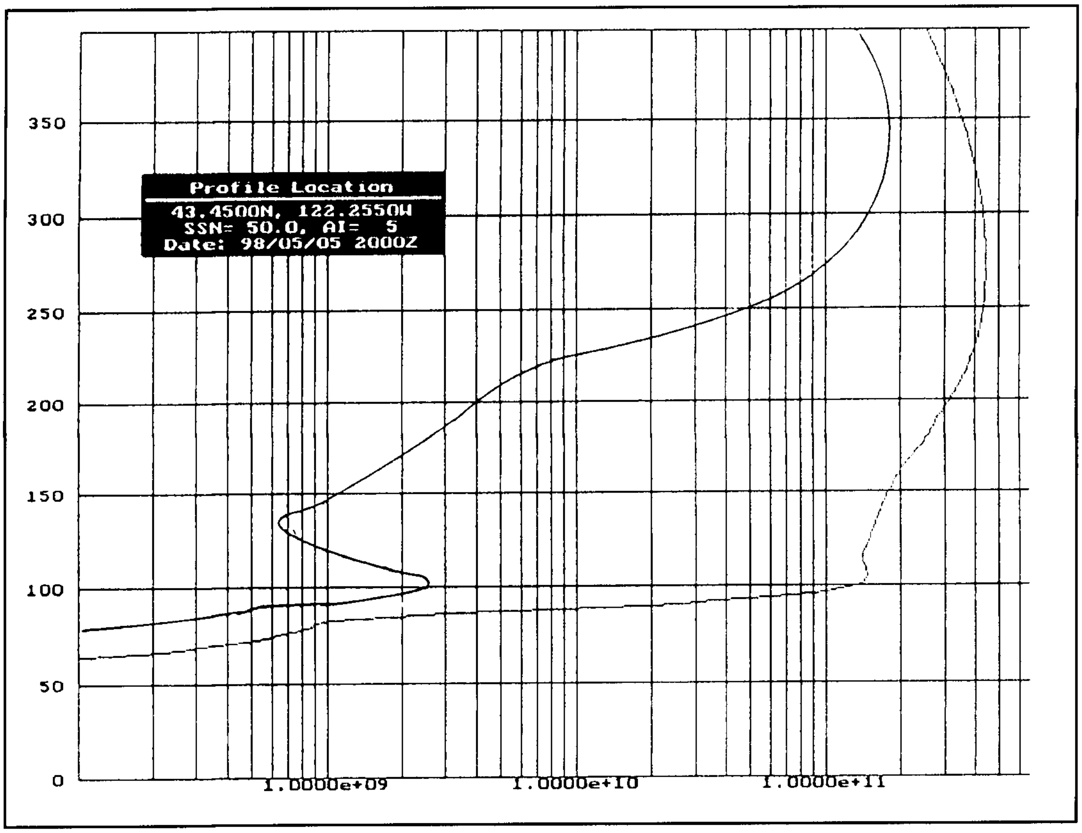

Figure 11. Electron density profiles for dawn and midday over LF path midpoint, May 5.

greater, during times of magnetic disturbance. This is because atmospheric gravity waves are generated by heating from energy deposition by auroral electrons and Joule losses by ionospheric currents.[18] Those waves can have wavelengths on the order of 1,000 kilometers and periods from 30 minutes to three hours. Thus, strong magnetic and auroral activity in the first five days of May could have provided the heating to excite the gravity waves.

Further, equator-ward motions of traveling ionospheric disturbances (TID) generated by gravity waves have been noted, with TIDs advancing equator-ward from both auroral zones at the same time and producing ionospheric effects at locations within 10 degrees of the geomagnetic equator.[19] On that occasion (November 9, 1979), an auroral substorm began with a magnetic excursion of -1400 nt in the horizontal component of the field on the record of the College, Arkansas, magnetometer. Magnetic activity persisted for two hours and was characterized by K = 6.

Turning to the present instance, the closest magnetometer to the LF path is located at Meanook, Alberta (54.6N, 246.7E). In the buildup of magnetic activity that developed in the first five days of May, the disturbance at Meanook was greater than that cited above, and the K-index was 6 or greater for 16 different three-hour periods. Moreover, the distance from Meanook to the midpoint of the LF propagation path is only 1400 kilometers, about one-fourth the distance the TIDs reached in the earlier event. In short, it was a time of continuing, intense energy deposition at auroral latitudes. This suggests atmospheric gravity waves were excited during that extended period, and, over the shorter distance where the wave action would remain strong, the waves could well have brought a significant disturbance to the LF propagation region at mid-latitudes.

Looking at the change in NPG signals, the decrease in the sunrise signature from 2.4 dB to 0.4 dB over the first five days of May, and the amplitude-number distribution of signals in **Figure 2**, the probability of such a sequence of values occurring at random is less than 1 in 100. That being so, one can consider that atmospheric gravity waves were indirectly associated with the effects. As for the mechanism, that would appear to be the ion-chemistry of the *D*-region.

In the LF propagation region, an atomic oxygen reservoir, as it were, is overhead, at 90 to 110 kilometers where the number density is on the order of 1011/cm^3 just before sunrise. On the other hand, the atomic oxygen density at 75 kilometers before sunrise is around 108/cm^3, and any significant downward circulation and mixing induced by atmospheric gravity wave motion would serve to increase the atomic oxygen content in the *D*-region. That, in turn, would affect the associative detachment rate of negative ions, releasing electrons to increase the electron density gradient.

The magnitude and distribution of the effect would depend on the details of the downward transport of O atoms, and the increase in electron density from electrons detached from negative ions would be in proportion to the increase in density of O atoms; e.g., a 50-percent increase in electron density from a 50-percent increase in atomic oxygen, etc. But, in the absence of any additional ion production, any change in the electron density due to a decrease in the negative-ion/electron ratio could only approach the level that would be expected from the nighttime sources of ionization. On that basis, the effect of atmospheric gravity-wave activity would be greatest just below the nighttime reflecting level.

In the absence of such transport of atomic oxygen, the effect of ionization by energetic electrons leaking from the radiation belt before sunrise would be to increase the electron density in the lower reaches of the *D*-region without any change in the negative-ion/electron ratio. As such, that would also change the initial reflection height of LF signals and result in a smaller change in path length or phase in the interference of skywaves and the groundwave at sunrise. The details of this type of effect would depend on the nature of the spectrum of the electrons coming down the field lines. Lacking that information in the present instance, the comparison of column ionization rates is about all that is warranted.

Finally, instead of changes in the *D*-region arising from disturbances coming down from above, it has been suggested that changes in the electron density profile come from below, due to solar EUV in the early part of sunrise being blocked by absorption in the ozonosphere.[20] This would prevent the dissociation of oxygen molecules into atomic oxygen, which then releases electrons from negative ions by associative detachment. It would also prevent photo-detachment by solar radiation. By that token, variations in the ozone altitude profile could contribute to the spread in daily signal recordings of NPG, noted earlier.

Conclusion

In connection with the possibility of atmospheric gravity waves indirectly affecting LF propagation, it was noted by the IPS Radio and Space Services of the Australian Space Forecast Centre that ionospheric critical frequencies during May 4 were enhanced in the northern Australian region and depressed in the southern region. While the use of satellite data on auroral electron influxes was limited to the northern auroral zone in the present study, there were comparable effects recorded on passes across the southern auroral zone. That being the case, an inquiry was made as to whether the ionospheric effects noted in the southern hemisphere were due to TIDs, from atmospheric gravity waves. Unfortunately, that proved inconclusive as the hourly sampling period of the ionosondes was too infrequent to provide sufficient details to determine whether TIDs were involved or not. However, more frequent observations, even at five-minute intervals, are planned for the future.

Given that there is no means of directly measuring the atomic oxygen density on a regular basis in the lower *D*-region, the circumstantial case for effects from atmospheric gravity waves will rise or fall on whether TIDs and similar LF effects are found in future major magnetic storms. This also depends on the continuation of efforts at monitoring LF signals.

As for the energetic electron influx during the second half of the period of interest, it was unusual in that it penetrated to such low latitudes.[14] Just how often such an influx will happen again is open to question, but there is little doubt that the energetic electrons leaking out of the radiation belt had an effect on the height of the LF reflection region.

A review of the levels of magnetic activity around the peak of solar cycle 22 shows that major magnetic storm levels were not unusual, being present about twice a month and having significant durations. It will be interesting to see if LF effects, such as those noted here, occur that frequently in the upcoming solar maximum. With the extensive solar warning network now in place, such effects could be looked for with reasonable hopes of success.

As noted earlier, the high energy electrons at low latitudes were also accompanied by electrons which were unable to reach the *D*-region. However, their energies were sufficient to penetrate to the ionospheric levels where 160-meter signals are propagated. That being the case, they represent yet another form of disturbance for operations on that band. In any event, the NOAA satellites are expected to continue in operation for the foreseeable future and the present LF monitoring program will continue, at least through the upcoming 160-meter DX season, so further results may be forthcoming as well as comparisons with conditions on the 160-meter band.

Acknowledgment

I am indebted to Dr. David S. Evans of NOAA for the satellite data on auroral electron

influx as well as energetic electron influx in the vicinity of the LF propagation path. In addition, I wish to acknowledge the prompt reply by Dr. Phillip Wilkinson, IPS Radio and Space Services, to my inquiry about TIDs in the southern hemisphere. ■

REFERENCES

1. R.W., "Schunk, Magnetosphere-Thermosphere-Ionosphere Coupling Processes," *Proceedings of the SCOSTEP Symposium*, XXVII COSPAR Plenary Meeting, Helsinki, 1988.
2. R.R. Brown, "Signal Ducting on the 160-Meter Band," *Communications Quarterly*, Spring 1998, pp. 65–82
3. A. Hall-Patch, *The Top Band Anthology*, Vol. 1, West Washington DX Club, July 1998.
4. A.D. Watt, *V.L.F. Radio Engineering*, Pergamon Press, 1967.
5. K. Davies, *Ionospheric Radio*, Peter Peregrinus Ltd., London, 1989
6. R.C. Whitten and I.G. Poppoff, *Fundamentals of Aeronomy*, John Wiley and Sons, 1971.
7. D. Bilitiza, *International Reference Ionosphere (IRI 90)*, National Space Science Data Center, Greenbelt, MD, 1990.
8. A. Brekke, *Physics of the Upper Polar Atmosphere*, John Wiley and Sons, 1997.
9. G.C. Reid, *Physics of the Sun*, Vol. 3, D. Reidel Publishing Company, 1986, p. 251.
10. R.R. Brown and R.A. Weir, Ionospheric effects of solar protons, *Arkiv. for Geophysik*, Vol 3, p. 523, 1962.
11. M. Menvielle and A. Berthelier, "The K-derived planetary indices, description and availability," *Review of Geophysics*, Vol. 29, p. 415, 1991.
12. R.R. Brown, "Electron precipitation in the auroral zone," *Space Science Reviews*, p. 311–387, D. Reidel, Dordecht, Holland, 1966.
13. J. Ortner, B. Hultqvist, R.R. Brown, T.R. Hartz, O. Holt, B. Landmark, J.L. Hook, and H. Leinbach, "Cosmic noise absorption accompanying geomagnetic storm sudden commencements," *Journal of Geophysical Research*, Vol. 67, p. 4169, 1962.
14. D. Evans, NOAA, private communication.
15. T. Kikuchi and D.S. Evans, "Quantitative study of substorm-associated VLF phase anomalies and precipitating energetic electrons on November 13, 1979," *Journal of Geophysical Research*, Vol. 88, p. 873, 1983.
16. International Geomagnetic Reference Field, NGDC, Utility Programs for Geomagnetic Fields, National Geophysical Data Center, Boulder, Colorado, 1996.
17. D.K. Bailey, R.R. Brown, and M.H. Rees, "Simultaneous forward-scatter, riometer and bremsstrahlung observations of a daytime electron precipitation event in the auroral zone," *Journal of Atmospheric and Terrestrial Physics*, Vol. 32, p. 149, 1970.
18. R.D. Hunsucker, "The Sources of Gravity Waves," *Nature*, Vol. 238, Nr. 6127, p. 204, July 1987.
19. L. Hajkowicz and R.D. Hunsucker, "A simultaneous observation of large-scale TIDs in both hemispheres following an onset of auroral disturbances," *Planetary Space Science*, Vol. 35, p.785, 1987.
20. G.C. Reid, "A study of the enhanced ionization produced by solar protons during a polar cap absorption event," *Journal of Geophysical Research*, Vol. 66, p. 4071, 1961.

PRODUCT INFORMATION

New Svetlana Web Site

Svetlana Electron Devices, Inc., invites you to browse their new Web site, The Svetlana Tube Zone, at <www.svetlana.com>. The site contains information on the tube industry with access to specific technical information. You will find:

1. Data sheets on Svetlana products, which can be downloaded in Adobe Acrobat format.
2. A tube search section that offers general characteristics on virtually every popular tube type ever made.
3. Online help and technical support which can be reached directly by e-mail.
4. A technical support section that includes Svetlana Technical Bulletins.
5. A list of related Web sites.

If you have any questions, please call, write, or e-mail Svetlana at 8200 South Memorial Parkway, Huntsville, Alabama 35802; Phone: (256) 882-1344; Fax (256) 880-8077; E-mail: <info@svetlana.com>.

Vibroplex Wooden Key Case for Original "Bug"

Vibroplex® now offers wooden key cases for the Original "Bug." Cases are handcrafted from hardwood, with brass hinges and handles. The interior is felt-lined and designed to hold your bug in place while transporting. On top of each case is a serialized Vibroplex logo plate.

Availability of these wooden cases is limited. The price is $119.95 plus shipping and handling. For information call The Vibroplex Co., Inc. at (334) 478-8873 or Fax (334) 476-0465.

Edited by Peter Bertini, K1ZJH
Senior Technical Editor

While there's no particular theme for this issue, we do offer three interesting notes. First, from K1BQT, "The Mini Sky Needle" tower alternative, for those who can't install a permanent tower at their QTHs. Second, from Amateur Radio the Journal of the Wireless Institute of America, *VK6UU, offers a VHF/UHF signal generator. Finally, VE2BRH, shares a useful accessory he came up with for the MFJ-259 SWR Analyzer. Enjoy!*
—de K1ZJH

The Mini Sky Needle

A tower alternative for antenna experimentation

Rick Littlefield, K1BQT

The RadioShack 36-foot, four-section telescoping mast (RS 15-5067) provides a great low-cost platform for lightweight antennas. You can raise or lower it quickly by loosening the locking clamps, and each mast section is interlocked so individual sections can't pull out accidentally. I use mine un-guyed, with the bottom section side-mounted to the building (in this case, my house) for support. To maximize load capacity, I mounted the rotor at the base—sky-needle style—where it turns the entire mast though a homemade thrust bearing located at the roofline (see **Figure 1**).

The rotor is a used Alliance HD-73 acquired on a swap net. While not a "monster" as far as rotors go, the HD-73 is readily available, fairly inexpensive, and rugged enough to do the job. Mine is plate-mounted on a shelf support that is lagged to the side of the building (pipe mounting could also be used if the base pipe is immobilized against rotation). The mounting shelf is built from hardwood using "screw-and-glue" construction and painted to match the house (see **Photo A**).

I installed the support bearing above the point where the first section of pipe flares in to fit the second section. The "bearing" is actually an aluminum casting sold at marine stores for supporting a wooden dock on 2-inch pipe. To ensure a good fit and smooth rotation, I finished the inside of the casting sleeve with a hand grinder and greased it prior to installation. If you install the bearing higher up on the second section of mast, you may need to sleeve the mast in to provide proper clearance. The mast should turn freely without binding, but should not be so loose as to rattle in the wind.

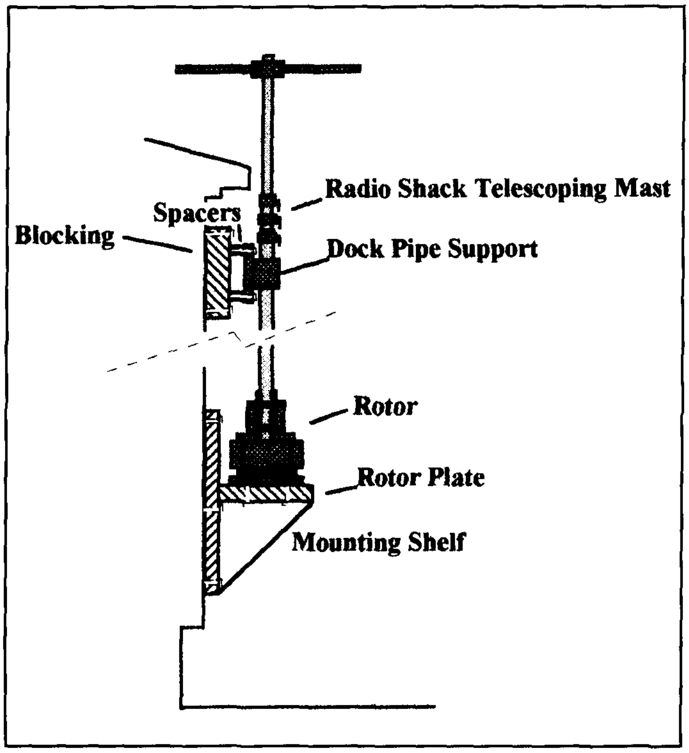

Figure 1. For rotor-plate mounting, a shelf is side-mounted to the building. The mount will be stronger if you are able to lag into support studs behind the wall sheathing.

Before installing, I test-assembled the entire structure horizontally on a level surface and made four standoff spacers for the support bearing. These were cut from aluminum tubing to the exact length required to "level" the mast (if the mast is level in the horizontal plane, it should be vertical when mounted to a sidewall).

Although I use the mast primarily for experimentation, one or more antennas are mounted on it most of the time where they regularly undergo the rigors of New England weather (including the disastrous ice storm of 1998). This survivability suggests the "sky needle" idea might work for more permanent residential installations where a larger tower would be prohibited.

However, one word of caution! What you install on the mast—and how far you extend it—deserves careful planning and consideration. When overloaded or subjected to severe weather, any un-guyed mast can (and will) turn

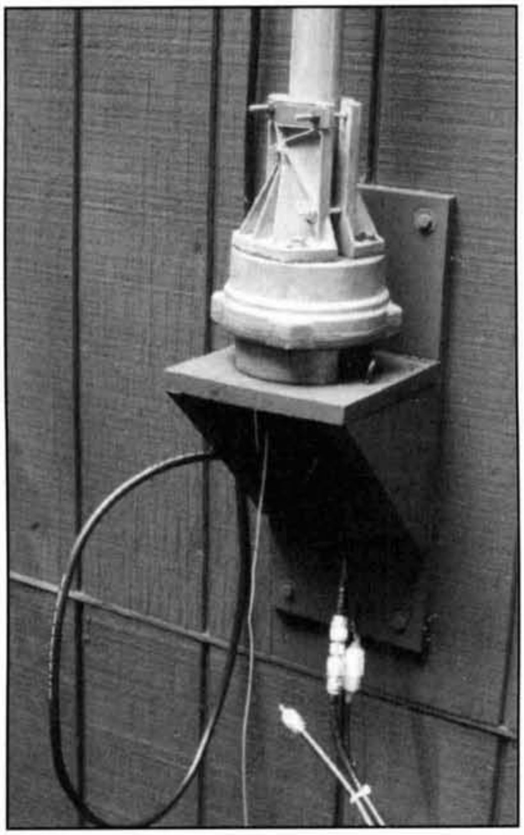

Photo A. The mounting shelf need not be large, as long as it is sturdy. For lightning protection, the mast is grounded to a small array of rods—and disconnects are provided for antenna and rotor cables.

into a long and powerful lever! This, in turn, may self-destruct in a matter of seconds—destroying antennas and damaging your roof! While a small two-pound Yagi might ride out windy conditions safely at full extension, heavier arrays must be "nested down" before severe weather hits.

Having said that, the "mini-needle" can provide a convenient and inexpensive alternative to a more permanent tower, especially for antenna experimentation. My total cost for the project, including a used Alliance rotor, was about $150.

VHF/UHF Signal Generator

A valuable piece of test gear

Will McGhie, VK6UU
Reprinted from Amateur Radio

I do not know how reproducible this circuit is. However, after spending some 50 hours to develop it over several months, I hope you will find it useful and, at the very least, that it will give you some ideas on how simple a signal generator can be for VHF and UHF.

A Signal Generator for the 2-Meter and 70-Centimeter Bands

If you build, service, or play around with voice repeaters, digipeaters, or FM radios in general, then a signal generator is a very valuable piece of test gear. This article is a design for a signal generator that covers the 2-meter and 70-centimeter bands. The generator is continuously variable in frequency and level, and has provision for audio input, be it voice, tone, or CTSS.

What Frequency?

Once the signal generator is working, how do you know what frequency it is on? It would be possible to calibrate the frequency and provide some form of dial but, in practice, I have not found this necessary. Open the mute on the radio under test and tune the signal generator across the band and you will find the correct frequency fairly easily. If it is a new radio you are tuning up, then use another radio as frequency marker. Find the required frequency on the working radio and then connect the radio to be tuned up to the signal generator.

Background

It is important to understand a bit about this design to gauge how it suits your requirements and what limitations the design might have. As I have mentioned, I don't know how reproducible this generator will be, as the method of construction is largely up to you.

I have had access to a commercial signal generator at work for many years but always wanted my own. Many years ago Dick Smith Electronics was getting rid of a companion VFO, the FV107, for next to nothing. I bought one and it lay around for a while until I modified the frequency of operation. The original VFO ran at about 5 MHz, and I was able to increase the frequency up to about 90 MHz. The circuit would just not go any higher without extensive changes; pity, I thought, as it would have been nice to get it up to 148 MHz for use as a signal generator.

As a compromise I set the VFO up at half the 2-meter frequency of 72 to 74 MHz, and it produced a nice signal on the 2-meter band due to the second harmonic. In fact, there was also a very healthy harmonic signal on 70 cm; so I had two signal generators for the price of one. This brings me to some very important points about a signal generator, and they are:

1. It must be frequency stable;
2. It must have smooth, easy frequency tuning; and

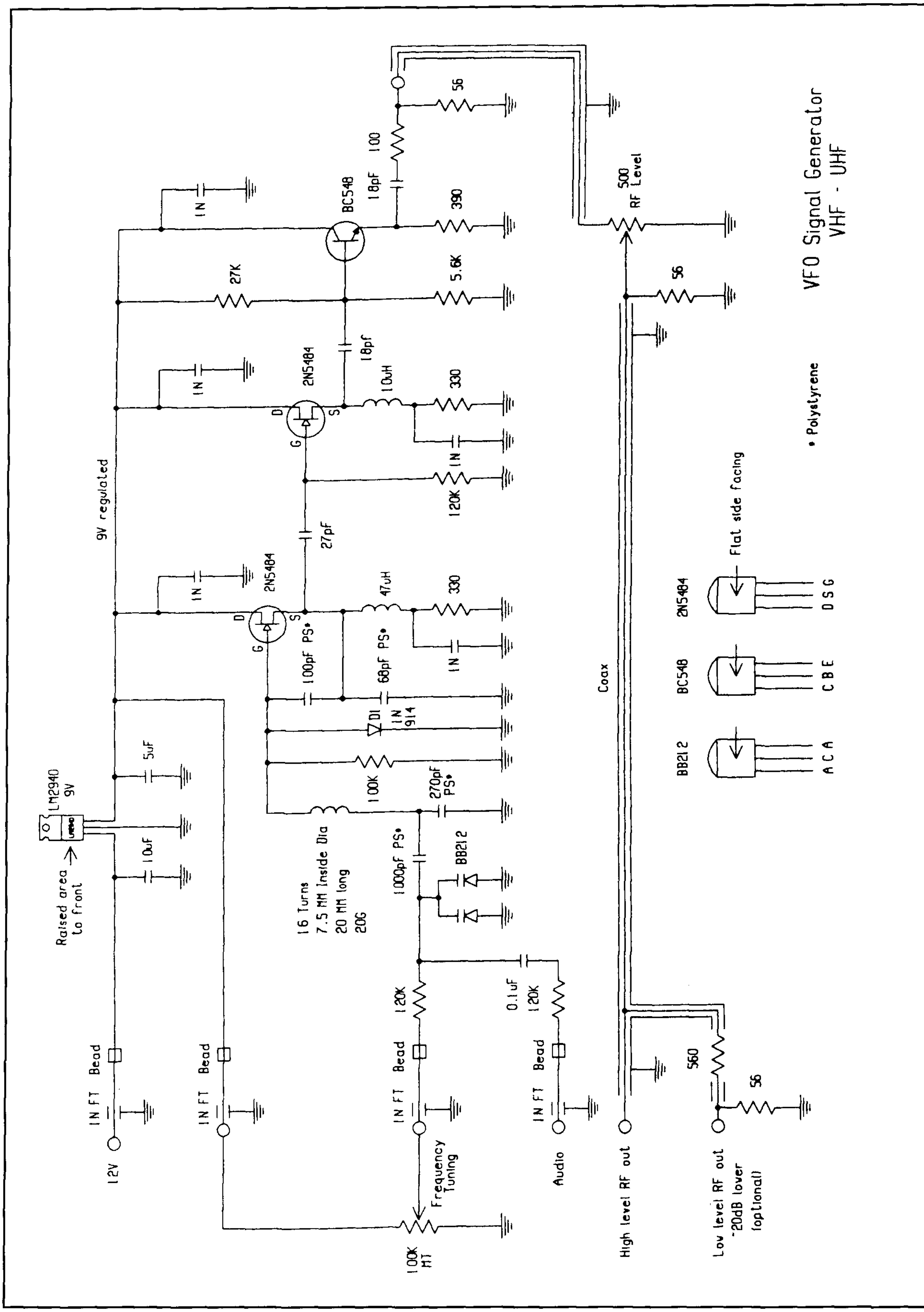

Figure 1. Schematic of the VHF/UHF signal generator. (Drawn by VK6UU.)

3. It must have as close to no signal leakage as possible.

Number 3 is perhaps the most important of all, and the most difficult to obtain. If a signal generator radiates a signal from itself via power cords or poor RF shielding, it is next to useless. If the radio you are testing is picking up just as much signal via other paths as it is receiving via the correct signal generator output, then accurate measurement and alignment of the radio is difficult at best.

As it turned out, having the signal generator operating at a sub-harmonic of the desired frequency is a good idea, the reason being that there is less 2-meter and 70-cm energy you have to shield against. Commercial signal generators usually operate on the same frequency as you require and, as such, have considerable RF shielding. The VFO unit is contained in a very thick metal box with extensive RF decoupling of all connections to the VFO. This is difficult to achieve in a homebrew unit.

Remember, the oscillator of a signal generator operating at the same frequency as you require for testing, provides a volt or more of signal and your radio, when tuned up, can hear down to a fraction of a millionth of a volt. By using the second harmonic there is about 40 dB less signal level to deal with and RF shielding is that much easier to achieve. True, you have less signal level available, but do you really require a volt of signal to align a radio? If it is that deaf then it requires basic adjustment before the signal generator is used. Enough of the basics now; on to the design as presented.

The Best Laid Plans...

I decided to do some minor modifications and, in the process, discovered the oscillator would not always oscillate. Try as I might the circuit was just not reliable enough. If I had problems with the design, what was the point of expecting others to reproduce the signal generator?

It may be that the oscillator running at around 73 MHz was not the correct design for this frequency. This forced a lot of thinking and finally a decision to lower the frequency of operation. It was then that I had a bright idea: lower the fundamental frequency of operation to around 29 MHz; 29.200 MHz times 5 is 146 MHz. The reason for picking this frequency is that most amateurs have an HF receiver that covers the 28 to 30-MHz band. This could be most useful for testing and setting up the signal generator.

What is the worst thing an oscillator can do? Answer, not oscillate. Sounds silly, but if you build an oscillator and it does not oscillate you have two problems. First, you may not realize it is not oscillating and second, once you discover it is not oscillating, how do you make it oscillate? To do this you require a means of checking to see if the circuit is oscillating and, if so, on what frequency. With many amateurs having limited test gear this is of the utmost importance. There is no point in designing a signal generator if most amateurs can't make it go. So the 29-MHz fundamental idea has a lot of merit.

The Circuit

Believe it or not, free running oscillators at 29 MHz are fairly stable provided the right components are used. This design, when listened to on 2 meters, drifts from switch-on, but only tens of kHz for a few minutes on the harmonic on 2 meters, and then settles down to remain on frequency, only requiring occasional frequency readjustment. I have found it now unusual to remain close to a given FM frequency all day. Every time the radio under test was turned on, the signal generator needed no adjustment.

In my original design I wanted to use easy-to-obtain components so I experimented with RFCs available from Dick Smith Electronics. These chokes come in all sorts of values; so, after a bit of trial and error, a circuit was produced where the main frequency determining inductor was one of these RFCs. However, the temperature stability, and hence frequency stability, of the circuit was terrible. I had to return to using an air-wound coil as shown in the circuit. The two RFCs in the source leads of the FETs are those discarded as oscillator inductors, but are not in critical areas of the frequency determining part of the oscillator.

The other important frequency determining parts of the circuit are the capacitors shown with PS* next to them; these are polystyrene capacitors and are very temperature stable. It is important to use these capacitors!

What makes producing a signal generator like this difficult from scratch is obtaining the correct frequency range. It is easy to make the circuit oscillate, but not so easy to make it oscillate on the frequency you want and over the tuning range you want. Using a hand-held transceiver to find the operating frequency after each modification is very difficult, as changes can result in the frequency shifting many tens of MHz, or, in some instances, not oscillating at all. I was able to use a spectrum analyzer for the ground work and this made it easy.

The frequency tuning is done using a varicap diode and a multi-turn potentiometer. A 20-turn pot is the best if you can find one; note that the value of the multi-turn pot is not important. Anywhere from 5 k to 1 meg works as it is just a means of obtaining a smooth variable voltage. I found that Radio Spares sells a range of multi-turn pots. A large knob on the potentiometer is important to give you good control. As a variation, a small fine-tune pot could be included in series with the main tuning pot.

The varicap diode is a BB212 available from Dick Smith Electronics and has a very wide capacitance differential (CD) of 22. At near zero volts the capacitance is about 600 pF, and 8 volts about 30 pF. The BB212 is two varicaps in one package and I joined the two together. The cathode is common inside the package with two anodes. Join the two anodes together. This then provides a variable capacitor from over 1000 pF down to about 50 pF. This brings me to an important point.

The circuit will stop oscillating if the total capacitance from the bottom of the oscillator inductor to grounds falls too low. I found this minimum value to be around 200 pF. Note the fixed 270 pF capacitor between the bottom of the inductor and ground. This is required as the varicaps can be tuned to a low capacitance that stops the circuit oscillating.

Is It Oscillating?

When you build up the circuit you want to know whether it is oscillating before you go any further. I found placing a finger on the oscillator inductor changed the voltage on the source resistor to ground. It was not much of a change but enough to indicate the circuit was oscillating.

Signal Level

A signal generator must have a level adjustment. This can be difficult to obtain. I tried various methods and the simplest was a potentiometer. Carbon pots do not make good RF level adjusters and don't take the signal level all the way down to zero if fed too high a level. This is because, even when fully down, there is some inductance, and at these frequencies that inductance means the pot does not drop to zero ohms. However, about 40 dB in range was obtained with a carbon pot. This lack of range with the carbon pot means that if you feed a signal level higher than 40 dB above the noise floor then you can't wind the level down into the noise.

Frequency Pulling

While on the subject of the RF level control, I found a small amount of frequency pulling when the RF level pot is turned fully up. On 2 meters it amounted to about 2 kHz, so I added another buffer stage to the design; however, this did not fix the frequency shift. I don't know if this problem is part of the design or a condition that may not occur with any other units that are made. I would be interested to know if you find the same problem.

Construction

My circuit was built on Tandy board. These boards come in a variety of sizes and look like Vero board, but with all the solder pads isolated so that you have to join pads rather than cut between them. It works well and is easy to use.

The entire circuit board was enclosed inside circuit board material, with the lid soldered on. With all leads in and out going through feed through capacitors and with ferrite beads on each of the leads, the RF shielding is more than adequate. The RF output is via a BNC socket, or "N" type, as you prefer.

This box is then mounted inside another box that contains the controls, power in and RF out, and is also made out of printed circuit board material. A BNC or "N" type connector is then added to the outside box and the RF fed from the first connector via coax. Using printed circuit board material results in an easy way of obtaining a fully screened RF box.

Further Thoughts

A few comments about the design. My unit ended up producing about 30 µV on 2 meters and 10 µV on 70 centimeters. The amount of RF output can be increased by changing the bias voltage on the last buffer transistor. I don't know why, but I found that lowering the base-to-ground resistor to about 2.7 k resulted in 100 µV on 2 meters.

If the output pot will not lower the signal level low enough, increase the 100-ohm resistor on the output of the last buffer stage, or reduce the value of the 18-pF capacitor on the output stage. Another method, as shown in the circuit diagram, is to include an attenuated output with two outputs from the signal generator, one high level and the other lower level.

Note the diode between the gate of the oscillator FET and ground. This is to limit the drive to the gate and it also reduces the amount of harmonics produced. So, if you want a lot more output (20 dB), remove the diode, but you will have to add a capacitor to compensate.

My unit tuned from about 28 MHz (140 MHz, 420 MHz) to 29.7 MHz (148.5 MHz, 445.5 MHz). If you only require the 2-meter band, then reduce the frequency range by adding resistors either side of the multi-turn pot. This will also give you smoother frequency control with more turns required to shift frequency.

The oscillator inductor is air wound and supported by simply soldering it onto the board. This inductor is vibration sensitive and acts like a microphone. To dampen this down, apply Silastic® over the coil. The wire I used is tinned copper and about 20 gauge. I was not sure of the size but it measured 30 thousandths of an inch on my micrometer. The coil turns are wound as close together as possible without touching.

Feedback

There are lots of possibilities to improve this design and I would like feedback on the design and attempts to build the generator. One idea that comes to mind is that the frequency tuning could be switched with different voltages to the varicap to give different band segments and hence slower main tuning.

The project is worth consideration as an RF signal generator which is worth its weight in gold for repeater site measurements. I hope to find the time to improve the design and provide greater signal output. Also, a design running at 146 MHz interests me. Does anyone have a circuit for a VFO circuit running at 146 MHz?

A Useful Accessory for the MFJ-259 SWR Analyzer

Build this handy female-to-BNC adapter

Remy Brodeur, VE2BRH

This article first appeared in RAQI, *June-July '94 and is reprinted with permission of the author.*

As stated in the (very well done) instruction manual for the MFJ-259 SWR Analyzer, besides doing a good job in measuring SWR, this unit can be used to measure velocity factors of coaxial lines, to adjust matching stub lengths, and to analyze LC circuits. To do so, it is suggested that one insert a 50-ohm resistor in series with the load analysis because an open-ended quarter-wavelength transmission line will act as a short circuit. In the same manner, a series type L-C circuit will also act as a short circuit at the resonant frequency. When placed in series with a 50-ohm resistor, such a short circuit will behave like a 50-ohm resistive impedance, thus exhibiting a perfect 1:1 SWR when presented to the MFJ-259, once the resonant frequency is found. If we were to perform the same measurements without the series resistor, the SWR would be infinity, a much more difficult point to find on the analyzer than a 1:1 ratio.

Construction

On the practical side, it is not always easy to insert a 50-ohm resistor in series with whatever load we wish to analyze. Because the MJF-259 connector is a SO-239 type, and the probe I am using for most of these kinds of tasks is terminated with a BNC connector, I found it was very convenient to build a PL-259 to female BNC adapter, incorporating the prescribed resistance (**Photo A**). As shown in **Figure 1**, such an adapter can built in 10 minutes, in three easy steps, using a PL-259 connector, a female, single-hole chassis-type BNC connector, and a 51-ohm, 1/4-watt resistor. (Resistors of 51 ohms are much easier to find than their precise 50-ohm counterparts. The single extra ohm is not enough to make much of a difference with the MFJ-259, and will certainly not alter the resonant frequency.)

Photo A. The author's PL-259 to female BNC adapter.

Conclusion

The project is simple to build, inexpensive, and will multiply by 10 the fun of using your MFJ-259 SWR Analyzer. I hope you will enjoy building and using such an adapter. ■

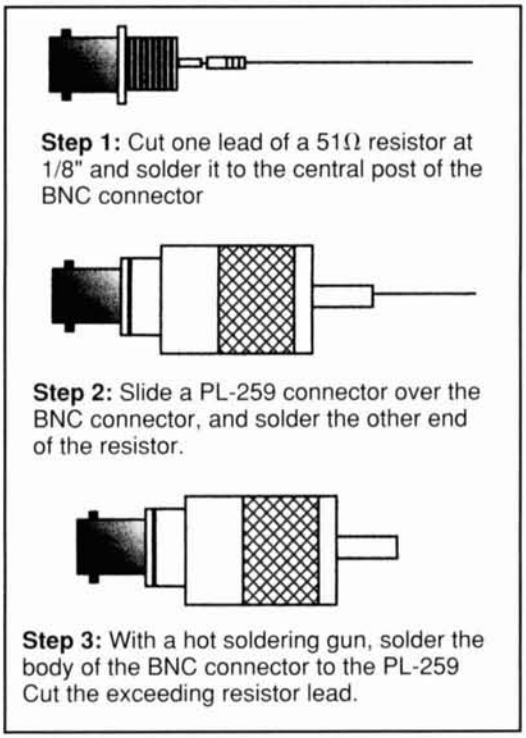

Figure 1. Construction details for the adapter.

COMMUNICATIONS QUARTERLY ARTICLE INDEX

FALL 1993–SUMMER 1998

ANTENNA EXOTICA

BALUNS

COMPUTERS

OPTICAL COMMUNICATIONS

PACKET

PROPAGATION AND METEOROLOGICAL EVENTS

QRP

QUARTERLY COMPUTING

QUARTERLY DEVICES

RECEIVERS

REVIEWS

TECHNICAL CONVERSATIONS

TEST EQUIPMENT

TEST PROCEDURES AND MEASUREMENT TECHNIQUES

THE FINAL TRANSMISSION

THE SOLAR SPECTRUM

TRANSCEIVERS

TRANSMITTERS

VHF/UHF

VIRTUAL EQUIPMENT

VLF OPERATION

It is appropriate to note here that this article depended dramatically on the proficiency of (and attention to detail by) Jerry Sevick. Postulations (theories, if you like) like this require confirmation—*physical* confirmation. The computer work, especially when espousing something new, *requires* physical confirmation. It can't be done simply by using *another computer program*—and that includes NEC.4!

W. J. Byron, W7DHD
Sedona, Arizona

Kirchoff's Laws: Still going...

Dear Editor:

In his article "Kirchoff's Laws: the classic cube problem," Jay Jeffrey treats a famous exercise for electrical engineering students: given a cube whose edges are identical resistors (say, 1Ω), determine its resistance between vertices at opposite ends if on of the cube's longest diagonals. This problem has become a classic because its method of solution is simple if the student (unlike Mr. Jeffrey) exploits the symmetry of a cube.

If you view a cube along one of its longest diagonals $\overline{AB}$ (see **Figure 1**), you'll see the symmetric network of **Figure 2**.

Suppose now that a 1 Amp constant current source is connected between points A and B. (See **Figure 3**).

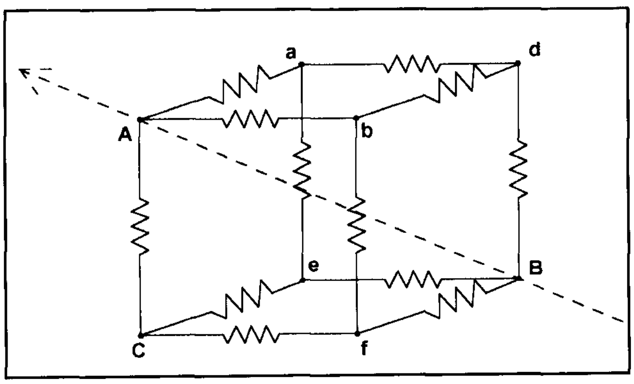

Figure 1. The cube along a diagonal.

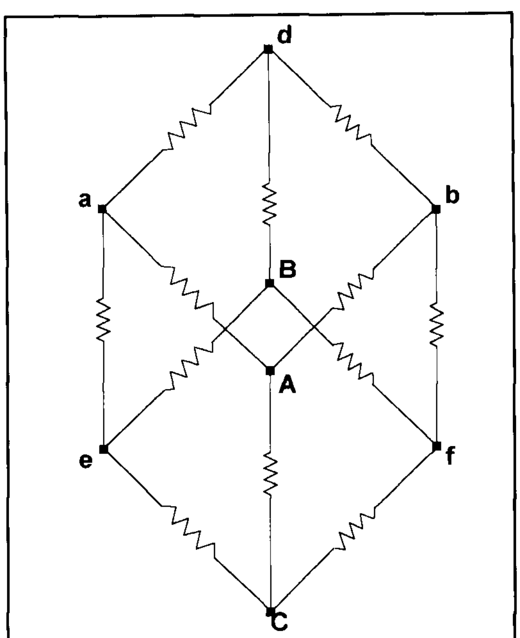

Figure 2. The symmetric network.

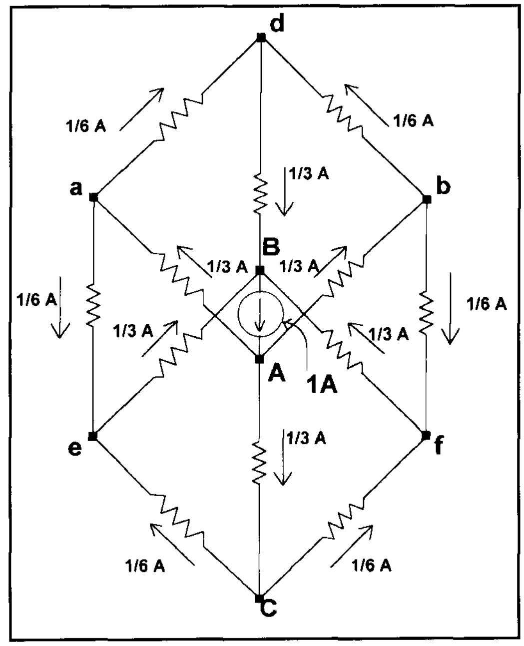

Figure 3. Connecting an amp source between A and B.

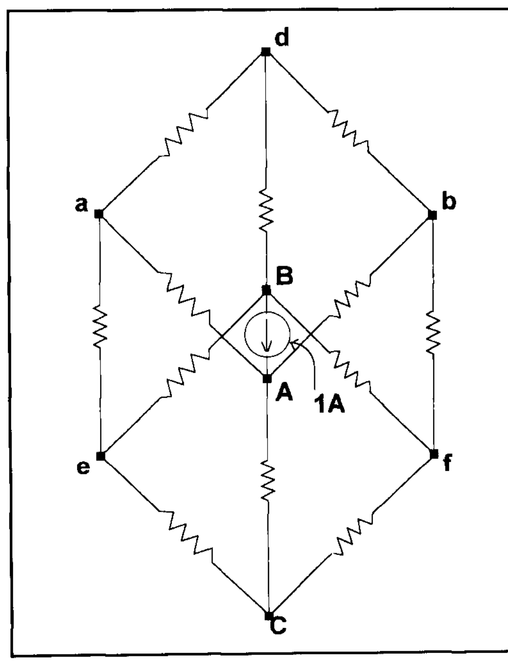

Figure 4. Current flows through into three identical resistors.

If the cube is rotated through a one-third turn (either clockwise or counterclockwise) around the axis $\overline{AB}$, the cube will appear unchanged except that the labels on its corners will change places; for example, rotating the cube one-third clockwise will move point a to point b and point b to point c, but otherwise the network will appear unchanged. Since nothing except arbitrary labels distinguishes one corner or one edge of the cube from another, there's no reason for more current to flow through resistor $\overline{Aa}$ than resistor $\overline{Ab}$ or $\overline{Ac}$: each resistor is identical and is connected identically to the rest of the network. Therefore, the 1A current divides equally among the three resistors that are connected to node A: 1/3A flows through each resistor ($\overline{Aa}$, $\overline{Ab}$, and $\overline{Ac}$).

Similarly, since the network is symmetric, there's no reason for more current from resistor $\overline{Aa}$ to flow through resistor $\overline{ad}$ than resistor $\overline{ae}$.

Hence the current from resistor aa divides equally between resistors $\overline{ad}$ and $\overline{ae}$, and 1/2 x (1/3A) = 1/6A flows through each resistor. A similar division of current occurs at the ends of resistors $\overline{Ab}$ and $\overline{Ac}$.

By the same reasoning that was applied to mode A, a current of 1/3A flows into each of the three identical resistors ($\overline{dB}$, $\overline{eB}$, $\overline{fB}$) that are connected to node B (see **Figure 4**).

The voltage difference between nodes A and B must be the same regardless of the path that's used to calculate the voltage difference. The voltage difference along resistor $\overline{Aa}$ is 1/3A x 1Ω = 1/3V.

The voltage difference along resistor $\overline{ad}$ is 1/6A x 1Ω = 1/6V.

And the voltage difference along resistor $\overline{dB}$ is 1/3A x 1Ω = 1/3V.

Hence the voltage difference between nodes A and B along the path AadB is 1/3V + 1/6V +1/3V = 5/6V.

Therefore, the resistance between nodes A and B is $\frac{(5/6V)}{1A} = 5/6\Omega$

The whole point of the "classic cube problem" is to avoid the complicated sets of linear equations that Mr. Jeffrey employed and to avoid that complexity by exploiting the symmetry of the cube.

Christopher Kirk, NV1E
Shrewsbury, Massachutts

And going!

Dear Editor:

In looking at your discussion in the Fall 1997 issue on the "Classic Cube Problem" there is a very easy solution for the case where all the resistors are the same or share some symmetry. Referring to **Figure 2** from the article; since R1=R2=R3, the currents in each resistor are equal (by symmetry) and the voltage drop across each is the same. Therefore points N, S, and T are at the same potential and we can connect them. Since they are all at the same potential, no change in current flow will occur in the new circuit. By the same reasoning we can connect O, Q, and U. This results in the circuit shown below (**Figure 1**). Using the 100k Ohm example given in the article we quickly get 83.33k Ohm for the total circuit as derived.

Peter Torrione
Norwood, New Jersey

Thank you!

Dear Editor:

I want to thank you again for something that I've thanked you for in the past. This time I have two more reasons. One reason is on the small side and the other is really big. I want to

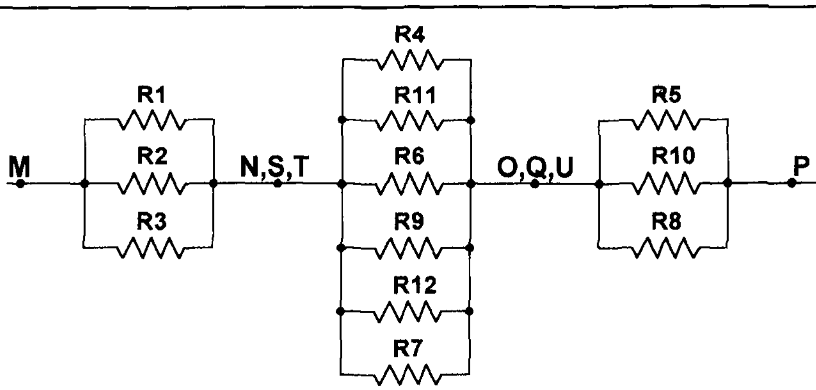

$$\frac{R}{3} + \frac{R}{6} + \frac{R}{3} = \frac{5R}{6}$$

IF R = 100k 33.33k + 16.62k + 33.33k = 83.33k

Figure 1. Circuit that results when connecting O, Q, and U.

thank you again for the help you've given me by editing my articles and forcing me to become a better writer. I now consider myself a fair technical writer, which is a big improvement from where I was six or seven years ago when you edited my first article for *Ham Radio*. Boy, was that a shock to my fragile male ego! I have an article in the last issue of *CommQuart* that has generated many favorable comments. It turned out well and I have you to thank for that.

Now for the BIG reason. In my job at Raytheon Defense Systems I do development of advanced systems, which requires me to write white papers and proposals. These go to various U.S. defense agencies. About a month ago, we won a major program based on a proposal we submitted. Due to the nature of the topic, I wrote about 60 percent of the technical part of the proposal and edited the remaining 40. After we won the bid, the customer said it was the best technical proposal they had ever seen. The complex technical issues were explained well and were easy to understand. Also, the text was very well written. THANK YOU!

Dick Webster, K5IU
Prosper, Texas

Note on the Teeny Twoer

Anyone interested in purchasing boards to build Rick Littlefield's "Teeny Twoer" (Summer 1998, page 98) may obtain them from FAR Circuits, 18 N 640 Field Court, Dundee, Illinois 60118-9269; <www.cl.ais.net/farcir/>. Boards are $11 each plus shipping and handling.

Reader finds Bruene's article noteworthy

Dear Editor:

I have recently read Mr. Warren B. Bruene's article "The Elusive Conjugate Match," and find it to be very noteworthy. I believe Mr. Bruene has proved his point by mathematical analysis beyond any doubt. His article should put to rest any misconceptions the article "Source Impedance of HT Tuned Power Amplifiers and the Conjugate Match" by Messrs. Belrose, Maxwell, and Rauch presents.

I recall from 30 years past that Mr. Maxwell was the head at Radio Corporation of America's (RCA) Astro-Labs (Satellite Communications) in Princeton, New Jersey. I had the pleasure and good fortune of meeting Mr. Maxwell, and he was generous in helping me derive a solution to specific antenna engineering problem. He was a colleague of the famous Dr. George Brown, Robert Lewis, and Epstein on one particular antenna project during the 1930s at RCA. I respect Mr. Maxwell and his knowledge of radio antenna engineering; however, I disagree with his recent article mentioned above.

Why do I mention Mr. Maxwell's connection to RCA? What is the significance? RCA maintained a school in New York City during the late 1960s and early 1970s; the curriculum was fundamental radio principles for the broadcasting industry. It is interesting that RCA Institute's *Radio Transmitter* manual treats the subjects of power amplifiers and pi tank networks far differently from Messrs. Belrose, Maxwell, and Rauch.

Quoting from the RCA text:

> Pi-Network Tanks. The pi-network tank performs the function of a resonant plate as well as a matching section for coupling the power amplifier to the antenna. The familiar pi-section appearance is apparent in figures 21d and figure 22. Note that C1 is the input capacitor. C2 the output capacitor, and tank conductor L1 is connected between them.
>
> First, to understand its role as resonant plate tank, refer to figure 22b. This is the same circuit as in figure 22a except for the rearrangement of components in the diagram. Also, the rf transmission line is temporally disconnected. The circuit now resembles the shunt-fed plate tank shown earlier. There is an additional component shown here, a large capacitor C2. However, C2 and C1 act in series to tune L1 to *parallel resonance*. Thus, the pi-network acts as a high-impedance plate load.
>
> Second, to understand the role of the pi-section tank as a matching section, refer to figure 22C. this is the same circuit as in b of the figure but now with rf transmission line connected. Since C2 is a large variable capacitor having a low reactance, it provides a means of adjusting the low output impedance of the pi-section tank to match the low input impedance of the transmission line. The pi-section tank thus acts as an efficient step-down device. It steps down the high-impedance value existing between 1 and 2 to a low impedance between 3 and 2.[1,2]

As we all know, parallel resonant circuits have a very high impedance, and, as the RCA text describes, the pi-network has two important functions working with the power amplifier circuit. Mr. Bruene states on page 28 of his article, and I cite his writing from paragraph seven: "For example, in IF stages of old tube receivers the tubes had a very high value of Rp (and Rs) compared to the IF load which the IF transformer places on them. There is no conjugate match." This point is well taken; according to RCA's manual the pi-network is a parallel resonant circuit presenting a high impedance.

Moreover, Dr. William Everitt's book *Communications Engineering* states "An Impedance-Transforming Theorem" describing the conjugate match (see page 243). Using RCA's definition of a pi-network's two functions with a PA, the conjugate match does not exist.[3,4]

Messrs. Belrose, Maxwell, and Rauch attempted further to justify their viewpoint adding to the confusion by mentioning the application of The venin and Norton's Theorems. They attempt to reduce a pi-network to a single equivalent resistance. Although, network transformations are employed in nodal analysis, I do not believe it is necessary to demonstrate to make the point. They also attempt to tie in the Maximum Power Transfer theorem to justify their viewpoint. It was commonly known during the early 1960s with the advent of SSB among radio amateurs that the dip and forward power readings do not coincide. However, Messrs. Belrose, Maxwell, and Rauch have stated otherwise in column one of their article (page 30). "If the amplifier is properly neutralized, the minimum plate current dip (indicating network resonance) will occur simultaneously with delivery of maximum output power." This is incorrect.

Mr. Bruene, as a first-class power amplifier design engineer, has demonstrated that Messrs. Belrose, Maxwell, and Rauch have stretched far to make the technical facts fit their own beliefs. My conclusions are that Mr. Bruene is correct and the other article's views are at the very least dubious in nature. However, readers will have to decide for themselves.

Walter J. Schulz, K3OQF/VQ9TD
Jim Thorpe, Pennsylvania

REFERENCES
1. *Oscillators, RF Amplifiers, Radio Transmitters, Transmitter Practices,* RCA Institutes, Inc., 1968.
2. *Resonance*, CREI Home Study Division, McGraw-Hill Book Club Co., 1969.
3. William Littell Everitt, E.E. Ph.D., Second Edition, *Communication Engineering*, McGraw-Hill Book Company, Inc., New York and London, 1937.
4. "AM/FM Transmitters: Appendix 1-Coupling Circuit Design," CREI Home Study Division, McGraw-Hill Book Club Co.

Regarding the Conjugate Match

Dear Editor:

Here are my thoughts on the conjugate-match controversy. There was a similar debate some years ago about the large-signal output impedance of solid-state devices, which seems to be virtually the same question. The issue is addressed in Section 13-4 of *Solid State Radio Engineering* (Wiley, 1980).

All circuit models have their uses—and limitations. I would like to try to put things into proper perspective.

1. Describing the performance characteristics of RF-power devices by analytical equations is often difficult or impossible. It is therefore very convenient to measure their performance and to plot the results (i.e., output power) as a function of load impedance (on a Smith chart). This is commonly called a "load-pull" characterization.

2. The conjugate of the impedance that produces maximum output power is often called the "large-signal impedance" of the device, and this is a simple way for one designer to tell

another how to replicate results. The power contours on a Smith chart are generally somewhat elliptical. If you try to draw too much power, the amplifier saturates. These behaviors lead to the notion of doing a conjugate match to draw maximum power from the device.

While the load-pull measurements, large-signal impedance, and conjugate-match concepts are often useful for design purposes, they do not represent a true, general characterization of the device for several reasons:

3. Large-signal characteristics are valid only for the specific circuit and test conditions. They are a "bulk" characteristic rather than a true characteristic. This concept is easily illustrated by a diode. If you drive 1 amp into a diode with a 0.7-volt cut-in voltage, you get an impedance of 0.7 ohms. If you drive 2 amps into the same diode, you get 0.35 ohms.

4. Load impedances for maximum power, maximum efficiency, and maximum linearity are generally different. How you load the device depends upon the class of operation (B versus E, for example), the supply voltage, power output, etc. This is not the case in a simple conjugate match.

5. There are reactive elements inside the RF-power device, but their values do not necessarily correspond to the reactance of the maximum-power load. The equivalent circuit models are considerably more complex than the conjugate-match model. The conjugate-match model does not naturally account for power loss in the device. I found it to be not at all useful for analyzing other modes of operation, such as classes D and E.

6. I've often used the analogy of trying to do a conjugate match to the electric outlet. Instead, you simply load it to get the desired power.

Equivalent-circuit models are used in programs such as SPICE to allow simulation of a device in a wide variety of circuits and conditions. Naturally, such models are only approximations of what really happens. The "true" characterization of an RF-power device requires the use of field and semiconductor theory. This is used in programs such as PISCES and SUPREM that are used in the design of semiconductors.

Frederick H. Raab, Ph.D., W1FR
Green Mountain Radio Research Company
Colchester, Vermont
<f.raab@ieee.org>

A few suggestions

Dear Editor:

I just received the last (Summer) issue of *Communications Quarterly*, to which I have been a subscriber since issue number 1. I started reading the editorial, and I do agree with it mainly. However, I have a few suggestions:

1. In *Communications Quarterly*, there seems to be a notable aversion to publishing e-mail addresses and sites, although these are, without doubt, the most convenient and fastest way to communicate nowadays. I do understand there is a certain fear that the Internet is eating our pastime, but, on the other hand, I think that the Internet can help us publicize ham radio.

So wouldn't it be interesting to place at least one e-mail address, say of the editor, in *Communications Quarterly*?

2. I'm getting a little tired of all the ELNEC/MININEC, etc. graphs. Though these programs do have their merits, I think there's a limit as to what should be published.

Few amateurs seem to use, for example, spreadsheets with simple programming to determine filters (lowpass/bp, etc.).

Four years ago, we started a balloon project at our university to stimulate the interest of the students and the radio amateurs of four provinces. They have shown quite a bit of interest, and actual flights are followed by a lot of hams. If you are interested, check out our Web site at:

<http://www.uccor.edu.ar/-jcoppens/glmain_e.html>

So enough for now. I do hope to continue this through e-mail. Faxing costs a few dollars per message, e-mail is free.

John Coppens, ON6JC/LW3HAZ
Argentina
<on6jc@amsat.org>
<jcoppens@linux2.uccor.edu.ar>

Thanks for your comments. I'll try to include more e-mail addresses with our articles to facilitate the exchange of information. My e-mail address, for anyone who'd like to drop me a line, is: <ka1stc@aol.com>.

Corrections

Grant Bingeman found two errors in his article "Phased Array Adjustment" (Summer 1998, page 29). First, **Equation 2** should read:

Z12 = -V2/I1

and I2R in the second paragraph on page 32 should read: I^2R. ■

Holiday Gift Ideas

Building and Using Baluns and Ununs
by Jerry Sevick, W2FMI

This volume is the source for the latest information and designs on transmission line transformer theory. Discover new applications for dipoles, yagis, log periodics, beverages, antenna tuners, and countless other examples.

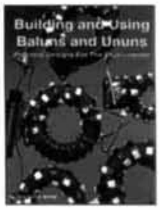

Order No. BALUN . . . $19.95

33 Simple Weekend Projects
by Dave Ingram, K4TWJ

Do-it-yourself electronics projects from the most basic to the fairly sophisticated. You'll find: station accessories for VHF FMing, working OSCAR satellites, fun on HF, trying CW, building simple antennas, even a complete working HF station you can build for$100. Also includes practical tips and techniques on how to create your own electronic projects.

Order No. 33PROJ.... $15.95

The Quad Antenna
by Bob Haviland, W4MB
Second Printing

An authoritative book on the design, construction, characteristics and applications of quad antennas.

Order No. QUAD...... $15.95

The VHF "How-To" Book
by Joe Lynch, N6CL

This book is the perfect operating guide for the new and experienced VHF enthusiast.

Order No. BVHF....... $15.95

The Vertical Antenna Handbook
by Paul Lee, N6PL

Learn basic theory and practice of the vertical antenna. Discover easy-to-build construction projects.

Order No. VAH....... $9.95

W6SAI HF Antenna Handbook
by Bill Orr, W6SAI

Inexpensive, practical antenna projects that work! Guides you through the building of wire, loop, Yagi and vertical antennas.

Order No. HFANT...... $19.95

McCoy on Antennas
by Lew McCoy, W1ICP

Unlike many technical publications, Lew presents his invaluable antenna information in a casual, non-intimidating way for anyone!

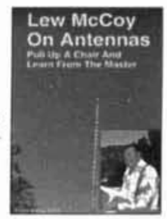

Order No. MCCOY $15.95

CQ Amateur Radio Almanac
by Doug Grant, K1DG

Free Almanac with orders over $75

Filled with over 600 pages of ham radio facts, figures and information. 1997 edition,next volume won't be published until 1999.

Order No. BALM97 .. ~~$19.95~~ $15.95

Keys, Keys, Keys
by Dave Ingram, K4TWJ

You'll enjoy nostalgia with this visual celebration of amateur radio's favorite accessory. This book is full of pictures and historical insight.

Order No. KEYS $9.95

The NEW Shortwave Propagation Handbook
by W3ASK, N4XX & K6GKU

A comprehensive source of HF propagation principles, sunspots, ionospheric predictions, with photography, charts and tables galore!

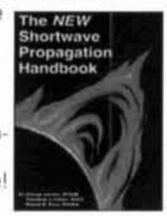

Order No. SWP......... $19.95

Amateur Radio Equipment Buyer's Guide

This New 144-page book is your single source for detailed information on practically every piece of Amateur Radio equipment and every accessory item currently offered for sale in the United States. From the biggest HF transceiver to Ham computer software, it's in the CQ Guide, complete with specs and prices. Over 2100 product listings (3100 including transceiver accessories!).

Also includes the most comprehensive directory anywhere of Ham product manufacturers and dealers in the USA, complete with phone and FAX numbers, web sites, and E-mail addresses, with 475 dealers and manufacturers listed.

Order No. EBG...... $15.95

Getting Started Videos- "How-To", Operating/Technical Tips, Techniques, and more!

Getting Started in Ham Radio– How to select equipment, antennas, bands, use repeater stations, grounding, basic soldering.

Getting Started in Packet–De-mystify packet. Info on making contacts, bulletin boards, networks, satellites.

Ham Radio Horizons–Step-by-step instructions for the prospective ham on how to get involved.

Getting Started in VHF–Intro to VHF. Repeater usage, packet, satellites and more exotic VHF op modes.

Getting Started in Amateur Satellites– How ops set up stations. Locate and track ham satellites.

Getting Started in DXing– Top DXers share experiences with equipment, antennas, op skills and QSLing.

Getting Started in Contesting– Advice and op tips from Ken Wolf, K1EA, K1AR and others!

$19.95 each–
Buy more and save!
Buy 2 or 3 for $17.95 each
Buy 4 to 6 for $15.95 each
Buy all 7 for your Club for only $99.95!!

ADVERTISER'S INDEX

Reach this dynamic audience with your advertising message, contact Don Allen, W9CW at 217-344-8653, FAX 217-344-8656, or e-mail: QtrlyAds@aol.com

.... POWER ON WITH ASTRON
SWITCHING POWER SUPPLIES ....

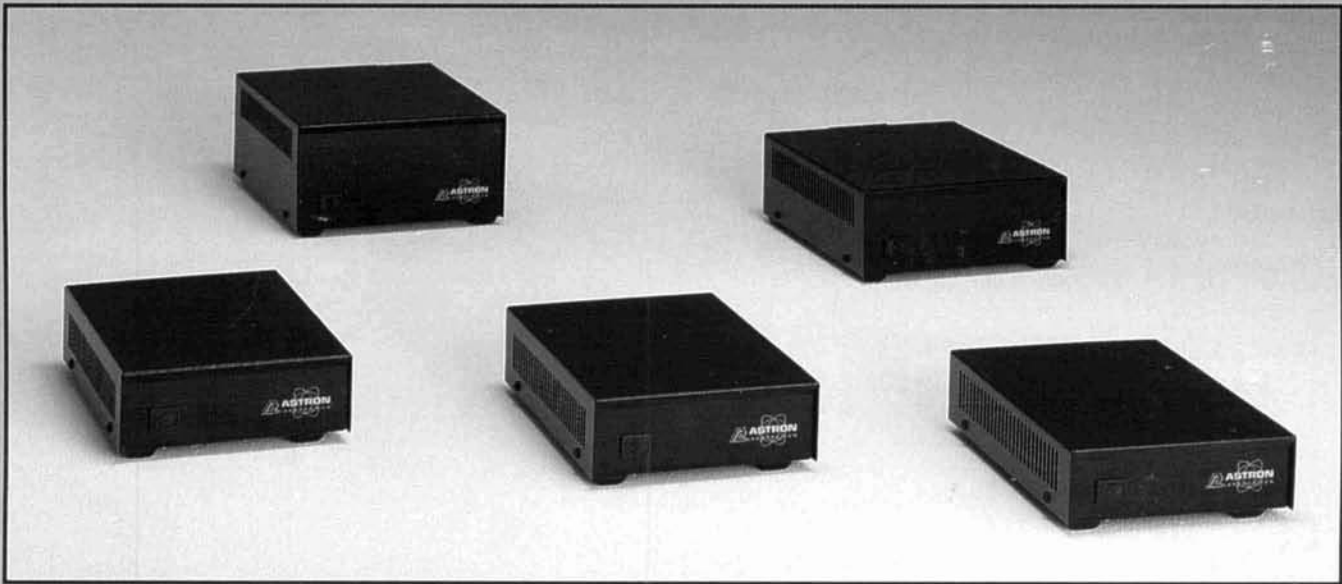

SPECIAL FEATURES:
- HIGH EFFICIENCY SWITCHING TECHNOLOGY SPECIFICALLY FILTERED FOR USE WITH COMMUNICATIONS EQUIPMENT, FOR ALL FREQUENCIES INCLUDING HF.
- HEAVY DUTY DESIGN
- LOW PROFILE, LIGHT WEIGHT PACKAGE.
- EMI FILTER
- MEETS FCC CLASS B

PROTECTION FEATURES:
- CURRENT LIMITING
- OVERVOLTAGE PROTECTION
- FUSE PROTECTION
- OVER TEMPERATURE SHUTDOWN

SPECIFICATIONS:
INPUT VOLTAGE: 90-132 VAC 50/60Hz
OR 180-264 VAC 50/60Hz
SWITCH SELECTABLE
OUTPUT VOLTAGE: 13.8 VDC

MODEL	CONT. AMP	ICS	SIZE	WT.(LBS)
SS-10	7	10	1 1/8 x 6 x 9	3.2
SS-12	10	12	1 3/8 x 6 x 9	3.4
SS-18	15	18	1 3/8 x 6 x 9	3.6
SS-25	20	25	2 7/8 x 7 x 9 3/8	4.2
SS-30	25	30	3 3/4 x 7 x 9 5/8	5

ASTRON CORPORATION

9 AUTRY, IRVINE, CALIFORNIA 92618
714-458-7277 FAX 714-458-0826
www.astroncorp.com